Identification of Novel Chemokine and Chemokine-like Mechanisms in Leukocyte Adhesion and Atherosclerotic Lesion Formation

Von der Fakultät für Mathematik, Informatik und Naturwissenschaften der RWTH Aachen University zur Erlangung des akademischen Grades einer Doktorin der Naturwissenschaften genehmigte Dissertation

vorgelegt von

Diplom-Biologin
Regina Krohn

aus Xanten, Deutschland

Berichter:
Universitätsprofessor Dr. med. Christian Weber
Privatdozent Dr. rer. nat. Christoph Peterhänsel
Tag der mündlichen Prüfung: 11.06.2008

The results of this work were in part published in:

Bernhagen, J., **Krohn, R.**, Lue, H., Gregory, J. L., Zernecke, A., Koenen, R. R., Dewor, M., Georgiev, I., Schober, A., Leng, L., Kooistra, T., Fingerle-Rowson, G., Ghezzi, P., Kleemann, R., McColl, S. R., Bucala, R., Hickey, M. J., Weber, C. (2007). MIF is a noncognate ligand of CXC receptors in inflammatory and atherogenic cell recruitment. *Nat Med* **13**, 587-96.

Krohn, R., Raffetseder, U., Bot, I., Zernecke, A., Shagdarsuren, E., Liehn, E. A., von Sandbrick, J. P., Nelson, P. J., Biessen, E. A., Mertens, P. R., Weber, C. (2007). Y-box binding protein-1 controls CC chemokine ligand-5 (CCL5) expression in smooth muscle cells and contributes to neointima formation in atherosclerosis-prone mice. *Circulation* **116**, 1812-20.

Table of Contents

Abbreviations

A	anti-
aa	amino acid (in single letter code)
Ab	antibody
apoE	apolipoprotein E
ATCC	American Type Culture Collection
BCECF/AM	2',7'-bis-(2-carboxyethyl)-5-carboxyfluorescein-acetoxymethyl
BSA	bovine serum albumin
CD	cluster of differentiation
cDNA	copy DNA
CHAPSO	3-[(3-Cholamidopropyl)dimethylammonio]-2-hydroxy-1-propanesulfonate
CHO	cell Chinese hamster ovary cell
CLF	chemokine-like function
Cy3	cyanine 3
DAPI	4',6-Diamidino-2-phenylindol
DDT	dithiothreitol
DMSO	dimethylsulfoxide
DNA	desoxyribonucleic acid
E. coli	*Escherichia coli*
EDTA	ethylenediaminetetraacetic acid
e.g.	for example (from Latin: exempli gratia)
EGTA	ethylene glycol-bis(2-aminoethylether)-N,N,N′,N′-tetraacetic acid
ELISA	enzyme-linked immunosorbent assay
FCS	fetal calf serum
FITC	fluorescein isothiocyannate
GAPDH	glyseraldehyde-3-phosphate dehydrogenase
H	hours
HEPES	4-2-hydroxyethyl-1-piperazineethanesulfonic acid
hIgG	human IgG
HRP	horse radish peroxidase
HUVEC	human umbilical vein endothelial cell
I domain	inverted domain
ICAM-1	intracellular adhesion molecule-1; CD54
IFN-γ	interferon-γ
IgSF	immunoglobulin superfamily
i.e.	that is (from Latin: it est)
i.p.	intrapericardial

JAM-A	junctional adhesion molecule-A; CD321
LFA-1	lymphocyte function-associated antigen-1; αLβ2; CD11a/CD18
mAb	monoclonal antibody
MHC	major histocompatibility complex
MM6	cell mono mac 6 cell
o.n.	overnight
pAb	polyclonal antibody
PBMC	peripheral blood mononuclear cell
PBS	phosphate buffered saline
PCR	polymerase chain reaction
PECAM-1	platelet endothelial cell adhesion molecule-1; CD31
PHA	phytohemagglutinin
PKC	protein kinase C
PMA	phorbol-12-myristate-13-acetate
PMSF	phenylmethanesulfonyl fluoride
PTX	pertussis toxin
SDF-1α	stromal cell-derived factor-1α; CXCL12
SDS-PAGE	sodium dodecyl sulfate-polyacrylamide gel electrophoresis
SEM	standard error of mean
siRNA	small interfering RNA
sJAM-A.Fc	soluble JAM-A.Fc protein
TBS	tris buffered saline
TEMED	N,N,N′,N′-tetramethylethylenediamine
TJ	tight junction
TNF-α	tumor necrosis factor-α
VCAM-1	vascular cell adhesion molecule-1; CD106
VLA-4	very late antigen-4; α4β1; CD49d/CD29
wt	wild-type

I Introduction

I.1 Atherosclerosis

Atherosclerosis is the principal contributor to cardiovascular disease, which recently is the major cause of death and illness in developed countries (Libby 2002). Atherosclerosis is a process, which begins with the formation of so-called “fatty streaks” beneath the endothelium of the artery wall, followed by the development of atherosclerotic lesions, which are composed of layers of lipid-laden macrophages and smooth muscle cells (SMC). As the disease progresses, these lesions develop into more complex fibrous plaques (atheromas) (Ross 1993). Eventually, by unknown mechanisms, these plaques may become unstable leading to rupture and subsequent thrombus formation rather than luminal narrowing results in clinical events such as myocardial infarction and stroke (Fig. I.1) (Hansson 2005).

Until the 1970s, atherosclerosis was linked with hypercholesterolemia without further knowledge of the mechanisms of plaque formation. Over the past decades, it has become evident that the retention of low-density-lipoproteins (LDL) and their oxidation (oxLDL) initiate an inflammatory response of the endothelium (Skalen *et al.* 2002; Leitinger 2003). After initiation of inflammation, endothelial cells (EC) and SMC as well as T lymphocytes and intimal macrophages secrete chemokines, which enhance the recruitment and transmigration of immune cells through the endothelium (Weber *et al.* 2004). Thus, atherosclerotic plaques contain a large quantity of activated immune cells producing effector molecules like radicals, inflammatory cytokines and proteases that can destabilize the lesions and initiate thrombus formation (Jonasson *et al.* 1986; Stemme *et al.* 1992; Hansson 2005).

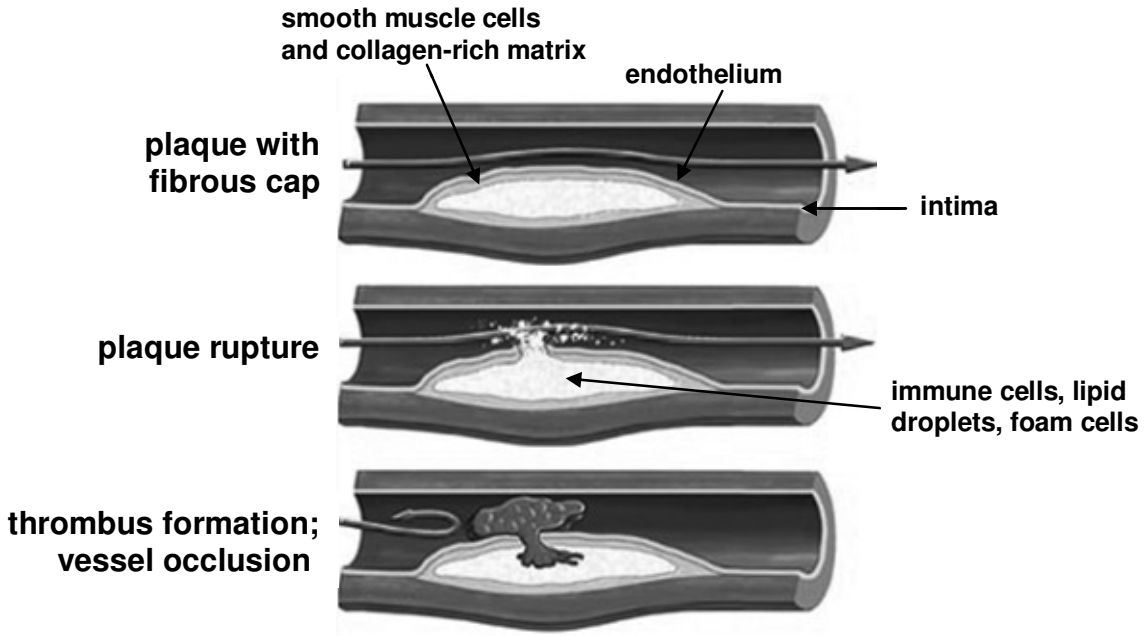

Fig.I.1: Plaque rupture. Atherosclerotic lesions form beneath the endothelium of the innermost layer of the vessel wall, the intima. They consist of inflammatory and immune cells, connective-tissue elements, lipids, and debris. The center of an atheroma is composed of lipid droplets, immune and foam cells. Activated immune cells secrete proteases, coagulation factors and radicals, which lead to plaque rupture. The leaking thrombogenic material leads to blood clotting and occlusion of the artery (Hansson 2005) (image: **http://www.nucleusinc.com).**

I.1.1 Therapeutic strategies

Besides bypassing the diseased artery, a common treatment of advanced atherosclerosis is the enlargement of the vessel lumen by balloon angioplasty with subsequent insertion of a metal tube, the so-called stent, which helps keeping the vessel from collapsing. The vessel injury caused by angioplasty and the use of bare-metal-stents, however, bear a high risk of re-narrowing of the vessel due to inflammatory processes, also called restenosis/in-stent-restenosis. The use of drug-releasing stents provided very promising results in preventing restenosis in randomized clinical trials, mostly performed with the antiproliferative agents sirolimus (Rapamycin) and paclitaxel (Muller *et al.* 2002).

For high-risk patients, such as diabetics, different drug therapies are employed to reduce various risk factors. Statins (HMG-CoA reductase inhibitors) are used to lower the blood cholesterol level. The pain killer acetylsalicylic acid (Aspirin®), which also inhibits platelet aggregation, is applied in low doses to prevent thrombosis. Furthermore, two different drug types are implemented to reduce the heart rate and blood pressure. Angiotensin converting enzyme (ACE) inhibitors prevent the activation of the

vasoconstrictive peptide angiotensin II, and β-blockers inhibit the stimulating effects of the stress hormones adrenalin and noradrenalin by antagonizing their receptors.

The establishment of aspirin, β-blockers, ACE-inhibitors, and lipid-lowering therapies have lowered the risk of future vascular events by about a quarter each in high-risk patients (Yusuf 2002). However, random clinical trials and observative data are very contradictory. Though treatments after coronary events improved and reduced mortality by about 50% in western developed countries in the past 20 years, cardiovascular disease remains the single leading cause of death because of unsatisfactory preventive therapies and an unhealthy lifestyle of patients. Therefore, a great effort is made in order to find new therapeutic approaches, e.g. by targeting inflammatory mediators like cytokines or chemokines.

I.2 Chemokines in atherosclerosis

Chemokines are a superfamily of small (most being 8-10 kDa) chemotactic cytokines that function in leukocyte trafficking and activation (Reape and Groot 1999). Approximately 40 different chemokines have been identified so far, which interact with about 17 different chemokine receptors expressed on different subsets of leukocytes. Chemokines can be classified according to the arrangement of the first two of four conserved cysteines at the N-terminus. The largest group is formed by the CC chemokines, where the cysteines are adjacent to each other, followed by CXC chemokines with the first cysteines separated by a single amino acid residue. Those chemokines are further classified according to the absence or presence of an N-terminal Glu-Leu-Arg sequence, the ELR motif. CXC chemokines containing the ELR motif, e.g. Growth related oncogene-α (Gro-α/CXCL1) and Interleukin-8 (IL-8/CXCL8) were found to be angiogenic factors in contrast to the ELR-lacking CXC chemokines like PF4, which mediates angiostasis (Maione *et al.* 1990; Strieter *et al.* 1995).

Fractalkine is the only member of the CX3C group with a 3 amino acid spacing between the N-terminal cysteines, and there has been described a XC group, which consists of two chemokines, lymphotactin-α and -β, possessing only two of the four cysteines (Moser and Willimann 2004). Another family termed chemokine-like-function (CLF) cytokines has recently been proposed for small molecular mediators like defensins and macrophage migration inhibitory factor (MIF) that cannot be assigned to the known chemokine families but share structural and functional features and can signal through

chemokine receptors, e.g. CCR6 (Yang *et al.* 1999; Degryse and de Virgilio 2003). The chemokines involved in atherosclerosis are listed in Table I.1.

Chemokine	Target	Receptor
CC Chemokine		
I-309/CCL1	MM	CCR8
MCP-1/CCL2	MM, TC, EC	CCR2
MIP-1α/CCL3	MM, TC	CCR1/5
MIP-1β/CCL4	MM, aTC, SMC	CCR5
RANTES/CCL5	MM, aTC, DC	CCR1/3/5
Eotaxin/CCL11	B, DC	CCR3
MCP-4/CCL13	MM, aTC	CCR2/3
TARC/CCL17	Th2, DC	CCR4
PARC/CCL18	rTC	Unknown
ELC/CCL19	aTC	CCR7
MDC/CCL22	aTC	CCR7
CXC Chemokine		
GRO/KC/CXCL1	MM, EC, SMC	CXCR1/2
IL-8/CXCL8	MM, EC, SMC	CXCR1/2
Mig/CXCL9	aTC	CXCR3
IP10/CXCL10	aTC?	CXCR3
I-TAC/CXCL11	MM, aTC, SMC	CXCR3
SDF-1α/CXCL12	TC, vascular progenitors	CXCR4
SR-PSOX/CXCL16	TC, NK	CXCR6
CX3C Chemokine		
Fractalkine/CX3CL1	MM, aTC	CX3CR1
CLF		
MIF	MM, TC	Unknown

Tab. I.1: Chemokines in atherosclerosis.
Cells affected by chemokines involved in atherosclerosis are monocytes/macrophages (MM), active or resident T cells or T cells in general (aTC, rTC and TC), smooth muscle cells (SMC), dendritic cells (DC), endothelial cells (EC), vascular progenitors and T helper cells (Th2) (adapted from Weber *et al.*, 2004).

Chemokines evoke cell responses by interacting with specific chemokine receptors, which are denominated according to their ligands (CXC, CC, XC, CX3C), plus R for receptor (Tab.I.1). These receptors are seven transmembrane-spanning receptors that signal through coupled heterotrimeric G proteins. Upon binding to their receptors chemokines induce a signal transduction cascade that leads to activation of protein kinases and an increase in intracellular Ca^{2+} (Horuk 2001). Eventually, cell activation leads to actin re-arrangement, shape change and cell movement.

Chemokines trigger the atherogenic recruitment of mononuclear cells (Charo and Taubman 2004; Weber et al. 2004). In this regard, chemokines immobilized on the endothelial surface rather than their soluble counterparts activate integrins such as the β_2 integrin lymphocyte function-associated antigen-1 (LFA-1) and very late antigen-4 (VLA-4), which mediate the arrest of rolling leukocytes on the arterial wall and their transmigration into the tissue to the site of inflammation (Fig.I.2) (Weber *et al.* 1999; Ley 2003; Laudanna and Alon 2006). In the context of atherosclerosis, this has been best established for the platelet-derived CC chemokine Regulated upon Activation, Normal T cell Expressed and Secreted (RANTES/CCL5), and for the CXC chemokines and CXCR2 ligands Gro-α and IL-8 (Charo and Taubman 2004).

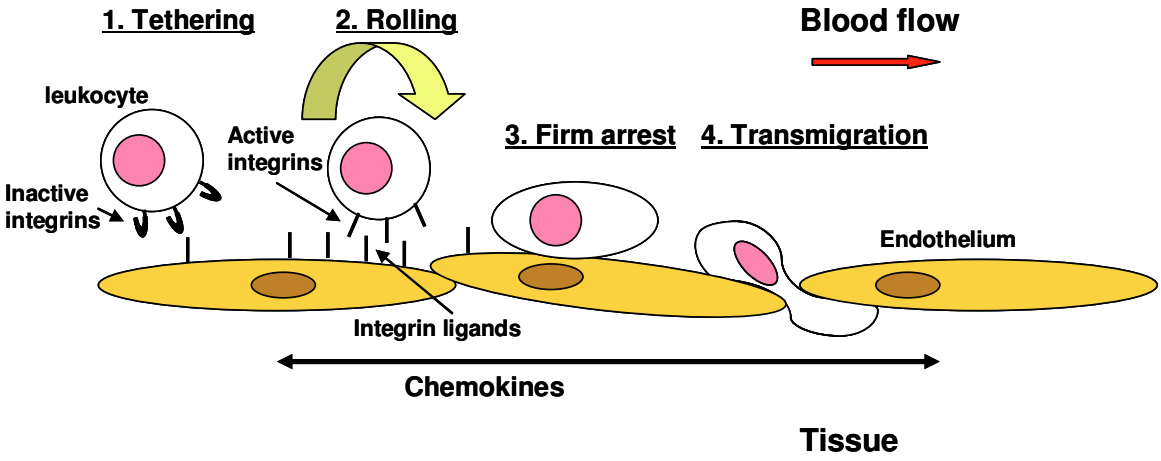

Fig.I.2: Leukocyte extravasation from the blood flow into inflamed tissue. A multistep cascade leads to the activation of integrins and their ligands by chemokines. The steps involved in this process are tethering, rolling, integrin activation, firm adhesion and transmigration across the endothelial layer modified from Sackstein (2005).

I.2.1 The chemokine RANTES in atherosclerosis

In the 1980's, RANTES has been identified as a CC-class chemokine expressed by T lymphocytes, which recruits T cells, eosinophils and macrophages to sites of inflammation (Schall *et al.* 1988; Schall *et al.* 1990). Further studies demonstrated an upregulation of RANTES in activated vascular SMC (VSMC) as well as its expression in several cell types involved in accelerated atherosclerosis and in neointimal lesions after vascular injury (Pattison *et al.* 1996; Jordan *et al.* 1997; von Hundelshausen *et al.* 2001). Here, it became evident that one of the major effectors of atherogenesis is the platelet-derived RANTES, which is deposited on the inflamed endothelium where it may trigger subsequent monocyte

arrest.

The known RANTES receptors are CCR1, CCR3 and CCR5. CCR1 and CCR3 are involved in RANTES-triggered eosinophil activation, though CCR3 seems to play a minor role in RANTES actions (Elsner *et al.* 1997). The effects of RANTES on leukocyte arrest and transmigration are mediated by specialized roles of CCR1 and CCR5, respectively (Weber *et al.* 2001), and a mouse model of atherosclerosis recently revealed that CCR5 but not CCR1 is the crucial receptor promoting atherogenesis (Braunersreuther *et al.* 2007), identifying CCR5 as a promising therapeutic target. Blocking the receptor with an antagonist called Met-RANTES (recombinant RANTES which retains its N-terminal methionine) significantly reduced injury-induced neointima hyperplasia and atherosclerosis progression in hypercholesterolemic mice (Veillard *et al.* 2004). Another therapeutic approach could be made by interfering directly with the chemokine production.

RANTES expression

Through the identification of a large number of consensus elements for T cell specific and ubiquitous DNA binding proteins in the RANTES promoter (Nelson *et al.* 1993) (Fig. I.3), some of the mechanisms regulating the expression of RANTES have been determined. For instance, promoter studies revealed the constitutive and interferon (IFN)-γ- or tumor necrosis factor (TNF)-α-inducible transcription factors IFN-regulatory factor 1 (IRF-1) and nuclear factor-κB (NF-κB or p50/p65), which synergistically activated the RANTES promoter (Genin *et al.* 2000; Lee *et al.* 2000). In monocytes and the monocytic cell line MonoMac6, a lipopolysaccharide (LPS)-inducible promoter module for cAMP response element binding protein/activator protein-1 (CREB/AP-1) has been identified (Boehlk *et al.* 2000). Additionally, RANTES expression in monocytes has been shown to be mediated by the constitutive binding of both CCAAT enhancer binding proteins (C/EPBs) (positions -125/-99) and Sp1 at position -73 and the binding of NF-κB following LPS stimulation (position -34) (Fessele *et al.* 2001). Another study using airway SMC revealed that AP-1 and nucleofactor of activated T cells (NF-AT) lead to TNF-α-induced promoter activation, whereas here NF-κB binding was not necessary (Ammit *et al.* 2002). Apart from IRF-1, NF-κB, AP-1 and other transcription factors, DNAse I footprinting also showed that the RANTES promoter contains possible binding sites for the Y-box binding protein-1 (YB-1) at positions -209 and -187 implying a regulatory role for YB-1 in RANTES expression (Nelson et al. 1993).

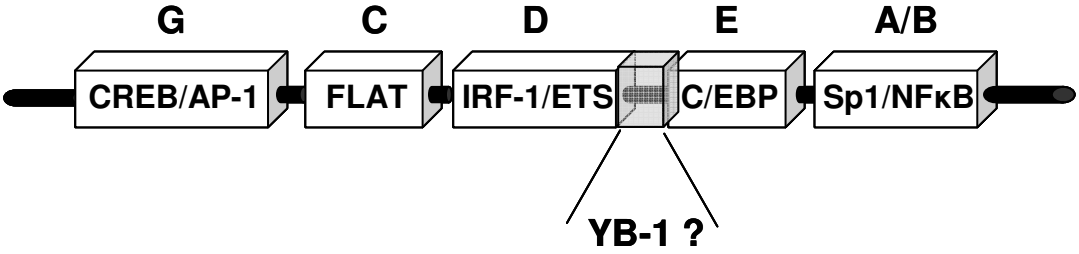

Fig. I.3: RANTES promoter modules. The RANTES promoter features 5 different regulation modules (A-G) for several transcription factors. Additionally, the promoter contains a possible binding region for YB-1 at position -187 to -209; FLAT = RANTES C site binding factor of late-activated T cells; Adapted from Fessele et al., 2002.

Transcription factor YB-1

The cold shock protein YB-1, also termed p50 and DNA binding protein B (dbpB), belongs to the evolutionary ancient and highly conserved group of Y-box binding proteins, which control the expression of a large number of gene products. In the cytoplasm it is cleaved by the 20s Proteasome and translocates to the nucleus (Sorokin *et al.* 2005), where it preferentially binds to a DNA sequence containing the so-called Y-box or inverted CCAAT-box (CTGATTGGC/TC/TAA) (Ting *et al.* 1994). This sequence is present in a variety of eukaryotic genes, such as those coding for the major histocompatibility complex (MHC) class II genes. By binding to this regulatory sequence, YB-1 can act either as a *trans*-repressor or -activator, and the inhibition or activation of a gene can be cell type-specific as shown for the matrix metalloprotease (MMP)-2 gene (Mertens *et al.* 1997). YB-1 not only controls gene expression on the DNA transcription level, but also on the translational level by splicing RNA precursors e.g. by interacting with the splicing factor SRp30c or binding to close proximity of the 5' cap-structure of the mRNA, thereby silencing and stabilizing the mRNA (Raffetseder *et al.* 2003; Evdokimova *et al.* 2006). Furthermore, YB-1 functions are likely beyond the regulation of gene expression, as it has been shown to relocate to the nucleus and bind to DNA repair proteins (Gaudreault *et al.* 2004).

An increased expression of YB-1 in certain inflammatory diseases has been described, e.g. by activated eosinophils in allergic asthma (Capowski *et al.* 2001), where YB-1 prolonged their survival and thus exacerbated disease, or by mesangial cells in

mesangioproliferative disease (van Roeyen *et al.* 2005). YB-1 might also play a role in atherogenesis, because the proximal promoter region of the RANTES gene displays two possible binding sites for YB-1, thus suggesting a regulatory role for YB-1 in the expression of the atherosclerosis-promoting chemokine RANTES.

I.2.2 The chemokine-like function chemokine Macrophage Migration Inhibitory Factor (MIF)

40 years ago, the cytokine MIF was first identified in context with delayed-type hypersensitivity as a T cell-derived inhibitor of random macrophage migration (Bloom and Bennett 1966; David 1966). It was later found to be also produced by other cells such as macrophages and monocytes and pituitary cells, where it is released in a "hormone-like" fashion (Bernhagen *et al.* 1993; Calandra *et al.* 1994). Nowadays, MIF is known to be an important mediator of host immune response promoting innate immunity by Toll-like receptor 4 upregulation and antagonizing the anti-inflammatory actions of glucocorticoids (Calandra and Bucala 1995; Roger *et al.* 2001). Moreover, in contradiction to its name, MIF recruits leukocytes to sites of inflammation in a chemokine-like manner as e.g. observed in a rat model of immunologically induced glomerulonephritis (Lan *et al.* 1997). Since the 1990's several immune-mediated diseases have been associated with MIF such as rheumatoid arthritis (RA) (Leech *et al.* 1999) and systemic lupus erythematosus (Hoi *et al.* 2006). An association of a MIF promoter CATT tetranucleotide polymorphism with the severity of these diseases has been documented (Baugh *et al.* 2002; Sanchez *et al.* 2006).

MIF and atherosclerosis

MIF's role in atherosclerosis progression has been established more recently. Schober *et al*. observed a significant reduction of macrophages and macrophage-derived foam cells in wire injury-induced neointimal lesions of hyperlipidemic mice after treatment with a MIF-blocking monoclonal antibody (mAb). Conversely, the content of SMC and collagen type I was increased indicating a more stable plaque phenotype. As an underlying mechanism, the authors found that incubation of aortic EC with recombinant MIF for 2 h can trigger monocyte arrest under flow conditions, while endothelial MIF mediates arrest after exposure to oxidized low-density-lipoprotein (oxLDL) (Schober *et al.* 2004). Accordingly, the retardation of diet-induced atherogenesis in LDL-receptor $(LDLR)^{-/-}$ mice by genetic

deletion of MIF was manifest by a decrease in intimal thickening, lipid deposition and protease expression (Pan *et al.* 2004). In a mouse model of spontaneous atherosclerosis, blockade of MIF also led to the reduction of macrophages in the aortic wall as well as to the inhibiton of several inflammatory mediators as ICAM-1, MMP-2 and TNF (Burger-Kentischer *et al.* 2006). These findings support a model, according to which MIF may directly affect endothelial-monocyte adhesion by a mode of action resembling that of immobilized chemokines in atherogenesis.

MIF structure and functional features

Human MIF consists of 115 amino acids (aa), has a molecular weight of 12.34 kDa and shows a 90% homology to murine MIF. The X-ray crystal structure revealed a MIF trimer of identical subunits (Sun *et al.* 1996), which form a circular protein with an interior hydrophobic solvent accessible channel with unknown function. Each monomer contains two antiparallel α-helices that pack against a four-stranded β-sheet (Fig. I.4, A). Reports about the oligomerization state of MIF have been contradictory and have varied with the techniques applied, and a study using gel filtration and cross-linking experiments proved that MIF forms monomers, dimers, and trimers in physiological solution, whereas the trimer is only a minor species (Mischke *et al.* 1998).

Apart from its unique structure that is not in line with neither structural group of chemokines, the MIF monomer bears a striking resemblance to the IL-8 dimer (Fig. I.3). Also, MIF displays a pseudo-ELR motif formed by an arginine (R11) and the aspartic acid residue at position 44 (D44) (Fig. I.4).

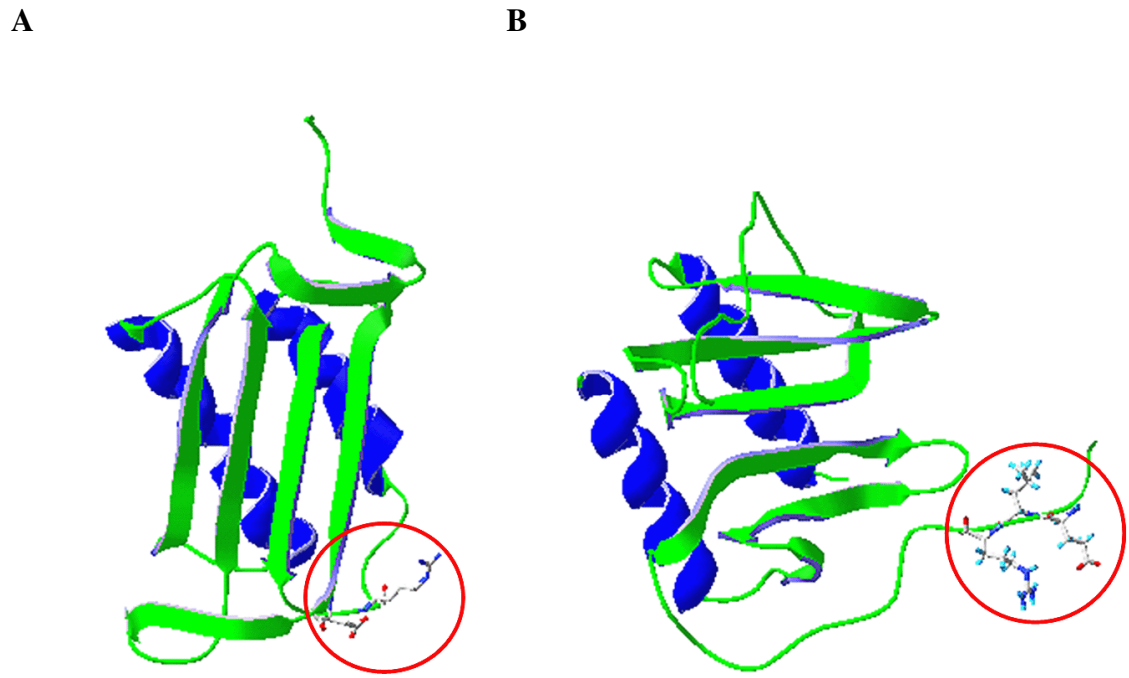

Fig. I.4: Architectural homology of the MIF monomer and IL-8 dimer. (A) MIF monomer with highlighted pseudo-ELR motif (red circle); (B) IL-8 dimer with side chains of one of the two ELR motifs (red circle).

Besides its similarity to IL-8, structural homologies of the MIF monomer and trimer with microbial enzymes have been disclosed (Chook *et al.* 1994; Subramanya *et al.* 1996), and in compliance with that, three enzymatic activities have been reported for MIF. First, a glutathione S-transferase activity and a tautomerase activity have been documented (Blocki *et al.* 1993; Rosengren *et al.* 1996), and it has been shown that MIF exhibits a thiol protein oxidoreductase activity and that this activity is dependent on the presence of the catalytic center that is formed by cysteine residues 57 and 60, the so-called CALC motif (Cys-Ala-Leu-Cys) (Kleemann *et al.* 1998). Mutation of the CALC motif did not only lead to the loss of the oxidoreductase activity, but also to the immunogenic function of MIF, whereas the inhibition of MIF's tautomerase activity by deleting or substituting the N-terminal proline did not interfere with its immunogenic function (Bendrat *et al.* 1997; Kleemann *et al.* 2000).

MIF interaction partners

MIF uptake into various immune and non-immune cell types by non-receptor mediated endocytosis and the identification of three intracellular proteins that directly interact with

MIF, supported the view that MIF fulfills intracellular functions:

1. The first intracellular MIF-binding protein, identified by yeast-two-hybrid screening, was the c-Jun activation domain binding protein-1 (Jab1), which is a component of the COP9 signalosome (Kleemann *et al.* 2000). By binding to Jab1, MIF prevents the activation of AP-1 regulated gene transcription and the degradation of the cell cycle inhibitor $p27^{Kip1}$. Thus, MIF blocks Jab1-mediated rescue from growth arrest (Fig.I.4). The authors suggested that MIF's counter-regulatory actions to glucocorticoids were mediated by blocking Jab1-binding to steroid hormone receptors. For the androgen receptor this theory was disproved; MIF did not modulate Jab1-mediated co-activation of the androgen receptor (Berndt *et al.* 2007).

Conversely, Jab1 is also associated with p53 degradation (Oh *et al.* 2006), and MIF has been shown to inhibit p53-mediated apoptosis and cell growth, thus linking inflammation and tumorigenesis (Hudson *et al.* 1999; Fingerle-Rowson *et al.* 2003). MIF-mediated apoptosis inhibition was associated with a reduced p53 level in the cell and dependent on cyclooxygenase 2 (Cox-2) (Mitchell *et al.* 2002) (Fig.I.4). These data point towards a possible cooperation between MIF and Jab1 in p53 degradation by inducing AP-1-mediated Cox-2 expression.

2. Jung *et al.* (2001) discovered that the thiol-specific antioxidant protein PAG binds to MIF under reducing conditions and that PAG dose-dependently inhibits MIF D-dopachrome tautomerase activity. Likewise, MIF inhibits the antioxidant activity of PAG.

3. As revealed by yeast-two-hybrid screening, BNIPL (Bcl-2/adenovirus E1B 19 kDa interacting protein 2-like), an apoptosis-associated protein interacts with MIF (Shen *et al.* 2003). The authors suggest that BNIPL may be involved in regulation of MIF-mediated cell proliferation.

4. The only known cell surface receptor for MIF is CD74, the invariant chain of major histocompatibility complex (MHC) II that is expressed in small quantities in a large number of cells (Leng *et al.* 2003). CD74 can mediate sustained activation of extracellular-regulated and mitogen-activated protein kinases (ERK-MAPK) and has been proposed to associate into a signaling complex with MIF, CD44 and Src-family tyrosine kinases (Shi *et*

al. 2006) (Fig.I.4). It has recently been demonstrated that protein kinase PI3K/Akt-mediated apoptosis was dependent on MIF-CD74-Src signaling triggered by exogenous MIF or endogenous MIF secretion, which was attenuated by Jab1 (Lue et al. 2007). Furthermore MIF's ability to inhibit p53-dependent apoptosis was dependent on CD74 and CD44 (Shi et al. 2006). Whether CD74 mediates MIF internalization and/or interaction with Jab1 still remains to be elucidated.

As not all cells targeted by MIF, i.e. neutrophils or fibroblasts express surface CD74, it seems likely that another receptor confers MIF's pro-inflammatory functions. Because the existing data on MIF's molecular mechanism do not explain how MIF exhibits its chemokine-like functions, and taking into account that the MIF monomer resembles the IL-8 dimer, it stands to reason that one or more chemokine receptors may be involved in MIF action (Fig.I.5).

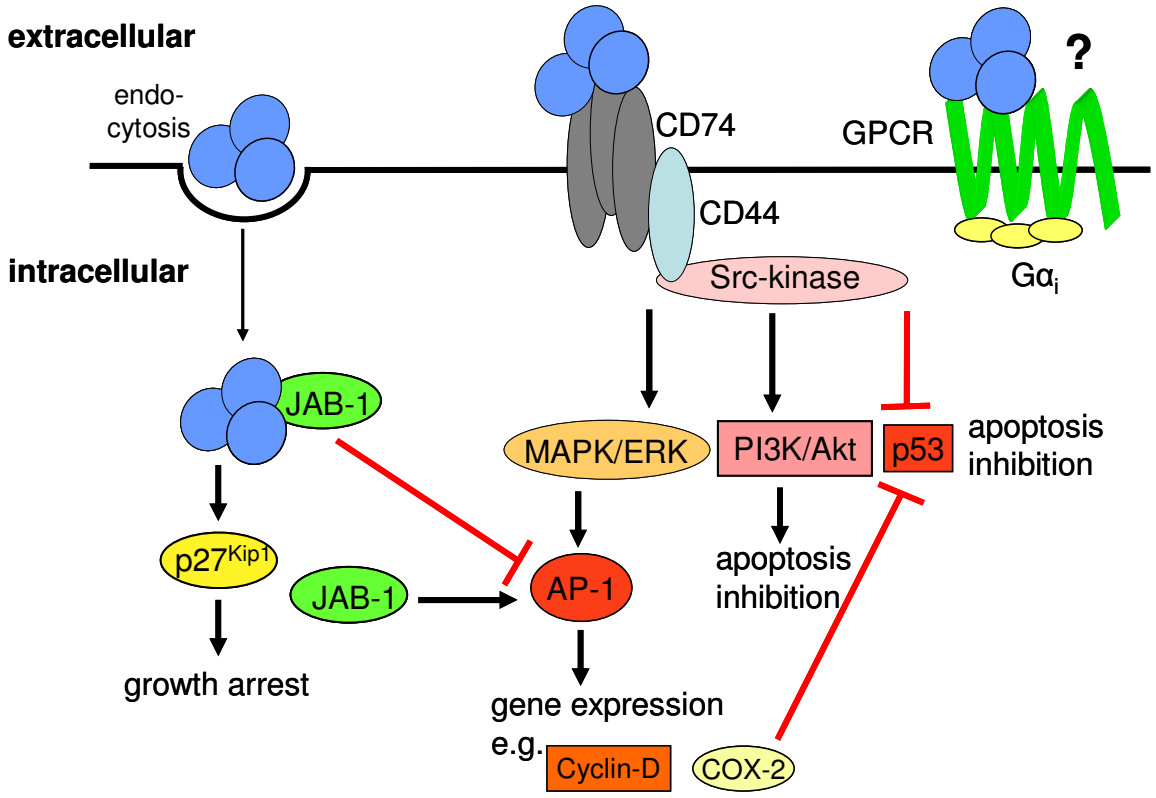

Fig.I.5: MIF's mechanism of action. MIF (blue trimer) is internalized and interacts with Jab1, thereby stabilizing p27kip1 and inhibiting AP-1-induced gene expression. MIF also binds to CD74, leading to a sustained activation of MAPK/ERKs through CD44 and Src-kinases, which promote gene expression. MIF-mediated apoptosis inhibition through PI3K/Akt depends on CD74 as well as apoptosis inhibition by p53 degradation. It remains to be elucidated, if Jab1 is involved in MIF-mediated p53 degradation. MIF may activate cells in chemokine-characteristic way through binding to a GPCR (modified from Morand *et al.*, 2006)

I.3 Aim of this study

This work was aimed at clarifying molecular mechanisms of two different mediators involved in atherogenesis. To get a better understanding of how chemokines and CLF chemokines trigger atherosclerosis and how their exacerbating effects on the disease may be diminished, two different approaches were pursued:

For one, the aim was to gain further insights in the expression regulation of a prominent chemokine, i. e. the CC chemokine RANTES. As the RANTES gene features two possible binding sites for the transcription factor YB-1 in the proximal RANTES promoter region, it was investigated if YB-1 regulates RANTES expression in vascular SMC and macrophages. Furthermore, the inflammatory effects of YB-1-regulated RANTES were analyzed in terms of leukocyte recruitment *in vitro* and neointima formation in a mouse model of restenosis.

The second approach intended to clarify the down-stream effects of a newly discovered CLF chemokine, i.e. the mediator protein MIF. In order to obtain a detailed overview of MIF's chemokine-like functions, it was tested whether MIF is able to provoke cell responses typical for a certain subclass of chemokines, the arrest chemokines, such as leukocyte arrest, integrin activation and calcium mobilization. Furthermore, it was tested if these chemokine properties are conferred by a chemokine receptor, and if MIF/GPCR interactions were required for inflammatory cell recruitment in atherogenesis.

Table II: Flow chart. Brief summary of the questions addressed in this study and performed experiments.

Identification of a protein involved in RANTES regulation	Identification of a MIF receptor and novel chemokine functions
Does YB-1 regulate RANTES expression in SMC and macrophages? DNA binding studies, promoter reporter studies with SMC and a macrophage cell line, real time-PCR, ELISA	**Does MIF trigger leukocyte arrest through GPCRs and CD74?** parallel plate flow chamber adhesion assays with blocking antibodies, real time-PCR, ELISA
Does YB-1-regulated RANTES mediated monocyte recruitment? parallel plate flow chamber adhesion assays	**Does MIF directly provoke rapid cell responses in a chemokine-like fashion?** integrin activation assay, calcium mobilization
Is YB-1 involved in atherosclerosis progression? mouse model of restenosis with lentiviral knock-down of YB-1, evaluation of plaque area and macrophage content, RANTES expression in plaque area	**Does MIF bind to a GPCR and is there an interaction of GPCRs and CD74?** FACS assay with fluorescein-MIF, coimmunoprecipitations
	What impact does a MIF/GPCR interaction have on inflammatory cell recruitment and atherosclerosis? *ex vivo* and *in vivo* perfusion of murine carotid arteries, peritonitis model, plaque regression experiments

II Material and Methods

Protocols were adapted from standard protocols (Sambrook and Russell, 2001) if not stated otherwise. All solutions were prepared with double distillated water (Heraeus Destamat, Heraeus, Germany) or Millipore water (Milli-Q Plus ultrapure purification, Millipore, MA). Reagents were from Fluka (Buchs, Switzerland), Sigma (Deisenhofen, Germany), or Roth (Karlsruhe, Germany) if not stated otherwise. All animal studies were approved by local authorities and complied with German animal protection law.

II.1 General equipment

autoclave	Systec 2540EL (Systec, Wettenberg, Germany)
balance	Analytical Plus, (Ohaus, Pine Brook, NJ, USA)
centrifuges	Eppendorf 5417C (Eppendorf, Hamburg, Germany), Heraeus
electroporators	Gene-pulser II (Bio-Rad, Hercules, CA, USA), Nucleofector
flow cytometers	FACSCalibur, FACSAria (BD Biosciences, San Jose, CA, USA)
fluorescence	plate reader SpectraFluor Plus (Tecan, Crailsheim, Germany)
gel electrophoresis	Mini-sub cell GT (Bio-Rad, Hercules, CA, USA)
laminar flow hood	Herasafe (Heraeus, Osterode, Germany)
microscopes	Olympus IX71 and BX51 (Olympus Optical,
PCR thermocyclers	MyCycler (Bio-Rad, Hercules, CA), DNA Engine Opticon (MJ
pH-meter	InoLab level 1 (WTW, Weilheim, Germany)
spectrophotometer	GeneQuant (Amersham Biosciences, Uppsala, Sweden)

II.2 General solutions

HH-buffer	Hank's buffered salt solution (HBSS), 0.5% (w/v) BSA, 10 mM HEPES, pH 7.4
MOPS-buffer	1% (w/v) human serum albumin, 145 mM NaCl, 4.7 mM KCl, 2mM $CaCl_2$, 1.2 mM $MgSO_4$, 5 mM glucose, 2 mM sodium pyruvate, 2 mM MOPS, and 1.2 mM NaH_2PO_4, pH 7.5
PBS	37 mM NaCl, 2.7 mM KCl, 1.5 mM KH_2PO_4, 8 mM Na_2HPO_4, pH 7.4 (PAA laboratories, Linz, Austria)
TBS	137 mM NaCl, 2.7 mM KCl, 25 mM Tris-HCl, pH 7.4

II.3 Mice

MIF-deficient mice (*Mif*$^{-/-}$) were crossbred with low-density lipoprotein receptor (LDLR)-deficient mice (*Ldlr*$^{-/-}$; Charles River Laboratories, Belgium) to establish *Mif*$^{+/-}$/*Ldlr*$^{-/-}$ mice (all C57BL/6). *Mif*$^{+/-}$*Ldlr*$^{-/-}$ animals of the F9 generation were used to generate *Mif*$^{-/-}$/*Ldlr*$^{-/-}$ mice and *Ldlr*$^{-/-}$ littermates. Transgenic mice were fertile and showed no phenotypical abnormalities.

Wild-type C57BL/6, Apolipoprotein E deficient (*Apoe*$^{-/-}$) and *Apoe*$^{-/-}$/Ccr5$^{-/-}$ mice were obtained from the local animal breeding facility (University Hospital, Aachen), and *Cxcr2*$^{-/-}$ mice on a BALB/c background and wild-type BALB/c mice were from the Jackson Laboratory (Bar Harbour, ME, USA). All studies with mice were approved by local authorities and complied with German animal protection law.

II.4 Chemokines, antagonists, and recombinant proteins

Biologically active recombinant human MIF, and labeled MIF with biotin or fluorescein, was from the Departmend of Biochemistry, University Hospital (UK) Aachen, Germany. Recombinant YB-1 was prepared from a pRSET vector (Invitrogen, Karlsruhe, Germany) containing an insert encoding for a hexahistidine T7 epitope-YB-1 fusion protein as described (Mertens *et al.* 1998).

The following chemokines were purchased from Peprotech (Rocky Hill, NJ, USA):

IL-8	interleukin 8/CXCL8
Gro-α	growth related oncogene-α/CXCL1
NAP-2	neutrophil activating peptide 2/CXCL7
RANTES	regulated upon activation normal T cell expressed and secreted/CCL5
IP-10	IFN-inducible protein 10/CXCL10
SDF-1α	stromal cell-derived factor 1α/ CXCL12
IFN-γ	interferon-γ
TNF-α	tumor necrosis factor-α

Recombinant human VCAM-1.Fc chimera was purchased from R&D Systems (Minneapolis, MN, USA). The small-molecule CXCR4 antagonist AMD3465 was provided by Anormed Inc. (Vancouver, Canada, USA) and the RANTES receptor antagonist Met-RANTES was kindly provided by Amanda Proudfoot (Serono International S.A., Geneva, Switzerland). Pertussis toxin (PTX) was obtained form Merck (Darmstadt, Germany).

II.5 Antibodies

II.5.1 Primary Antibodies

RII115	mouse-αhuman CXCR2 monoclonal antibody (mAb) (kind gift of A. Ludwig and E. Brandt, Department of Immunology and Cell Biology, Forschungszentrum Borstel)
327C	mouse-αhuman mAb, which binds to an activation epitope corresponding to the extended high affinity conformation of $\alpha_L\beta_2$ (Shamri et al. 2005) (provided by D. Staunton, Department of Biomedical Engineering, Genome and Biomedical Sciences Facility, University of California at Davis)
Ka565	rabbit-αhuman MIF pAb (Department of Biochemistry, University Hospital Aachen (UK Aachen, Germany)
α-SMA	mouse-αhuman α-actin mAb (clone 1A4, Dako, Glostrup, Denmark)
Mac2	rat-αmouse mAb (clone M3/38, Cedarlane Laboratories, Ontario, Canada)
αRANTES	goat-αhuman mAb (clone C19, Santa-Cruz Biotechnology, CA, USA)
αYB-1	pAb raised against an oligopeptide within the N-terminal domain of YB-1 (P.R. Mertens, UK Aachen)
MOMA-2	rat-αmouse mAb, macrophage marker (clone MCA519, AbD Serotec, Düsseldorf, Germany)
CD3	mouse-αhuman mAb, T-cell marker (clone PC3/188A, Santa-Cruz Biotechnology)

II.5.2 Directly conjugated antibodies

CXCR2-FITC	mouse-αhuman mAb, FITC-conjugated (clone 6C6, BD Pharmingen, Heidelberg, Germany)
CD115-PE	rat-αmouse mAb, PE conjugated, monocyte marker (clone AFS98, eBiosciences, San Diego, CA, USA)
Gr-1-perCP	rat-αmouse mAb, perCP-conjugated, mature granulocyte marker (clone RB6-8C5, BD Pharmingen)
F4/80-Biot	rat-αmouse mAb, biotinylated, mature macrophage marker (clone A3-1, Serotec)

II.5.3 Blocking antibodies

NIHIIID9	mouse-αmouse MIF mAb raised against purified recombinant mouse MIF (Lan et al. 1997)
αGro-α	mouse-αhuman mAb, clone 20326 (R & D Systems, Minneapolis, MN, USA)
αKC	rat-αmouse mAb, clone 124014 (R&D Systems)
αIL-8	mouse-αhuman mAb, clone 6217 (R & D Systems)
αSDF-1α	mouse-αhuman/mouse mAb, clone 79014 (R & D Systems)
αCXCR1	mouse-αhuman mAb, clone 42705 (R & D Systems)
αCXCR2	mouse-αhuman mAb, clone 48311 (R & D Systems)
αCXCR4	mouse-αhuman mAb, clone 44708 (R & D Systems)
αCD74	mouse-αhuman (clone M-B741, BD Pharmingen)
TS1/18	mouse-anti human mAb, specific for the β2 subunit of human αLβ2, purified from hybridoma cell supernatants by protein G chromatography (performed by Line Fraemohs, UK Aachen)
HP2/1	mouse-αhuman mAb, specific for the α_4 subunit of human VLA-4 (Immunotech, Marseille, France)

II.5.4 Isotype controls

mouse IgG_1/IgG_{2b}/IgG_{2a}	(all from R & D Systems)
rat IgG1/ IgG2b/ IgG2a	(all from Serotec)
rabbit IgG	Department of Biochemistry, UK Aachen

II.5.5 Secondary antibodies

goat-αmouse-IgG	fluorescein isothiocyannate (FITC)-conjugated (Sigma)
donkey-αmouse-IgG	FITC-conjugated (Santa-Cruz Biotechnology)
goat-αrabbit-IgG	FITC-conjugated (Santa-Cruz Biotechnology)
donkey-αrat-IgG	FITC-conjugated (Santa-Cruz Biotechnology)
donkey-αgoat-IgG	cyanine 3 (Cy3)-conjugated (Santa-Cruz Biotechnology)
donkey-αmouse-IgG	Cy3-conjugated (Santa-Cruz Biotechnology)
goat-αmouse-IgG	horseradish peroxidase (HRP)-conjugated (Serotec)

II.6 Mammalian cell culture

Cell culture with mammalian cells was performed under sterile conditions in a laminar flowhood. Cells were maintained in a CO_2-incubator at 37°C and a humidified 5% CO_2 atmosphere. Cells were cultured in growth medium supplemented with 10-20% (v/v) fetal calf serum (FCS), 4 mM L-glutamine and 50 µg/ml gentamicin or penicillin (100 U/mL)/streptomycin (100 µg/mL) (PAA, Pasching, Austria) to avoid contamination with bacteria. Cells used in this study and their optimal growth media are listed in (Tab.II.1). FCS was incubated at 56°C for 30 min to inactivate the complement system and stored at -20°C until use. All media and solutions used for cell culture were from Gibco if not stated otherwise and purchased sterile or sterilized through a 0.2 µm filter. All cell lines were regularly tested to be mycoplasma free by the VenorGeM Mycoplasma detection kit™ (Minerva Biolabs, Berlin, Germany).

II.6.1 Culturing of adherent cell monolayers

Adherent cell lines were grown until confluence and then passaged by trypsinization. The monolayer was first washed with phosphate buffered saline (PBS) and then incubated 1-2 min with 0.25% (v/v) trypsin/0.04% EDTA at 37°C. After detachment of the monolayer, trypsin was inactivated by the addition of medium containing FCS. For subculturing, cells were harvested by centrifugation (5 min, 200 g, at room temperature (RT)) and then split with a subculturing ratio between 1:3 and 1:10.

II.6.2 Culturing of cells in suspension

Cells growing in suspension were cultured at a density of 10^5 - 10^6 cells/ml. Cells were harvested by centrifugation (5 min/200 g/RT).

II.6.3 Freezing and thawing of mammalian cells

Freeze stocks of cell lines were stored in 1.8 ml cryovials in liquid nitrogen. Cells were first harvested and then resuspended at a concentration of 10^6 – 10^7 cells/ml in ice-cold complete medium containing 10% (v/v) dimethylsulfoxide (DMSO). The cryovials were placed overnight (o.n.) at -80°C in a cryocontainer to assure slow cooling and then transferred to liquid nitrogen for long-term storage. For thawing of cells, cryovials were rapidly thawed in a 37°C water bath. Cells were slowly added to 4 mL warm growth medium, centrifuged and resuspended in growth medium.

Tab.II.1: List of the primary cells and cell lines used in this study

Primary cells	Origin/Phenotype	Source	Medium
HAoEC	human aortic endothelial cells	PromoCell (Heidelberg, Germany)	Endothelia Growth Medium MV (PromoCell)
HVSMC	human vascular smooth muscle cells (SMC) from Arteria mammaria	provided by R. Blindt, Med. Clinic I, UK Aachen	Smooth Muscle Cell Growth Medium 2 (PromoCell)
rSMC	SMCs from media and neointima of Sprague-Dawley rats	from Alma Zernecke, Institute for Molecular Cardiovascular Research (IMCAR), UK Aachen	isolated and cultured as described (Zeiffer et al. 2004)
HCASMC	human coronary artery SMCs	PromoCell	Smooth Muscle Cell Growth Medium 2 (PromoCell)
T cell blasts	from peripheral blood mononuclear cells (PBMCs) healthy donors		RPMI 1640 + 10% FCS, 2 mM glutamine, 5 µg/mL PHA, 100 U/mL IL-2
neutrophils	from PBMCs of healthy donors		not cultured
monocytes	from PBMCs of healthy donors		not cultured
Cell lines	**Origin/Phenotype**	**Source**	**Medium**
MonoMac6	human acute monocytic leukemia	from Ziegler-Heitbrock, University fo Leicester, UK	RPMI 1640 + 10% FCS, 1x MEM non-essential amino acids, 9 µg/ml insulin, 1 mM oxalacetate and 1 mM pyruvate
CHO/ ICAM-1	chinese hamster ovary cells expressing inter-cellular adhesion molecule-1 (ICAM-1)	Revotar (Henningsdorf, Germany)	DMEM/F12-GlutaMax + 10% FCS, 800µg/mL G418
SVEC	Simian virus transduced mouse endothelial cells	ATCC (Manassas, USA)	DMEM + 10% FCS
Jurkat	human T cell leukemia cells	ATCC	RPMI 1649 + 10% FCS
L1.2	murine pre-B lymphoma	from Dr. M. Locati , University of Milano, Italy	RPMI 1640 + 10% FCS, 1 mM pyruvate, 50 µM β--mercaptoethanol, 10 mM HEPES
HEK-293	human embyonic kidney	ATCC	DMEM/F12-GlutaMax + 10% FCS
RAW264.7	murine macrophages	ATCC	DMEM + 10% FCS

II.6.4 Isolation of PBMC

PBMC were isolated from venous blood of healthy donors by Ficoll-hypague density gradient centrifugation. After dextran sedimentation, the plasma supernatant was carefully overlayed on Biocoll separating solution, density 1.077 g/ml (Biochrom, Berlin, Germany) and centrifuged (20 min/450 g/RT/without brake). The PBMC interface layer was harvested, diluted in PBS and centrifuged (5 min/400 g/RT). The mononuclear cells were washed twice with PBS, and the viability was determined by trypan blue exclusion.

II.6.5 Isolation of T cells

Total T cells from PBMC (0) were isolated by use of the CD3 Dynabeads™ (Miltenyi Biotec, Bergisch Gladbach, Germany) according to the manual. Subsequently the T cells were cultured in RPMI 1640 medium containing 10% FCS. In order to stimulate proliferation of the T cells, the medium was supplemented with 100 U/mL IL-2 and 5µg/mL phytohemagglutinin (PHA), which initiates mitosis. After 3-4 days cells were transferred to fresh medium containing 100U/mL IL-2. Cells were employed in flow adhesion experiments after 7-8 days (II.9.2).

II.6.6 Isolation of monocytes

Monocytic cells were isolated from PBMC (0) via depletion of non-monocytic cells. By use of the Monocyte Isolation Kit II (containing a cocktail of biotin-conjugated antibodies against CD3, CD7, CD16, CD19, CD56, CD123 and CD235a (Glycophorin A), as well as αbiotin MicroBeads) and the autoMacs™ device (Miltenyi Biotec, Bergisch-Gladbach, Germany) according to the recommended protocol, monocytes were isolated by negative selection.

II.6.7 Isolation of neutrophils

After Ficoll-hypague density gradient centrifugation of venous blood (0) the pellet contains neutrophils and erythrocytes. In order to remove erythrocytes, the pellet is resuspended in ~ 20 mL erythrocyte lysis buffer and incubated RT for 5 min. Cells were washed with PBS and kept on ice until further use.

Erythrocyte lysis buffer: 155 mM NH_4Cl

10 mM $KHCO_3$

0.1 mM EDTA

pH = 7.3

II.7 RNA and DNA techniques

II.7.1 Transformation of *E. coli*

E. coli (strain DH5α) were cultured in LB medium at 37°C with vigorous shaking. For growth on solid media, a bacteria suspension was spread on a LB agar plate or a single bacteria colony was inoculated to achieve single colony growth. The LB plates were incubated inverted o.n. at 37°C. For culturing of bacteria transformed with a plasmid conferring antibiotic resistance, growth medium was supplemented with the appropriate antibiotic. For long-term storage of bacteria at -80°C, LB medium was supplemented with glycerol to a final concentration of 15% (v/v). All solutions used for bacteria work were autoclaved or filter-sterilized.

Bacteria growth medium

Bacteria growth medium was autoclaved for 20 min at 121°C. LB agar medium was allowed to cool to 50°C before addition of antibiotics.

LB medium: 0.5% (w/v) yeast extract,

1% (w/v) peptone 140,

1% (w/v) NaCl

LB agar medium: LB medium with 1.4% (w/v) agar

Preparation of heat-shock competent *E. coli*

DH5α cells were prepared mainly as described (Chung *et al.* 1989). 5 mL LB medium were inoculated with DH5α and incubated on at 37°C shaking. Then 100 mL LB medium were incubated with 750 µL of the o.n. culture for 1 to 2 h at 37°C until the optical density at 600 nm (OD_{600}) was approximately 0.4, indicating the early exponential growth phase. OD_{600} was measured in a spectrophotometer with pure medium as reference. The culture was centrifuged (10 min/3000 g/4°C), and the pellet was resuspended in 10 mL ice-cold TSS buffer. 500 µL aliquots were frozen immediately in liquid nitrogen and stored at -80°C.

TSS buffer: 10% (w/v) polyethyleneglycol (PEG) 8000 (Promega)

5% (v/v) DMSO

20 mM $MgCl_2$

in 1x LB medium (II.7.1)

Heat-shock transformation of competent *E. coli*

100 µl thawed competent *E. coli* were gently mixed with 1-5 ng of plasmid DNA, and incubated for 30 min on ice. The bacteria were heatshock treated for 90 sec in a 42°C waterbath, and then incubated for 2 min on ice. After addition of 900 µL LB medium, the bacteria were incubated for 1 h at 37°C with gently shaking. The bacteria were spread on selective LB agar plates and incubated on at 37°C to select for transformed bacteria.

II.7.2 Plasmids

pcDNA3.1	Invitrogen
pcDNA3.1/CXCR1	(UMR cDNA Resource Center, Rolla, MO, USA)
pcDNA3.1/CXCR2	(UMR cDNA Resource Center)
pcDNA3.1/CXCR3	(UMR cDNA Resource Center)
pcDNA3.1/his-CD74	(UMR cDNA Resource Center)
pSG5	Stratagene, La Jolla, CA
pSG5/YB-1	provided by Dr. Peter Mertens (Department of Nephrology and Clinical Immunology, UK Aachen, RWTH Aachen University, Aachen, Germany)
H1.Empty	lentiviral expression vector RRl-cPPt-H1.PreSIN (Seppen et al. 2002) containing the H1 instead of the cytomegalovirus (CMV) promoter
H1.shYB-1	RRl-cPPt-H1.PreSIN containing the H1 promoter and a YB-1 siRNA (kindly provided by Dr. Erik A. Biessen, Division of Biopharmaceuticals, Leiden Amsterdam Center for Drug Research, Leiden University, The Netherlands)
pGL3	luciferase reporter vector (Promega)
pGL3/RANTES	pGL3 containing the RANTES promoter (Ute Raffetseder, Department of Nephrology and Clinical Immunology, UK Aachen)
pGL3/-168	containing the truncated RANTES promoter lacking the Y-box (generated by PCR of a -974 nucleotide RANTES 5' upstream fragment based on previously described pGL3-based plasmid constructs (pGL3; Promega, Madison, WI) (Fessele et al. 2001)

II.7.3 Miniprep: Small-scale purification of plasmid DNA

Plasmid DNA was purified from a bacteria culture by alkaline lysis as described (Sambrook and Russell 2001) mL o.n. culture was centrifuged (1 min/7000 g/RT) and the pellet was resuspended in 100 µL buffer 1. For lysis of the bacteria, 200 µL of buffer 2 was added followed by gently mixing and 5 min incubation at RT. The mixture was neutralized by 200 µL ice-cold buffer 3, gently mixed, and incubated for 5 min at -20°C. The suspension was spun down (20 min/20000 g/RT) to remove proteins, cell debris and chromosomal DNA. The supernatant with plasmid DNA was transferred to a new eppendorf tube mixed with 500 µL isopropanol and centrifuged (20 min/20000 g/RT). The pellet with plasmid DNA was washed with 70% (v/v) ethanol, air dried and resuspended in 50 µL 10 mM Tris-HCl, pH 8.5.

Buffer 1: 50 mM glucose

25 mM Tris-HCl, pH 8.0

10 mM EDTA, pH 8.0

Buffer 2: 200 mM NaOH

1% (w/v) SDS

Buffer 3: 3 M potassium acetate, pH 5.5

II.7.4 Midiprep and Maxiprep: Large-scale purification of plasmid DNA

Large-scale purification of plasmid DNA from bacteria o.n. culture was performed using

the Qiagen Plasmid Midi or Maxi Kit™ (Qiagen, Hilden, Germany) according to the manufacturer's instructions.

II.7.5 Restriction endonuclease digestion of DNA

Restriction endonucleases (MBI Fermentas, Ontario, Canada) were used to digest double-stranded DNA for analytical purposes. Restriction endonucleases recognize specific palindromic sequences and cleave a phosphodiester bond at each strand at that sequence. Restriction endonuclease digestion of DNA for analytical purpose was done according to the manufacturer's instructions. 0.2-1 µg DNA were digested with 5-10 U restriction enzyme in a volume of 20 µL. Digests were incubated for 1 h at 37°C or as recommended by the supplier. Reaction buffers were supplied by the manufacturer.

II.7.6 Agarose gel electrophoresis

Separation of DNA fragments from digest was done by agarose gel electrophoresis. The negatively charged DNA fragments migrate towards the anode in an electric field at a rate determined by the size. DNA samples were diluted with DNA loading buffer and separated on a 1-2% (w/v) agarose gel dissolved in TAE electrophoresis buffer containing 0.1 µg/mL ethidium bromide. After electrophoresis at 110 V, the DNA was visualized on a UV light transilluminator and photographed for documentation.

DNA loading buffer (6x):	30% (v/v) glycerol
	6 mM EDTA
	0.25% (w/v) bromophenol blue
	0.25% (w/v) xylenecyanol

TAE electrophoresis buffer (1x):	40 mM Tris-acetate
	1 mM EDTA

II.7.7 Quantification of DNA and RNA

DNA and RNA concentration was determined by measuring the absorbance at 260 nm (A_{260}) in a spectrophotometer using a quartz cuvette. For double-stranded DNA an $A_{260} = 1$ corresponds to 50 µg DNA/mL, and for RNA an $A_{260}=1$ corresponds to 40 µg RNA/mL. The absorbance at 280 nm was also measured to estimate DNA and RNA purity. Pure DNA or RNA has an A_{260}/A_{280} ratio of 1.8-2.0 at pH 7.0.

II.7.8 Sequencing of DNA

The sequence of DNA constructs were screened by a commercial sequencing service (MWG Biotech, Martinsried, Germany) and the sequence data were verified on the basis of the corresponding electropherogram.

II.7.9 Transfection of eukaryotic cells

Stable transfection of L1.2 and HEK-293 cells

L1.2 cells stably expressing the chemokine receptors CXCR1, CXCR2 or CXCR3 and HEK-293 (HEK) cells stably expressing CXCR2 were generated by electroporation with subsequent selection: 10^7 L1.2 or HEK cells growing in log phase (passaged the day before transfection) were transfected with 10 µg plasmid DNA (pcDNA3.1, pcDNA3.1/CXCR1, pcDNA3.1/CXCR2 or pcDNA3.1/CXCR3) using the gene-pulser II electroporator (Bio-Rad) with the parameters 260 V, 975 µF, 200 Ω. After 48 hours cultivation in growth medium, transfected cells were selected with G418 sulfate at 800 µg/ml. G418-resistent cells were subcloned by limiting dilution in 96-well plates with flat bottom and clones were analyzed by flow cytometry with the mAbs αCXCR1, αCXCR3, αCXCR2-FITC and the respective isotype controls.

Transient transfection of Jurkat T cells, VSMC, HCASMC and L1.2 cells

2×10^6 VSMC and HCASMC (grown until 80% confluence) were transfected with 3 µg pSG5/YB-1 or vector control using the HAoSMC Nucleofector Kit and the Nucleofector™ device (Amaxa) according to the manufacturer's manual. Transfected VSMC were cultivated in 25 cm² flasks for 24 h in non-selection medium and further processed for gene expression determination via real time-polymerase chain reaction (PCR) (II.7.10).

HCASMC were cultured in 35 mm² dishes for 24 h to 48 h and employed in a flow adhesion assay (II.9.2). The same system was employed for the transfection of Jurkat T cells with the expression vector pcDNA3.1/CXCR2. Here, the Cell Line Nucleofector Kit V was used. Cells were split to a concentration of 1×10^6 cells per mL one day before the transfection.

II.7.10 Quantitative real time-PCR

To determine IL-8, Gro-α, YB-1 or RANTES gene expression, a real time-PCR was performed using the QuantiTect Kit with SYBRGreen™ (Qiagen) and specific primers according to manufacturer's protocol. The real time-PCR technique is based on the ability of the fluorescent dye SYBRGreen to bind to double-stranded DNA, i.e. the increase in double-stranded DNA can be directly detected. Thus, the increase of fluorescence over the reaction time can be associated with the employed mRNA concentration.

RNA from HUVEC, HAoEC, or HVSMC was isolated using the RNeasy Mini Kit™ (Qiagen) following digestion of genomic DNA using the RNase-free DNase set (Qiagen) according to the manufacturer's protocol. After determination of the RNA amount (I.5.6), up to 1 µg messenger RNA (mRNA) was reverse-transcribed with the Omniscript RT Kit (Qiagen) using oligo-dT primers. RNA was reverse-transcribed into cDNA at 37°C for 1 h. 100 ng cDNA were assessed in the real time-PCR reaction. The housekeeping gene glyceraldehyde 3-phosphate dehydrogenase (GAPDH) was used as a reference gene.

Reverse transcription: 2 µL 10x reverse transcription buffer

2 µL dNTP mix (5 mM each)

2 µL 10 µM oligo-dT primer (MWG Biotech)

1 µL RNase inhibitor (10 U/µL)

1 µL Omniscript reverse transcriptase

1 µg template RNA

H_2O to a final volume of 20 µL

Real time-PCR 2 µL cDNA or H_2O

20 µL 2x QuantiTect SYBR Green PCR Master Mix

forward primer to a final concentration of 0.5 µM

reverse primer to a final concentration of 0.5 µM

RNase free water to final volume 40 µL

Real time-PCR Program:

1. Initial activation	95℃, 15 min	
2. Denaturation	94°C, 15 sec	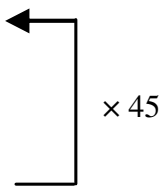
3. Annealing	55°C, 30 sec	× 45
4. Extension	72°C, 30 sec	
5. Plate read		

The relative mRNA expression is estimated as follows:

$\Delta C_t = C_t(\text{target}) - C_t(\text{reference})$

$\Delta\Delta C_t = \Delta C_t - \Delta C_t(\text{target control})$

relative mRNA expression: $2^{-(\Delta\Delta Ct)}$

C_t: Cycle number at which the fluorescence intensity exceeds a determined threshold

Primers for real time-PCR:

YB-1:	5'-CACCTTACTACATGCGGAGACCT-3',
	5'-TTGTCAGCACCCTCCATCACT-3'
RANTES:	5'-TTGCCTGTTTCTGCTTGCTC-3',
	5'-TGTAACTGCTGCTGTGTGGT-3'
GAPDH:	5′-GCCTCAAGATCATCAGC-3′;
	5′-ACCACTGACACGTTGGC-3′

GRO-α: 5′-AGGGAATTCACCCCAAGAAC-3′,

5′-TAACTATGGGGGATGCAGGA-3′

IL-8: 5′-TCTGCAGCTCTGTGTGAAGG-3′,

5′-AATTTCTGTGTTGGCGCAGT-3′

II.8 Protein assays

II.8.1 Electrophoretic mobility shift assay (EMSA)

For preparation of nuclear extracts, HCASMC were lysed in ice-cold hypotonic buffer. Sequential centrifugation at 1000 g for 10 min and 5000 g for 5 min was performed at 4°C to pellet nuclei, yielded by addition of high salt extraction buffer for 20 min on ice. After final centrifugation at 15000 g, supernatant containing nuclear proteins was collected and concentrations determined by Bio-Rad protein assay using bovine serum albumin as standard. Extracts were stored at -80°C until performance of EMSA.

Recombinant YB-1 was prepared from a pRSET vector (Invitrogen) containing an insert encoding for a hexahistidine T7 epitope-YB-1 fusion protein (Mertens *et al.* 1998). Synthetic DNA-probes corresponding to the sense as well as antisense strands of the RANTES promoter sequences -204/-173 were end-labeled by means of the Biotin 3' End DNA-labeling Kit™ (Pierce, Rockford, IL, USA), which uses terminal deoxynucleotidyl transferase to catalyze nontemplate-directed nucleotide incorporation onto the 3'-OH end of DNA. Double-stranded DNA was generated by mixing equal amounts of labeled complementary oligos and incubating the mixture for 1 h at room temperature. The nucleotide sequences were:

5'-CCGGTACCCATTGGTGCTTGGTCAAAGAGGAAACTGATGAGCTCACTCAG ATCTGC-3' (sense)
5'-GCAGATCTGAGTGAGCTCATCAGTTTCCTCTTTGACCAAGCACCAATGGGT ACCGG-3' (antisense)

Biotin-labeled DNA was incubated with affinity-purified recombinant YB-1 protein

(II.4) (by Ute Raffetseder, UK Aachen) or nuclear cell extract for 20 min on ice, subjected to gel electrophoresis (II.7.6) on native 6% polyacrylamide gels, and transferred to nylon membranes. Bands were visualized by streptavidin-HRP conjugate and chemiluminescent substrate (LightShift chemiluminescent EMSA kit, Pierce). For supershift analyses, peptide-derived affinity-purified rabbit αYB-1 antibody (peptide antibody against amino acids 185-206) was incubated with nuclear proteins 12 h prior to addition of probes. The binding reaction was as above and samples were subjected to electrophoresis in 6% polyacrylamide gels.

Lysis buffer: 10 mM HEPES (pH 7.9)

1.5 mM $MgCl_2$

10 mM KCl

0.5 mM DTT

supplemented with a proteinase inhibitor cocktail (Complete Mini, Roche, Mannheim, Germany)

Extraction buffer: 20 mM HEPES/KOH (pH 7.9)

1.5 mM $MgCl_2$

420 mM NaCl

0.2 mM EDTA

25% glycerol

II.8.2 Enzyme-linked immunosorbant assay (ELISA)

The IL-8 and RANTES concentrations in the supernatants of stimulated and unstimulated HAoEC or YB-1 overexpressing SMCs were detected via ELISA. HAoEC were incubated with MIF (50 ng/mL) or TNF-α (100 U/mL) for 2 h at 37°C, and the levels of IL-8 in the supernatant were quantified using the Quantikine ELISA Immunoassay (R&D Systems) (Fig.II.1). RANTES secretion by YB-1-transfected SMCs (0) was also determined via a Quantikine ELISA Kit (R&D Systems). These Kits contained a 96 well polystyrene microplate (12 strips of 8 wells) coated with mAbs against IL-8 or RANTES, which

immobilized the proteins on the well surface. After binding of a HRP-conjugated detection pAb and reaction with a substrate, a color change according to the protein content was measured at a wavelength of 450 nm with an ELISA reader and evaluated via XFluor™ Software (Tecan, Crailsheim, Germany).

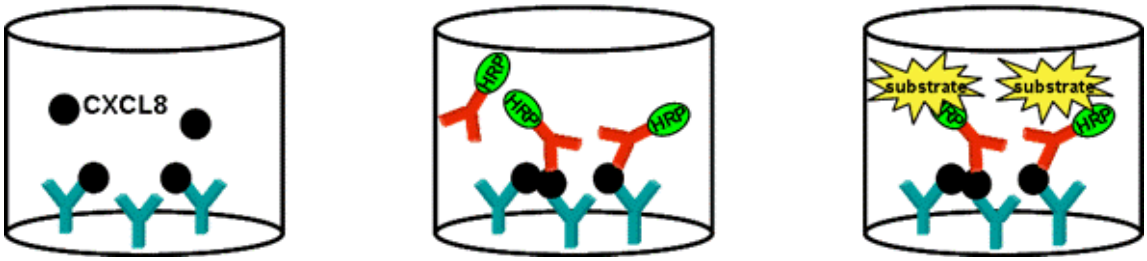

Fig.II.1: ELISA. From left to right: mAbs specific for e.g. IL-8 coated to polystyrene microplate bind to the IL-8 proteins from cell supernatants and immobilize the protein on the microplate. Secondary HRP-conjugated αIL-8-Abs bind to the immobilized protein and oxidize a substrate resulting in a color change of the substrate solution, which can be detected and evaluated by an ELISA-reader.

II.8.3 Flow cytometry

Flow cytometry can be used to just analyze cells by their size, granularity and protein expression (by e.g. FITC-conjugated detection Abs) or to sort cell populations (FACS = Fluorescent activated cell sorting). In a buffer stream one cell at a time passes by an argon laser, which excites fluorescently labeled cells. Measurements of the size (forward scatter) and granularity (sideward scatter) are independent from the fluorescence signal.

Measurement of fluorescence intensity using fluorescence labeled Abs was done to examine the expression of chemokine receptors on the cell surface or the activation of the αLβ2 integrin activation (II.9.3). The results were displayed as histograms showing the logarithmic distribution of the fluorescence intensity or as diagrams demonstrating the change in mean fluorescence intensity (MFI). For receptor expression determination, 1×10^5 cells were resuspended in PBS with specific Ab or IgG isotype control (10 µg/mL) and incubated for 30 min on ice. After washing, the cells were incubated with a FITC-conjugated detection Ab (10 µg/mL) for 30 min on ice. The cells were washed and analyzed immediately by flow cytometry in a FACSCalibur (BD Biosciences).

The change of MFI as a cause of chemokine-mediated Ca^{2+} influx (II.9.4) was measured with the FACSAria System and evaluated with FlowJo Software (BD Biosciences).

II.8.4 Coimmunoprecipitation

For extraction and precipitation of the CXCR2/CD74 complex, L1.2 cells expressing human recombinant human CXCR2 (II.7.9) and CD74 as well as untransfected cells were washed with ice-cold PBS and resuspended in nondenaturing lysis buffer to a final concentration of 5×10^6 cells/mL. After 30 min incubation on ice, cell debris was spun down at 14500 × g for 20 min. The clear supernatants were incubated with 30 µL protein A-sepharose beads for 1 h on a roller mixer. After centrifugation of the beads the supernatants were incubated with 2.5 µg αCXCR2 antibody (RII115) or the respective isotype control for 1 h. Subsequently 30 µL of pre-blocked protein G-sepharose beads (2 h incubation with 2.5% BSA and 2.5% Roti-Block™ (BioRad, Hercules, CA, USA) at 4˚C) were added to the supernatants and incubated over night. All incubations were carried out at 4˚C. Precipitates were washed three times with wash buffer and once with PBS. Proteins were eluted with 60 µL hot elution buffer.

The pull down of the MIF/CXCR2 complex was performed similarly: 5×10^6 HEK cells stably expressing CXCR2 and control transfectants (0) were incubated with biotin-MIF (1µg) for 30 min at 4˚C, spun down and lyzed with 1 mL lysis buffer. After centrifugation of cell debris, lysates were incubated with 100 µl Dynalbeads M280 Streptavidin (10 mg/ml) (Invitrogen) for 30 min at 4˚C. The Dynalbeads were collected by Dynal magnetic partical concentrator. The beads were washed three times with 1:5 diluted lysis buffer. The precipitated proteins were eluted by boiling the beads in SDS loading buffer.

Non-denaturing lysis buffer:
1% (w/v) Triton X-100
1% (w/v) (CHAPSO) (Calbiochem)
50 mM Tris-HCl (pH 7.4)
100 mM NaCl
15 mM EGTA
0.02% (w/v) sodium azide

10 mM iodoacetamide

supplemented with a proteinase inhibitor cocktail (Complete Mini, Roche, Mannheim, Germany)

Wash buffer: 0.1% (w/v) Triton X-100

50 mM Tris-HCl (pH 7.4)

100 mM NaCl

15 mM EGTA

0.02% (w/v) sodium azide

Elution buffer: 1% (w/v) SDS

100 mM Tris-HCl (pH 7.4)

10 mM dithiotreitol (DTT)

II.8.5 SDS-polyacrylamide gel electrophoresis (PAGE)

After immunoprecipitation of CXCR2, the protein and co-immunoprecipitated CD74 were analyzed by SDS-PAGE. SDS binds to polypeptides resulting in a negative charge directly proportional to protein size. Protein samples were first concentrated in a stacking gel before migrating into the resolving gel. Electrophoresis was carried out at 200 V. The resolving gel was further analyzed by western blotting (II.8.6)

Resolving gel: 12% (w/v) acrylamide/Bis

375 mM Tris-HCl, pH 8.8

0.1% (w/v) SDS

0.1% (w/v) ammonium persulfate

0.1% (v/v) TEMED

Stacking gel:	5% (w/v) acrylamide/Bis
	125 mM Tris-HCl, pH 6.8
	0.1% (w/v) SDS (sodium-dodecylsulfate)
	0.1% (w/v) ammonium persulfate
	0.1% (v/v) TEMED
Electrophoresis buffer:	(10x) 250 mM Tris base
	1.92 M glycine
	1% (w/v) SDS

II.8.6 Western blot analysis

Separated proteins from a SDS-PAGE (II.8.6) were transferred to a nitrocellulose membrane and detected using specific primary Abs and HRP-conjugated secondary Ab. The proteins were transferred from the gel to the nitrocellulose membrane (Hybond-ECL, Amersham Biosciences, Uppsala, Sweden), at 90 V for 1 hour in ice-cold blotting buffer. Nonspecific binding sites on the membrane were blocked with 5% (w/v) nonfat milk in TBS for 1 hour at RT. Thereafter, the membrane was incubated with a primary Ab diluted in blocking buffer for 1 hour at RT or o.n. at 4°C. After 3 times washing with TBS/0.05% (v/v) Tween, the membrane was incubated with a HRP-conjugated secondary Ab diluted in TBS for 1 hour at RT or on at 4°C. In the presence of hydrogen peroxide (H_2O_2) the protein-bound HRP converted the substrate ECL (enhanced chemiluminescence) (Pierce, Rockford, IL, USA) to a light-emitting carbonyl, and the specific protein bands were visualized via exposure to an autoradiografic film (Kodak, Rochester, NY,USA).

Blotting buffer (1x)	25 mM Tris base
	192 mM glycine
	10% (v/v) methanol
	0.005% (w/v) SDS

II.8.7 Histochemistry

Serial tissue sections of the left common carotid artery (II.10.1) of *Apoe*$^{-/-}$, Met-RANTES-treated *Apoe*$^{-/-}$ and *Apoe*$^{-/-}$/*Ccr5*$^{-/-}$ mice were stained according to MOVAT's pentachrome staining. After paraffin removal by dipping the cover slides with the tissue sections in baths of xylene and graded alcohols are stained with the following dyes. Cover slides are washed with acetic ethanol and water in between each staining step.

1. Staining with Alcian blue (Sigma) for 20 min to visualize mucins and glycosaminoglycans:

Staining solution:	Alcian blue	1% (w/v)
	in acetic acid (1%)	

2. Staining with orcein (Merck) and haematoxylin for 30 min to visualize elastic fibers and cell nuclei:

Staining solutions:

A:	orcein	1% (w/v)
	in ethanol (70%)	
	acetic acid (25%)	0.5% (v/v)
B:	haematoxylin	15% (w/v)
	in ethanol (100%)	

C:	iron(III)-chloride	10% (w/v)
	in water	
D:	iodine	1% (w/v)
	potassium iodide	2% (w/v)
	in water	

Two volumes of solution B are mixed with one volume of solutions A, C, and D.

3. Staining with Brilliant Crocein Scarlet MOO (Sigma) for 10 min:

Staining solutions:

Solution A:	Brilliant Crocein Scarlet	0.1% (w/v)
	in glacial acetic acid	
Solution B:	acid fuchsin	0.1% (w/v)
	In acetic acid	(0.5% v/v)

Working solution: volumes of A and 1 volume of B

4. Staining with saffron for 15 min:

Staining solution:	saffron	6% (w/v)
	in ethanol (100%)	

After staining, the sections are washed in ethanol and xylol to remove water and covered with Entellan (Merck).

Stained tissue:

Nuclei	dark violet/black
Cytoplasm	pink/red
Elastic fibers	violet/black

Collagen	yellow/yellow-green
Extracell. matrix	blue/blue-green
Muscle	red

II.8.8 Immunofluorescence

Confluent HAoEC and CHO-ICAM-1 cells grown on glass slides were incubated with MIF (50 ng/mL) for 2 h at 37˚C. After washing with phosphate-buffered saline (PBS) and fixation with 2% paraformaldehyde/PBS (PFA), cells were stained for surface-bound MIF using the polyclonal rabbit MIF antibody Ka565 (1:500) followed by a FITC-conjugated goat αrabbit Ab, and mounted with Vectashield containing DAPI (Vector Labs, Burlingame, CA).

Tissue sections of aortic roots (II.10.2) or the left common carotid artery (II.10.1) of *Apoe*$^{-/-}$ mice were stained for CD3, MOMA-2, α-SMA, Mac2, RANTES or YB-1. For detection, Cy3- or FITC-conjugated secondary Abs were used (II.5.5). The relative macrophage or T cell content was determined by quantifying the area positive for Mac2 or CD3. Images were recorded with a Leica DMLB fluorescence microscope and charge couble device (CCD) camera.

II.9 Functional assays

II.9.1 Luciferase reporter assay

The Promega luciferase assay system (Mannheim, Germany) was employed in order to quantitatively analyze YB-1-triggered activation of the RANTES promoter. HCASMC and RAW264.7 cells were transfected with the reporter vector pGL3/RANTES (II.7.2, II.7.9) containing the full length RANTES promoter or the truncated promoter (pGL3/-168) upstream of a modified firefly luciferase gene. Moreover, the cells were co-transfected with the YB-1 overexpression vector pSG5/YB-1, or promoter activation by endogenous YB-1 was attenuated by means of short hairpin RNA (shRNA) generated by pSuperduper plasmid (OligoEngine, Seattle, WA, USA) with the sequence 5'-GGTCATCGCAACGAA GGTTTT-3' introduced as a tail-to-tail tandem repeat corresponding to base pairs (bps) 285 to 305 of the human YB-1 coding sequence (accession nr. J03827) (provided by Ute Raffetseder). As indicated, human IFN-γ (100 U/mL) was added to the cells. YB-1-

triggered luciferase expression was measured 24 h after transfection in a single tube luminometer (Sirius, Berthold Detection Systems, Pforzheim, Germany). Results were calculated as fold-changes relative to luciferase activity measured with pGL3 plasmid without promoter.

II.9.2 Parallel plate flow chamber adhesion assay

MonoMac6, Jurkat T cells and Jurkat cells transiently expressing CXCR2, L1.2, and primary monocyte or T cell arrest on CHO-ICAM-1monolayers, HAoEC, SVEC, HCASMC or VCAM-1.Fc was analyzed in a parallel wall chamber under laminar flow condition. CHO-ICAM-1 cells, HAoEC, SVEC, pSG5/YB-1 transfected or untransfected HCASMC were grown to confluence in 35 mm dishes or plates coated with VCAM-1.Fc (0.5 μg/mL) were pre-incubated with MIF (50 ng/mL), IL-8 (10 ng/mL), IP-10 (500 ng/mL), SDF-1α (100 ng/mL) or control buffer for 2 h at 37˚C. Leukocytes were directly incubated with MIF (250 ng/mL), IL-8 (100 ng/mL) or SDF-1α (100 ng/mL) as indicated. The arrest of L1.2 transfectants on SVEC monolayers was assessed in the presence or absence of the CXCR4 antagonist AMD3465 (10 μM). Monocytes and T cells (2.5-5×10^5/mL) labeled with calcein-AM (Molecular Probes/Invitrogen, Paisley, UK) in HH buffer (II.2) were pretreated with PTX (0.5 μg/mL) for 2 h or with blocking mAbs against β_2, α_4, CD74, CXCR4 (all 10 μg/mL), CXCR1 (30 μg/mL), CXCR2 (3 μg/mL), or isotype-matched control IgG at corresponding concentrations for 30 min and perfused at 1.5 dyn/cm^2. In particular experiments the HAoEC monolayers were incubated with blocking Abs against Gro-α, IL-8, and MIF. In certain approaches HCASMC were incubated with the RANTES receptor antagonist Met-RANTES. After 5 min, the number of adherent cells was quantified in multiple fields (0.24 mm^2 each, >10 per treatment) by analysis of images recorded with a long integration 3CCD video camera (JVC, Japan) using AnalySIS software (Soft Imaging System, Münster, Germany). For analysis of arrest on CHO-ICAM-1 cells, background adhesion to vector-transfected CHO cells was subtracted.

II.9.3 αLβ2 integrin activation assay

MonoMac6 cells or primary monocytes (5 × 10^5 cells/mL) were stimulated with MIF (50 ng/mL) in assay buffer without Ca^{2+}/Mg^{2+} at 37˚C for indicated periods. Incubation of cells

without MIF for 30 min served as negative control. As a positive control, cells were incubated with 3 mM Mg^{2+} and 1 mM EGTA (ethylene glycol bis(2-aminoethyl-ether)-N,N,N'N'-tetraacetic acid). Cells were fixed with 2% PFA, reacted with 327C (10 µg/mL) and αmouse-IgG FITC conjugate and analyzed by flow cytometry. Activation of αLβ2 was reported by the increase in MFI (Shamri *et al.* 2005).

II.9.4 Calcium mobilization assay

The activation of cells due chemokine/GPCR interaction causes a rapid influx of Ca^{2+} and the release of Ca^{2+} from the endoplasmic reticulum. This calcium mobilization can be visualized by the fluorophore Fluo-4. Fluo-4 AM (Molecular Probes, Eugene, OR, USA) is a calcium indicator, which can be loaded into cells. After the uptake, the lipophilic acetoxymethyl group is cleaved off the originally hydrophilic fluorophore by cellular esterases. Upon binding to cytosolic Ca^{2+}, Fluo-4 exhibits an increase in MFI, which can be detected by flow cytometry (II.8.3).

Neutrophils and L1.2/CXCR2 transfectants were labeled with 0.9 µM Fluo-4 AM in assay buffer for 45 min at 37 ˚C. Subsequently cells were once washed with assay buffer and resuspended to a final concentration of $2x10^6$/ml - 500 µl per sample. Calcium mobilization in respond to a stimulus, e.g. MIF was detected via the FACSAria. Samples were homogenized by passing them through pre-separation filters (Miltenyi) just prior to the FACS measurement. Baseline fluorescence was recorded for 10 sec. Then the stimulus was added to the cells and the change in MFI was recorded for another 2 min. For determining desensitization, a second stimulus was given after the measurement and the MFI was recorded another 2 min.

Assay buffer:
- 4.6 mM KCl
- 1 mM $CaCl_2$
- 130 mM NaCl
- 5 mM glucose
- 20 mM HEPES
- 0.1% human serum albumin

II.10 Animal experiments

II.10.1 Mouse model of arterial wire-injury and lentiviral transduction

Apoe$^{-/-}$ mice were fed a Western type diet (containing 0.25% cholesterol and 15% cacaobutter, SDS, Sussex, UK) from 1 week prior to surgery and throughout the experiment. Transluminal wire injury of the left common carotid artery was performed as described (Lindner *et al.* 1993; Schober *et al.* 2002; Schober *et al.* 2003) (Fig.II.2). A 0.014-in flexible angioplasty guidewire was advanced into the common carotid artery via the left internal carotid artery and endothelial denudation was achieved by three rotational passes. For lentiviral transfer, the lumen of the carotid artery was incubated with the H1.shYB-1 or H1.empty (II.7.2) carrying lentivirus solution (10^{10} i.u./mL) for 15 min. directly after wire-injury. Two groups of *Apoe*$^{-/-}$ mice (n = 6 each) were treated with MetRANTES (40 µg 3 times a week) after wire injury and lentiviral transduction. Animals were sacrificed at 4 weeks after injury. Starting at the bifurcation serial tissue sections (5 µm) were obtained from left common carotid arteries. For morphometry, ten sections (each 50 µm apart) were stained with Movat's pentachrome (II.8.7), and subjected to planimetric analysis (Diskus software, Hilgers, Königswinter, Germany).

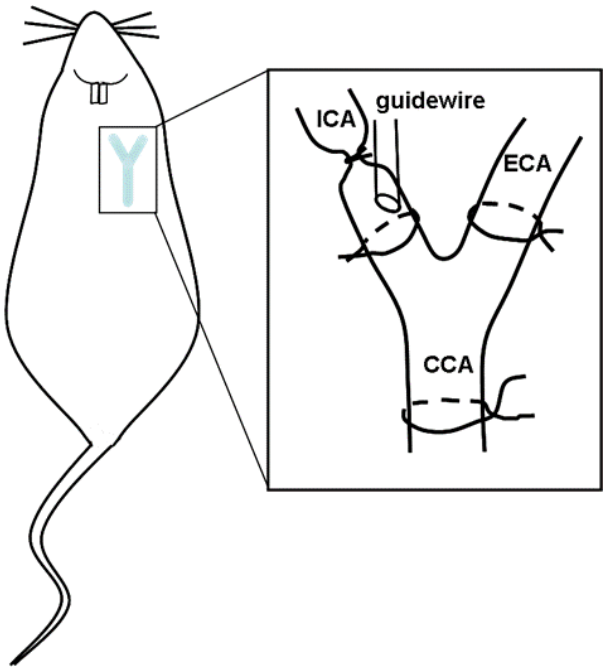

Fig. II.2: Arterial wire-injury.
A flexible guidwire is introduced into the internal carotid artery (ICA) and advanced into the common carotid artery (CCA). The endothelial denudation is achieved by three rotational passes.

II.10.2 Mouse model of atherosclerotic disease progression

Apoe$^{-/-}$ mice (C57BL/6) were fed an atherogenic diet containing 21% fat (Atromin) for 12 weeks and sacrificed. Subgroups were injected with blocking MIF mAb (NIHIIID.9), blocking αSDF-1α mAb (II.5.3), blocking αGro-α antibody (II.5.3), or vehicle/PBS starting at 12 weeks of diet and subsequently twice weekly (50µg intraperitoneally (i.p.)) until sacrifice at 16 weeks of diet. Hearts were harvested by *in situ* perfusion fixation with 4% PFA. The extent of atherosclerosis was assessed in aortic roots by staining of 5 µm transversal sections (3-6/mouse) for lipid deposition with Oil-red-O. After staining with Oil-red-O for 30 min, the tissue sections were washed with PBS until the buffer remained clear and quantified by computerized image analysis (Diskus software, Hilgers, Aachen, Germany). The relative content of macrophages and $CD3^+$ T cells was determined by mAb staining for MOMA-2 and CD3 detected by FITC-conjugated secondary antibody (II.8.7). Images were recorded with a Leica DMLB fluorescence microscope and CCD camera.

II.10.3 *Ex vivo* perfusion and intravital microscopy of murine carotid arteries

In order to study the MIF-mediated leukocyte arrest on early atherosclerotic endothelium, we performed cell adhesion assays under flow conditions in murine carotid arteries. Preparation for *ex vivo* perfusion of murine carotid arteries was performed as described (Huo *et al.* 2001). *Apoe*$^{-/-}$, *Mif*$^{+/+}$*Ldlr*$^{-/-}$ and *Mif*$^{-/-}$*Ldlr*$^{-/-}$ mice were fed an atherogenic diet containing 21% fat (0.15% cholesterol, 19.5% casein; Altromin, Germany) for 6 weeks. Wild-type *Mif*$^{+/+}$ and *Mif*$^{-/-}$ mice were treated with TNF-α (1 µg) by i.p. injection 4 h before perfusion experiments. The common carotid artery and the internal branch were ligated and a catheter was inserted through incision of the common carotid artery cranial to the suture. Arteries were transferred onto the stage of an Olympus BX51 microscope equipped with a saline immersion 20× objective and superfused with PBS at 37°C. MonoMac6 cells labeled with calcein-AM were pre-treated with CXCR2, CD74 mAbs or isotype control or the artery was perfused with blocking MIF mAb NIHIIID.9 (60 µg/mL) for 30 min. Arteries were perfused with monocytic cells (10^6/mL) in MOPS-buffer at a flow rate of 4 µL/min using a syringe pump (GENIE; Kent Scientific Corporation,

Litchfield) and adhesive interactions with the vessel wall (arrest, rolling) were recorded by stroboscopic epifluorescence illumination (Drelloscop 250; Drello, Mönchengladbach, Germany). At 10 min of perfusion, cells not moving for >30 s were defined as firmly adherent, and arrest was quantified in all segments of the artery.

For *in vivo* microscopy, the left carotid artery was surgically exposed in anesthetized mice 4 h after i.p. injection of TNF-α (1 µg/ml) and rhodamin G (100µL 0.02%; Molecular Probes) was administered into the lateral tail vein. After 30 min, adhesive interactions of labeled leukocytes with the common carotid artery were visualized *in situ* using a Zeiss Axiotech microscope (water immersion objective; Zeiss, Munich, Germany) with a 100 W HBO mercury lamp for epi-illumination (Osram, Eichstätt, Germany). The number of cells adherent to the artery wall was quantified in at least three fields of observation at 20× magnification.

II.10.4 Bone marrow repopulation

For bone marrow transplantation femurs and tibias were aseptically removed from donor *Cxcr2*$^{-/-}$ or *BALB*/c control mice. Marrow cavities were flushed and single cell suspensions prepared. Donor cells (3×10^6) were administered by tail vein injection into 6-8 week old *Mif*$^{+/+}$ or *Mif*$^{-/-}$ mice 24 h after an ablative dose of whole-body irradiation (2x6 Grays (Gy)).

Model of acute inflammation in the peritoneal cavity

Wildtype C57BL/6 mice reconstituted with *Cxcr2*$^{+/+}$ or *Cxcr2*$^{-/-}$ bone marrow cells were injected i.p. with 200 ng MIF in sterile PBS. After 4 h, the peritoneal exudate was harvested by an i.p. lavage with sterile PBS. The number of immigrated neutrophils was analyzed by quantifying the number of Gr-1$^+$CD115$^-$F4/80$^-$ cells by flow cytometry using fluorochrome-conjugated mAbs detecting CD115, Gr-1, F4/80 or appropriate IgG isotype controls (II.5.2).

II.11 Data illustration and statistical analysis

Graphs display results as mean ± SEM of 3 to 10 independent experiments, if not indicated otherwise. To compare data, one-way analysis of variance (ANOVA) and Newman-Keuls post-hoc test or an unpaired Student's t-test with Welch's correction was performed using GraphPad Prism 4. Differences with at least $P<0.05$ were considered as statistical significant.

III Results

III.1 The Role of YB-1 in RANTES-mediated atherosclerosis

III.1.1 YB-1 binds to a Y-box in the RANTES promoter

To detect additional regulatory elements involving YB-1 within the RANTES promoter, its sequence was compared with those of the Y-boxes of the MMP-2 and the DNA polymerase α gene. A sequence with homologies with known YB-1 binding motifs was identified within the proximal RANTES sequence between -204 and -173 base pairs from the start codon, containing several matching nucleotides but also an inverted repeat motif (Fig. III.1.1). In the preliminary investigation, an electrophoretic mobility shift assay using nuclear extracts of HASMC and rYB-1 was performed. The gel electrophoresis revealed that YB-1 bound to the biotin-labeled RANTES promoter element (Fig. III.1.2).

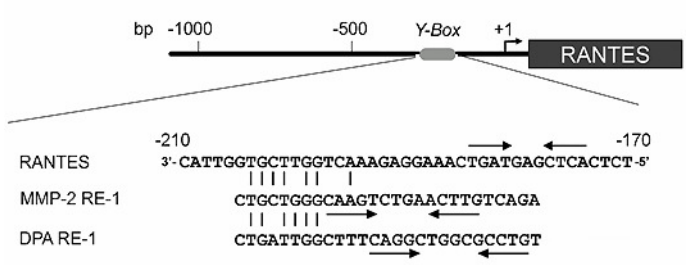

Fig. III.1.1: YB-1 recognition elements in the RANTES promoter. Sequence alignment of the proximal CCL5/RANTES gene promoter with known YB-1 binding motifs in the MMP-2 and DNA-polymerase α (DPA) genes revealed similarities of the sequence -210/-170 bps with known YB-1 binding motifs, that are matching nucleotides within the Y-box and the presence of a 3' localized inverted repeat motif (indicated by arrows).

While recombinant YB-1 bound to the single-stranded proximal sense (SS1) (Fig. III.1.2, A, lane 4) and antisense (SS2) promoter region (Fig III.1.2, A, lane 6), no binding to a double-stranded DNA probe (DS) was observed (Fig. III.1.2, A, lane 2). Specificity of binding was confirmed by inhibition of YB-1 binding to the single stranded antisense probe in the presence of homologous competitor DNA (hom.C) at 500-fold molar excess (Fig. III.1.2, A, lane 7-9). Complex formation of the same mobility with the single stranded antisense probe was observed when testing nuclear extracts derived from SMC (NE_{SMC}) (Fig. III.1.2, A, lane 10). Furthermore, the SS2-NE_{SMC} complex mobility was

supershifted with a YB-1 specific antibody (Fig. III.1.2, B, lane 2), supporting the assumption that YB-1 functions in the regulation of RANTES promoter activity.

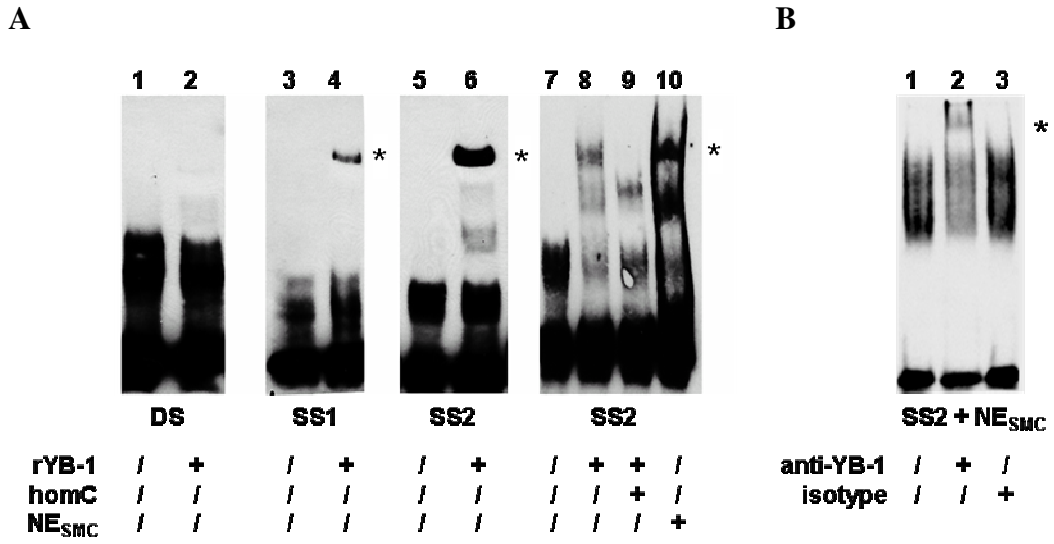

Fig. III.1.2: Conventional DNA binding studies (EMSA) demonstrated binding of rYB-1 to the RANTES promoter element. Synthetic DNA-probes corresponding to the sense as well as antisense strands of the RANTES promoter sequences -204/-173 were end-labeled with biotin in order to visualize the bands by streptavidin-horseradish peroxidase conjugate and chemiluminescent substrate. Sense (SS1) and antisense (SS2) strands of the -204/-173 element were preferentially bound by YB-1 as compared to the double-stranded probe (DS) (compare lane 2 with lanes 4 and 6, complex indicated by *). Specificity of binding was confirmed by diminished bands after inclusion of homologous competitor DNA (homC.) (lane 9). With SMC nuclear extract (NE_{SMC}) a complex of the same mobility formed with the antisense strand (SS2) probe (lane 10). (C) Binding of a YB-1 specifc Ab resulted in a supershift of the SS2/NE_{SMC} complex (lane 2) while the isotype control did not bind to the complex (lane 3).

III.1.2 The increased expression of YB-1 and RANTES correlate in inflammatory SMC

Because an upregulation of chemokines has been identified in neointimal SMC with a pro-inflammatory phenotype (Jordan et al. 1997), the expression of YB-1 and RANTES in rat SMC isolated from the media and neointima of balloon-injured aortas was determined. Indeed, RANTES mRNA expression was markedly increased in neointimal SMC compared with medial cells, as determined by quantitative real time-PCR analysis. In parallel, the expression of YB-1 mRNA was increased 3- to 4-fold in neointimal versus medial rSMC (Fig. III.1.3), suggesting a role for YB-1 in the regulation of RANTES in injured or pro-inflammatory SMC.

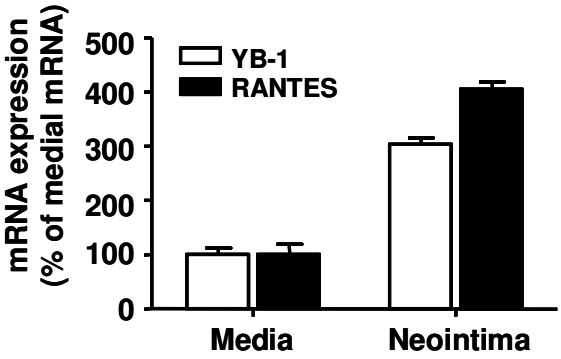

Fig. III.1.3: YB-1 and RANTES expression correlated in inflamed rSMC. The expression of YB-1 and RANTES in both neointimal and medial rat SMC was examined by real time-PCR. Results represent two experiments in duplicate.

III.1.3 YB-1 controls the transcriptional activity and protein expression of RANTES in HVSMC

In order to study regulatory effects of YB-1 on RANTES expression in human VSMC, a luciferase reporter assay was employed (Fig. III.1.4). Whereas transfection with empty vector pGL3 alone had no effect, transfection with a reporter construct harbouring the proximal 1014 base pairs (full-length) of the RANTES promoter (pGL3/RANTES) caused a moderate increase in luciferase activity (Fig.III.1.4, A). Co-transfection with YB-1 (pSG5/YB-1) and pGL3/RANTES led to a significant induction of luciferase activity in hSMC. The induction by YB-1 was almost completely attenuated in cells co-transfected with a plasmid coding for a reporter construct with a truncated RANTES promoter lacking the Y-box (pGL3/-168). Conversely, luciferase activity conferred by the full-length promoter pGL3/RANTES was significantly inhibited by co-transfection of YB-1 shRNA (Fig. III.1.4, B). To determine the efficiency of YB-1 knock-down, a real time-PCR was performed with the shRNA transfected cells. An about 50% decrease of YB-1 mRNA was achieved by shRNA transfection (Fig. III.1.4, C).

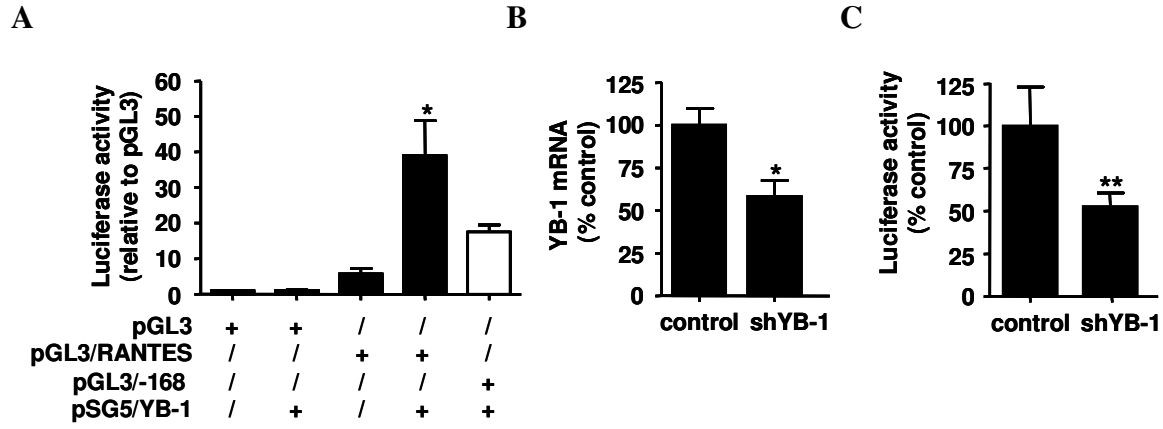

Fig. III.1.4: YB-1 induced RANTES promoter activation in human HVSMC. The effect of YB-1 on RANTES promoter activation in human SMC was determined using a luciferase reporter assay. (A) HVSMC were co-transfected with pSG5/YB-1 to overexpress YB-1 and vector without promoter (pGL3), reporter construct with full-length RANTES promoter reporter (pGL3/RANTES) or with truncated promoter (pGL3/-168). Overexpression of YB-1 increased RANTES promoter activation (*P<0.05, when compared to pGL3/RANTES transfected cells). (B) Knock-down of YB-1 by shRNA (shYB-1) significantly reduced promoter activity in hSMC.). Both pGL3/RANTES and pSuperduper co-transfected HVSMC served as controls (**P<0.01, when compared to control). (C) Transfection of HVSMC with YB-1 shRNA (shYB-1) resulted in a 50% decrease in YB-1mRNA compared to control-transfected cells (*P<0.05, when compared to control).

Next the effect of YB-1 transfection (pSG5/YB-1) on RANTES mRNA and protein expression was studied by real time-PCR analysis and ELISA. Overexpression of YB-1 mRNA in transfected hSMC was associated with a marked up-regulation of RANTES mRNA levels compared to control cells transfected with empty vector pSG5 (Fig. III.1.5, A). Similarly, RANTES protein secretion was significantly increased in HVSMC overexpressing YB-1 and inhibited by shRNA knock-down of YB-1 (shYB-1, Fig. III.1.5, B).

As other cells in addition to SMC are involved in atherosclerotic lesion formation, the RANTES promoter regulation by Yb-1 was also tested in the murine macrophage cell line RAW264.7. In contrast to SMC, the luciferase reporter assay revealed a negative effect of YB-1 on RANTES promoter activity (Fig. III.1.6). YB-1 overexpression reduced the basal luciferase activity in pGL3/RANTES transfected cells. To stimulate RANTES promoter activation the macrophages were stimulated with (100U/mL) IFN-γ. This activation was significantly down-regulated by YB-1.

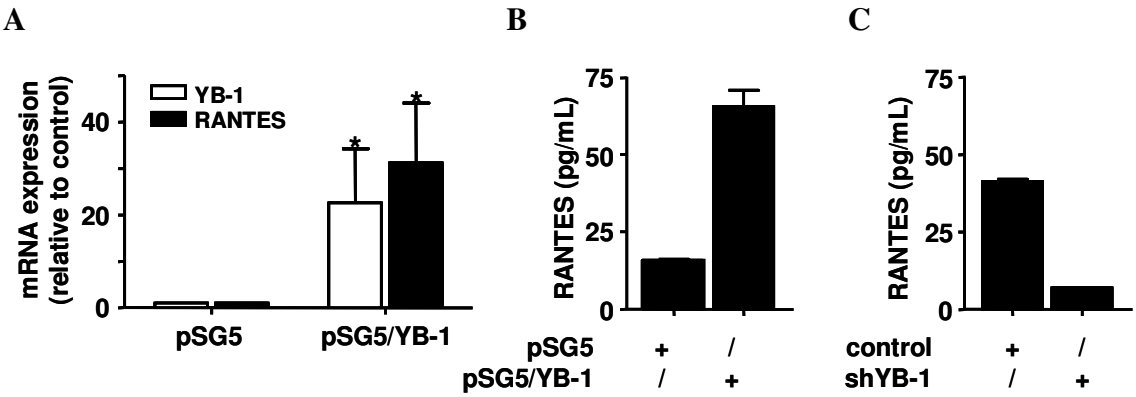

Fig.III.1.5: YB-1 induced RANTES expression in HVSMC. (A) RANTES and YB-1 expression in HVSMC 48 h after transfection with the YB-1 overexpression vector pSG5/YB-1 was examined via real time-PCR. Both RANTES and YB-1 mRNA levels were increased after transfection (*P<0.05, when compared with control transfectants). (B) The level of RANTES protein in HVSMC supernatants was increased with YB-1 overexpression as determined by ELISA. (C) YB-1 knock-down via shRNA transfer led to an attenuated RANTES expression compared to pSuperduper (control) transfected cells. Results represent 2 independent experiments in duplicate (B and C).

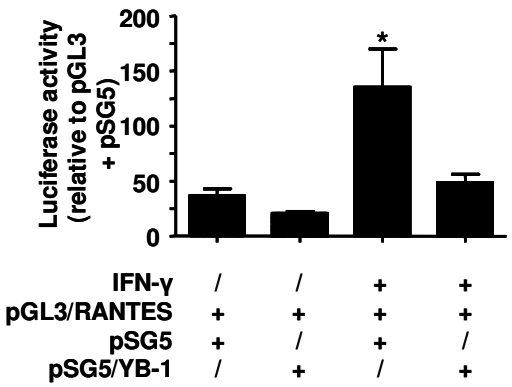

Fig. III.1.6: YB-1 inhibited RANTES promoter activity in the macrophage cell line RAW264.7. A luciferase reporter assay was performed with RAW264.7 cells. Cells were transfected with the RANTES reporter construct and pSG5 control vector or YB-1 overexpression vector pSG5/YB. Luciferase activity was measured in those transfectants with or without IFN-γ stimulation; (*P<0.05, when compared with pSG5/YB-1 transfected IFN-γ stimulated cells).

III.1.4 YB-1 induces monocyte adhesion by regulating RANTES expression in HCASMC

As RANTES has been established to control monocyte recruitment (von Hundelshausen et al. 2001; Schober et al. 2002), the role of YB-1-mediated RANTES expression in MonoMac6 cell arrest on coronary artery SMC (HCASMC) was analyzed under flow conditions (Fig. III.1.7). Compared to vector-transfected controls, transfection of HCASMC monolayers with pSG5/YB-1 to overexpress YB-1 significantly increased monocyte arrest. This increase was mediated by YB-1-induced RANTES protein expression, as evidenced by the inhibition after pre-treatment of MonoMac6 cells with the

RANTES receptor antagonist Met-RANTES. Thus, YB-1-mediated RANTES expression supported increased monocyte recruitment.

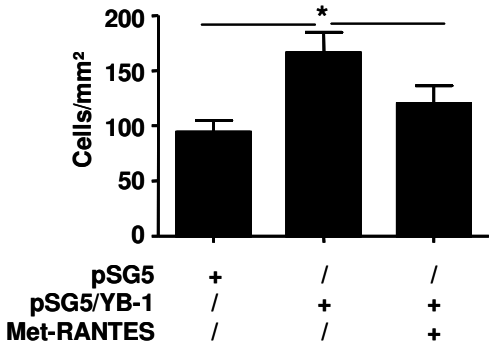

Fig. III.1.7: YB-1-mediated RANTES triggered monocyte arrest under shear flow. HCASMC were transfected with the pSG5/YB-1 and grown in 35 mm² dishes until confluence. The cell monolayers were perfused with calcein AM-labeled MonoMac6 cells at 1.5 dyne/cm^2. Adherent MonoMac6 cells were counted after 2 min of perfusion; (*P<0.05, when compared to control transfectants or Met-RANTES treated CASMC).

III.1.5 Knock-down of YB-1 protects against neointima formation

Because YB-1 and RANTES mRNA levels are up-regulated in inflammatory neointimal SMC (Fig. III.1.3), the next aim was to investigate the role of YB-1 in atherosclerotic lesion formation. Therefore an *in vivo* mouse model of accelerated atherosclerosis was employed. Carotid arteries of *Apoe*$^{-/-}$ (Ccr5$^{+/+}$), Met-RANTES-treated *Apoe*$^{-/-}$ and *Ccr5*$^{-/-}$*/Apoe*$^{-/-}$ mice were luminally transfected with lentiviral shRNA targeting YB-1 or empty vector immediately after wire-induced endothelial denudation injury (performed by Ilze Bot, Institute of Biopharmaceutics, Leiden University, The Netherlands). Lentiviral shRNA transfer led to an approximately 2.5-fold decrease of YB-1 expression in *Apoe*$^{-/-}$ mice as revealed by immunofluorescence (Fig. III.1.8 and Fig. III.1.9). The expression of YB-1 and RANTES was colocalized in neointimal cells but also in medial cells of carotid arteries after injury, and lesional RANTES expression was almost completely abolished after knock-down of YB-1 in H1.shYB-1-treated arteries (Fig. III.1.8, A). Of note, YB-1 in vascular lesions was predominantly expressed in colocalization with α-SMA$^+$ SMC (Fig. III.1.8, B), but not with Mac-2+ macrophages (Fig. III.1.8, C).

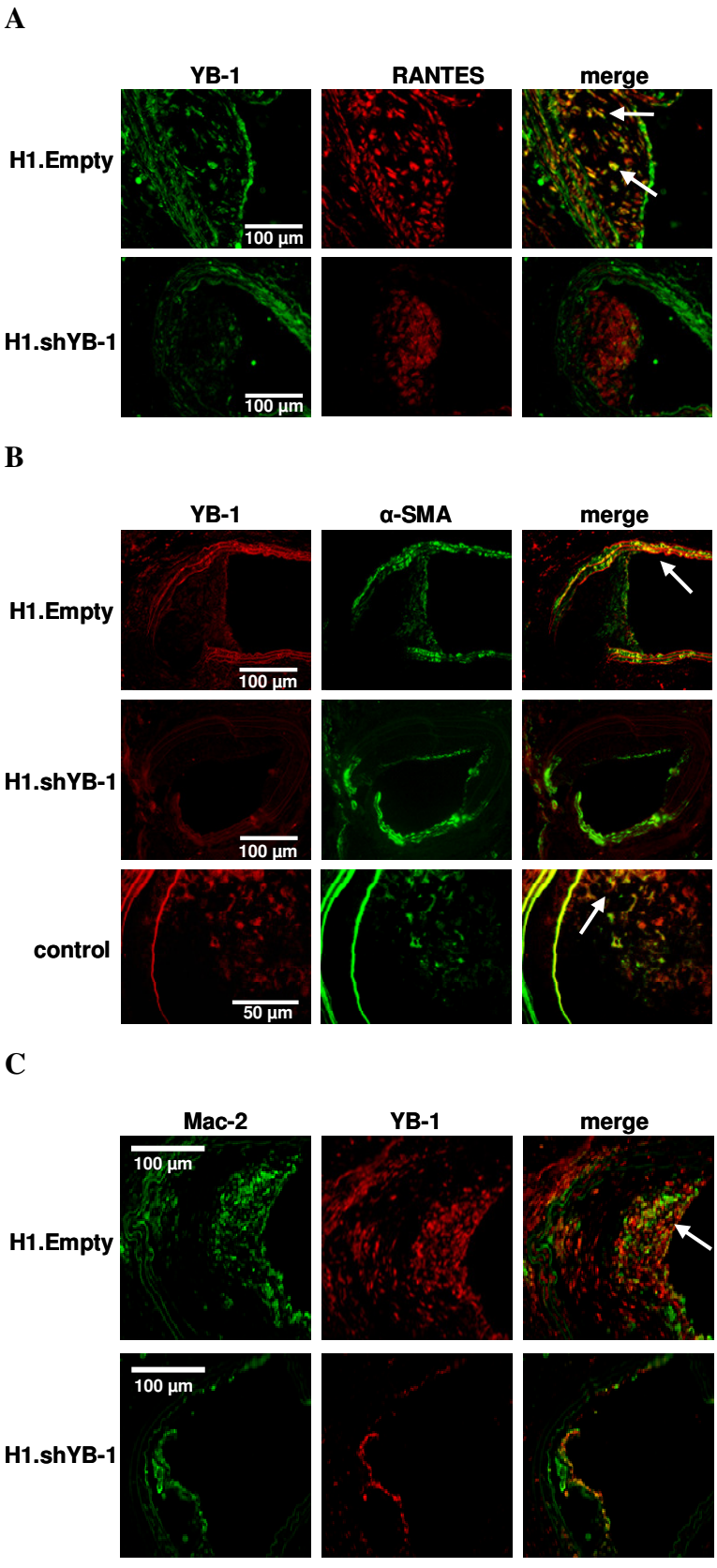

Fig. III.8: YB-1 colocalized with RANTES and the SMC marker α-SMA in lesions of murine carotid arteries. Serial sections of control and H1.shYB-1-treated carotid arteries were stained for YB-1 and RANTES, α-SMA or Mac-2.
(A) Double immunofluorescence staining for YB-1 and RANTES revealed their co-expression in the neointima of control (H1.empty) carotid arteries (arrows).
(B) Doublestaining for YB-1 and α-SMA demonstrated a strong YB-1 expression in medial (arrow) area of control transfected carotid arteries, as well as in the neointimal area of untransfected vessels (control, arrow).
(C) No relevant colocalization of YB-1 with the macrophage marker Mac-2 was found in the plaque area (C; arrow). YB-1 and RANTES expression was markedly reduced in H1.shYB-1-treated arteries (A-C).

Analysis of the lesional areas in the carotid artery after 4 weeks revealed a significant reduction in the neointima and media in YB-1 shRNA (H1.shYB-1) in comparison to control (H1.empty)-treated *Apoe*$^{-/-}$ animals (Fig. III.1.9). YB-1 knock-down in Met-RANTES-treated or *Ccr5*$^{-/-}$*/Apoe*$^{-/-}$ mice did not lead to a significant change in the media and neointima size compared to empty vector-treated animals (Figure III.1.10), indicating that the YB-1 effect on atherosclerotic lesion formation is mediated through RANTES alone.

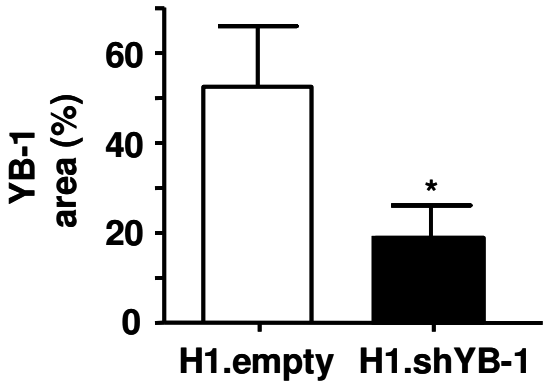

Fig III.1.9: YB-1 expression in the lesional area in *Ccr5*$^{+/+}$ H1.shYB-1 treated animals was significantly reduced. Analysis of 5-6 sections of 5 carotid arteries by immunofluorescence staining for YB-1 revealed that the expression was 2.5-fold higher in H1.empty-treated vessels compared to arteries with YB-1 knock-down (*P<0.05, when compared with H1.empty-transfected carotid arteries).

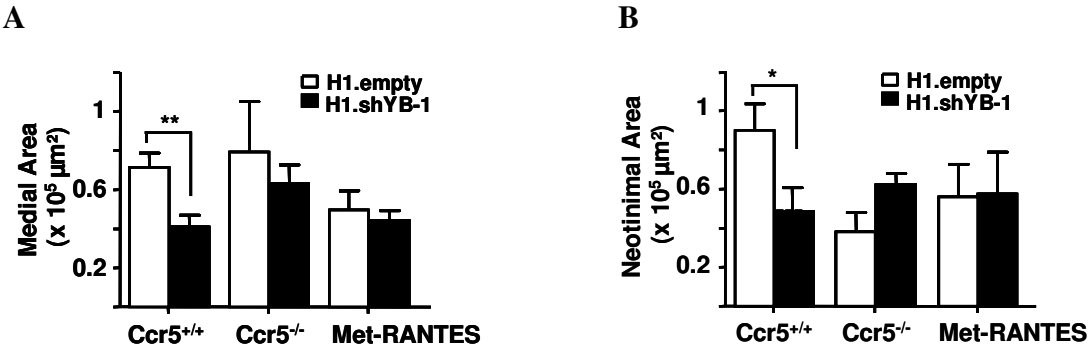

Fig. III.1.10: Vascular remodelling after wire injury was RANTES-mediated. Serial tissue sections of carotid arteries were stained with Movat's pentachrome, and the medial (A) and neointimal (B) area was analyzed. Treatment of *Apoe*$^{-/-}$ (*Ccr5*$^{+/+}$) carotid arteries with H1.shYB-1 showed a significant decrease in both the medial and neointimal area (*P<0.05, when compared with H1.empty-transfected carotid arteries; **P<0.01, when compared with H1.empty-transfected carotid arteries). *Ccr5*$^{-/-}$ and Met-RANTES-treated animals displaced a similarly reduced neointimal area as the *Ccr5*$^{+/+}$ mice, which were treated with YB-1 shRNA (B), but the plaque area was not further reduced, when those carotid arteries were treated with H1.shYB-1.

The infiltration of macrophages in the lesion is a major event in atherosclerosis progression. Therefore, the macrophage content in carotid arteries with and without lentiviral knock-down was compared in *Apoe*$^{-/-}$ mice. As shown in Fig. III.1.11, the inhibition of vascular remodelling in H1.shYB-1-treated *Apoe*$^{-/-}$ mice was associated with a significant decrease in the medial and neointimal content of Mac-2^{+} macrophages in H1.shYB-1- compared to H1.empty-transfected carotid arteries.

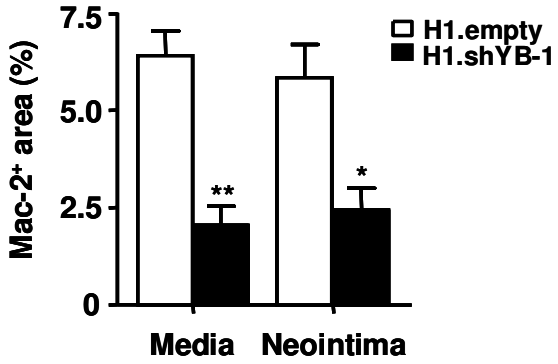

Fig. III.1.11: The macrophage content in lesions with YB-1 knock-down was significantly reduced. Serial tissue sections were stained for the macrophage marker Mac-2. Macrophage infiltration in the lesional area (media and neointima) of H1.shYB-1-treated carotid arteries 4 weeks after wire injury were compared with H1.empty-transfected carotid arteries; (*P<0.05 and **P<0.01, when compared with H1.empty-transfected carotid arteries).

III.1.6 Interference with chemokine functions or regulation mechanisms

The above-presented study intented to find out, if and how YB-1 is involved in RANTES expression regulation and how this regulation affects RANTES-mediated atherosclerosis. Unsterstanding the expression regulation of a chemokine is one important step towards finding a suitable therapeutic target. Nevertheless, a direkt blockade of the chemokine receptor activation or the interaction of a chemokine or CLF chemokine with other molecules by small molecule antagonists may also be a promising approach to the treatment or various diseases. The following study intented to identify a receptor for the CLF chemokine MIF and novel chemokine functions of the CLF chemokine MIF, as well as new insights in MIF's impact on atherogenesis.

III.2 The CLF chemokine MIF and atherosclerotic lesion formation

III.2.1 MIF triggers monocyte arrest in flow through CXCR2

Due to the findings that the MIF monomer bears a structural resemblance to the IL-8 dimer (Fig. I.4) (Sun *et al.* 1996) and given the fact that Gro-α, IL-8 and their receptor CXCR2 have been identified as major ligand-receptor pairs promoting monocyte arrest (Gerszten *et al.* 1999; Weber *et al.* 1999), a flow adhesion assay, using blocking mAbs and pertussis toxin (PTX), was employed to explore whether MIF-induced monocyte arrest was dependent on $G_{\alpha i}$ protein-coupled activities of CXCR2. Confluent HAoEC were pretreated with MIF for 2 h to immobilize it on the monolayer surface (Fig. III.2.1). Then, calcein-stained monocytes or cells of the MonoMac6 cell line were perfused over the cell monolayer at 1.5 dyn/cm², resembling physiological shear flow. MIF presentation provoked a substantial increase in the arrest of primary monocytes and MonoMac6 cells after 2 min of perfusion, an effect specifically blocked by a MIF mAb (Fig. III.2.2). The MIF-triggered but not spontaneous monocyte arrest was ablated by the CXCR2 mAb or PTX, consistent with the established role of $G_{\alpha i}$ activity in chemokine receptor signaling. Furthermore, mAbs against the classical CXCR2 agonist chemokines Gro-α and IL-8 did not interfere with the arrest-promoting function of MIF (Fig. III.2.2, A).

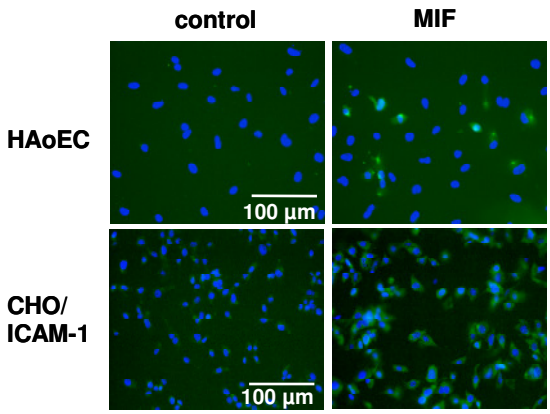

Fig. III.2.1: MIF was immobilized on the cell surface of HAoEC and CHO/ICAM-1 cells. Immunofluorescence using a rabbit MIF antiserum, followed by the respective FITC-conjugated mAb, revealed surface presentation of MIF (green; blue: cell nuclei) on HAoEC and CHO/ICAM-1 cells after pretreatment for 2 h. In contrast, MIF was absent in buffer-treated cells (control).

To further exclude the presence of CXC chemokines (e.g. with an ELR-motif) specialized in triggering integrin-dependent arrest, CHO cells expressing the β2 integrin ligand ICAM-1 were also employed as a model system to dissect the mechanisms utilized

by MIF to promote monocytic cell arrest (Fig. III.2.3). Under flow conditions, ICAM-1 expression supported the constitutive arrest of MonoMac6 cells. Exposure of the CHO transfectants to MIF for 2 h led to its immobilization on the cell surface (Fig. III.2.2) and, similar to exposure with IL-8, increased monocytic cell arrest (Fig. III.2.3, A). MIF-induced adhesion was fully sensitive to PTX and inhibited by a blocking β2 mAb (Fig. III.2.3, A), confirming the role of $G_{\alpha i}$ signaling in β2 integrin-mediated arrest induced by MIF. Both primary monocytes and MonoMac6 cells express the IL-8 receptors CXCR1 and CXCR2 (Weber et al. 1999). While a blocking CXCR1 mAb had no significant effect and blocking CXCR2 substantially but not fully attenuated the arrest functions of MIF, combining these mAbs completely inhibited monocytic cell arrest triggered by MIF. In addition to CXCR2, the MIF-binding membrane protein CD74 was involved in MIF-induced monocyte arrest, as shown by mAb inhibition (Fig.2.3, B). None of the mAbs significantly inhibited spontaneous arrest (data not shown). This clearly indicates that CXCR2 mediates the arrest function of MIF. Moreover, fully efficient arrest appeared to involve adjuvant functions of CD74 and, to a minor extent, CXCR1.

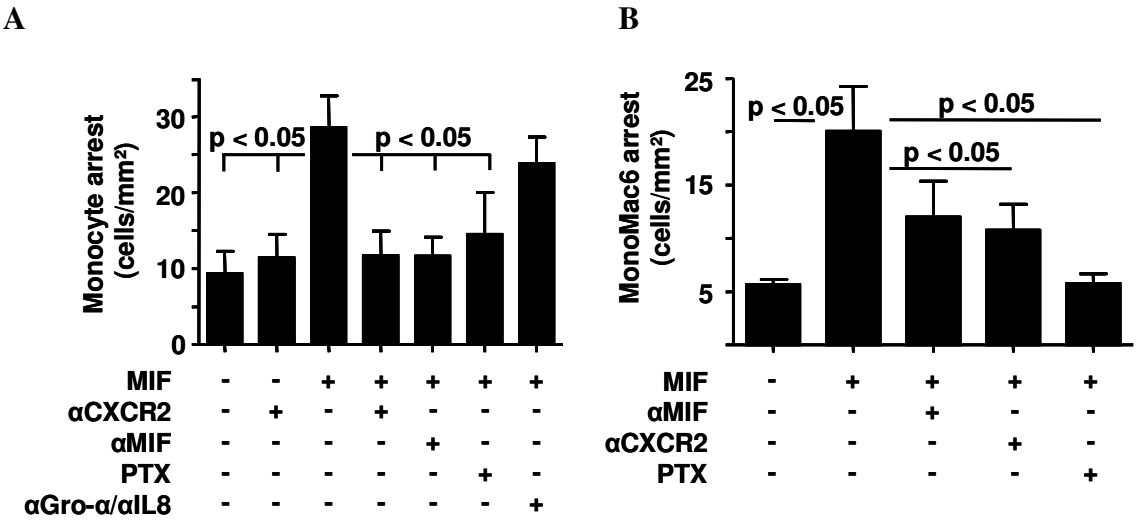

Fig. III.2.2: MIF-triggered arrest of monocytes and monocytic MonoMac6 cells on endothelial cells was mediated by CXCR2. Human aortic endothelial cells were perfused with human primary monocytes (A) and cells of the human monocytic MonoMac6 cell line (B). Adherent HAoEC monolayers were preincubated with or without recombinant MIF (50 ng/mL) for 2 h and perfused with monocytic cells at a flow rate of 1.5 dyn/cm² for 2 min. MIF-mediated arrest of primary monocytes or MonoMac6 cells was inhibited by pretreatment with mAbs to MIF or CXCR2, or with pertussis toxin (PTX) as indicated. Monocyte arrest is expressed as cells/mm². The blocking mAbs against Gro-α and IL-8 did not have an effect on MIF-triggered monocyte arrest (A).

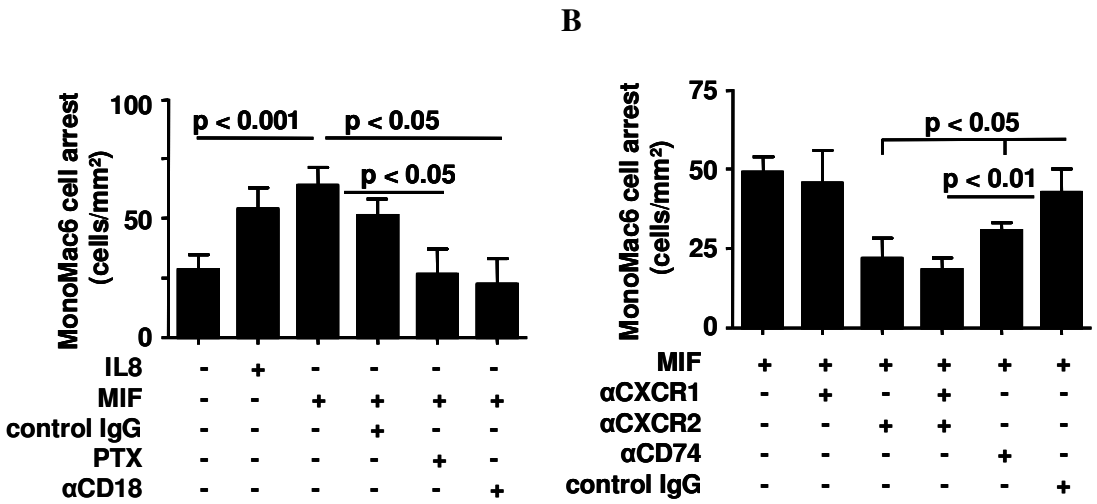

Fig. III.2.3.: β2 integrin-mediated arrest induced by MIF was abolished by PTX and αCXCR2 and αCD74 mAbs. MIF-treated CHO/ICAM-1 monolayers were perfused with MonoMac6 cells at 1.5 dyn/cm^2 for 2 min. Binding to vector-transfected CHO cells was subtracted. (A) MIF provoked a similar adherence of the cells as IL-8 and cell arrest was significantly blocked by PTX or the antibody TS1/18, which specifically binds the β2-subunit of αLβ2. (B) MIF-mediated MonoMac6 arrest was monitored after pre-treatment with blocking mAbs against CXCR1 and/or CXCR2 or CD74.

III.2.2 MIF triggers T cell arrest in flow through CXCR4

The next aim was to evaluate whether the potential ligand function of MIF extends to other CXCRs. Isolated and activated T cells do not express CXCR2 or the expression is very low (Cockwell *et al.* 2002; Takata *et al.* 2004), but MIF has been shown to activate T cells and to induce signaling processes through Src-family kinases (Calandra and Roger 2003; Lue *et al.* 2006). Since the CXCR4 ligand SDF-1α has been implicated in integrin-dependent arrest of T cells via the Src-family kinase p56^{lck} (Feigelson *et al.* 2001; Weber *et al.* 2001), flow adhesion assays were performed to explore if MIF can act through CXCR4. MIF or SDF-1α immobilized on HAoEC triggered the arrest of primary human IL-2-stimulated effector T cells. MIF-induced but not spontaneous T cell arrest was inhibited by a mAb against CXCR4 and was sensitive to PTX (Fig. III.2.4, A). Presentation of MIF or SDF-1α on CHO/ICAM-1 transfectants supported the αLβ2-dependent arrest of Jurkat T cells, an effect specifically inhibited by blocking CXCR4 (Fig. III.2.4, B).

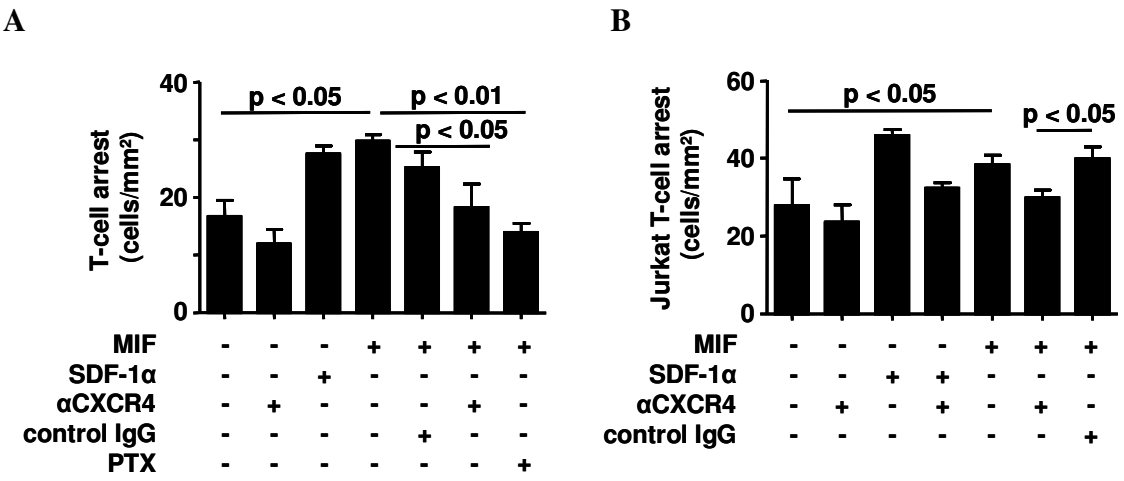

Fig. III.2.4: MIF triggered T cell adhesion on CHO/ICAM-1 monolayers through CXCR4. MIF-treated CHO/ICAM-1 monolayers were perfused with primary human T cells and Jurkat T cells at 1.5 dyn/cm^2 for 2 min. Then firmly adherent cells were counted. Binding to vector-transfected CHO cells was subtracted.

Since MonoMac6 cells and primary monocytes showed a strong CXCR2-dependent response to MIF stimulation, Jurkat T cells that do not express endogenous CXCR2 (Fig.III.2.5, A), were transiently transfected with pcDNA3.1/CXCR2, and flow experiments were performed with these cells 48 h after transfection. CXCR2 expression was confirmed via FACS analysis prior to the experiments (Fig. III.2.5, B). As revealed by the arrest data (Fig. III.2.6), ectopic expression of CXCR2 in Jurkat T cells further increased MIF-triggered arrest corroborating that CXCR2 imparts enhanced responsiveness to MIF in leukocytes.

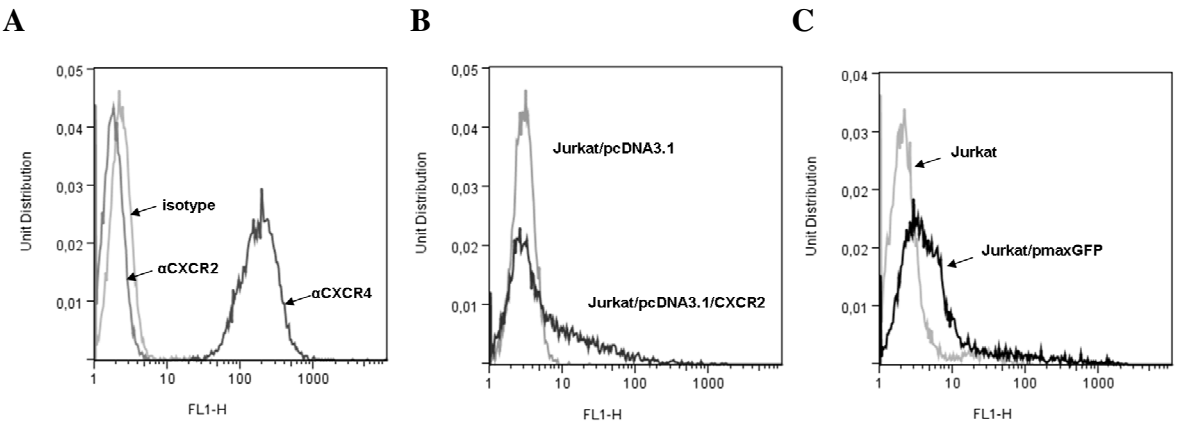

Fig. III.2.5: FACS analysis of Jurkat cells. (A) Jurkat cells were stained for CXCR2 and CXCR4, or treated with isotype control. (B) Jurkat cells were transfected with control vector (Jurkat/pcDNA3.1) or CXCR2 expression vector (Jurkat/pcDNA.3.1/CXCR2) via the Amaxa Nucleofector device. After 24 h, CXCR2 expression was confirmed by an αCXCR2/FITC mAb. (C) Transfection efficiency was determined by transfection of the Jurkat cells with a provided vector coding for the green fluorescent protein (pmaxGFP); Transfection efficiencies were ~70%.

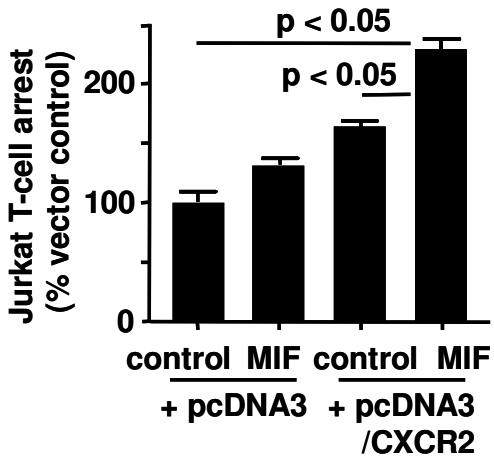

Fig. III.2.6: CXCR2 expression led to an increased T cell arrest in response to MIF. Jurkat T cells were transfected with the CXCR2 overexpression vector pcDNA3/CXCR2. 48 h afterwards, the cells were perfused over CHO/ICAM-1 cell monolayers. Cell arrest is given in % of empty vector transfectant cells.

Further experiments to elucidate the role of CXCR2 receptor in MIF action were performed using murine L1.2 pre-B lymphoma cells transfected to express either CXCR1, CXCR2, or CXCR3, and controls expressing endogenous Cxcr4 only. These experiments were carried out in the presence or absence of the CXCR4 antagonist AMD3645. Expression of CXCR1, CXCR2 and CXCR3 was verified prior to the flow adhesion experiments (data not shown). While MIF triggered the arrest of the CXCR2 transfectants and Cxcr4 expressing cells with similar efficacy as the *bona fide* ligands IL-8 and SDF-1α, the CXCR1 and CXCR3 transfectants were only responsive to IL-8 and IP-10, respectively, but did not respond to MIF (Fig. III.2.7). These results establish that CXCR2

and CXCR4 but not CXCR1 or CXCR3 support MIF-induced arrest functions.

Besides the arrest function, the chemotactic activity is a crucial feature of chemokines causing blood cells to transmigrate through the vessel wall to sides of inflammation. In parallel to the flow adhesion experiments, transmigration assays were performed by the members of the Institute of Biochemistry under supervision of Jürgen Bernhagen. According to the results of the cell arrest in shear flow, MIF displayed chemokine-like functions by stimulating monocyte, T cell and neutrophil chemotaxis through CXCR2 and CXCR4 (Bernhagen *et al.* 2007).

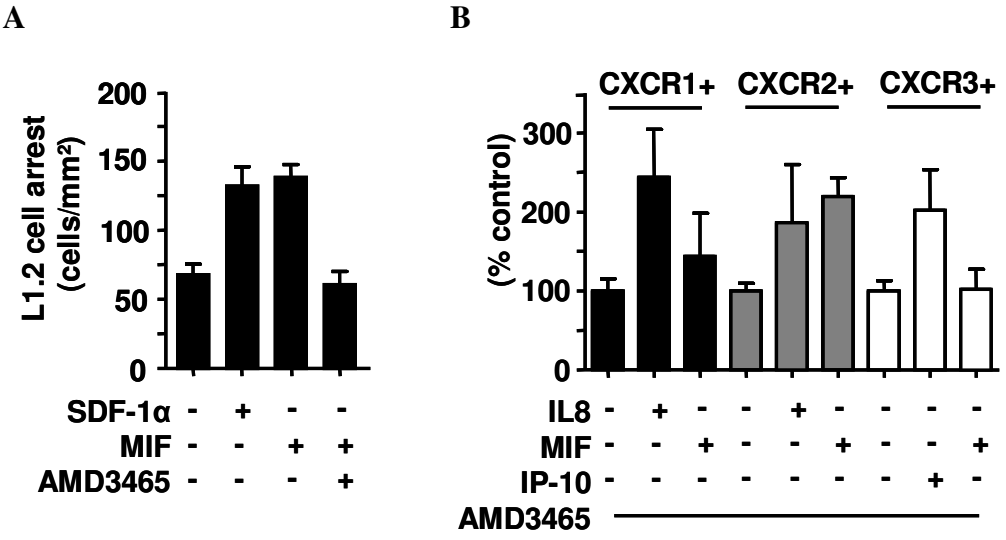

Fig. III.2.7: MIF induced cell arrest through CXCR2 and CXCR4, but not through CXCR1 or CXCR3. SVECs were perfused with L1.2 transfectants stably expressing CXCR1, CXCR2 or CXCR3, and with controls expressing only endogenous CXCR4, in the presence of the CXCR4 antagonist AMD3465. Arrest is quantified as cells/mm² (A) or as percentage of control cell adhesion (B). Data are results from one representative experiment (n = 3 measurements) of four experiments.

III.2.3 MIF triggers rapid activation of leukocytes

To investigate if MIF induces other typical arrest chemokines engaging CXCR2, HUVEC and HAoEC were incubated with MIF (50 ng/mL) for 2 h. The expression of the CXCR2 ligands IL-8 and Gro-α was determined via real-time-PCR (Fig. III.2.8) IL-8 protein concentration in cell supernatants were detected with an ELISA (Fig III.2.8). TNF-α-treated cells served as positive controls. In contrast to TNF-α, pre-incubation of HAoEC and HUVEC with MIF for 2 h did not show an increase in IL-8 or Gro-α mRNA expression. Also, the IL-8 concentration in cell supernatants of both cell types was not increased after MIF incubation.

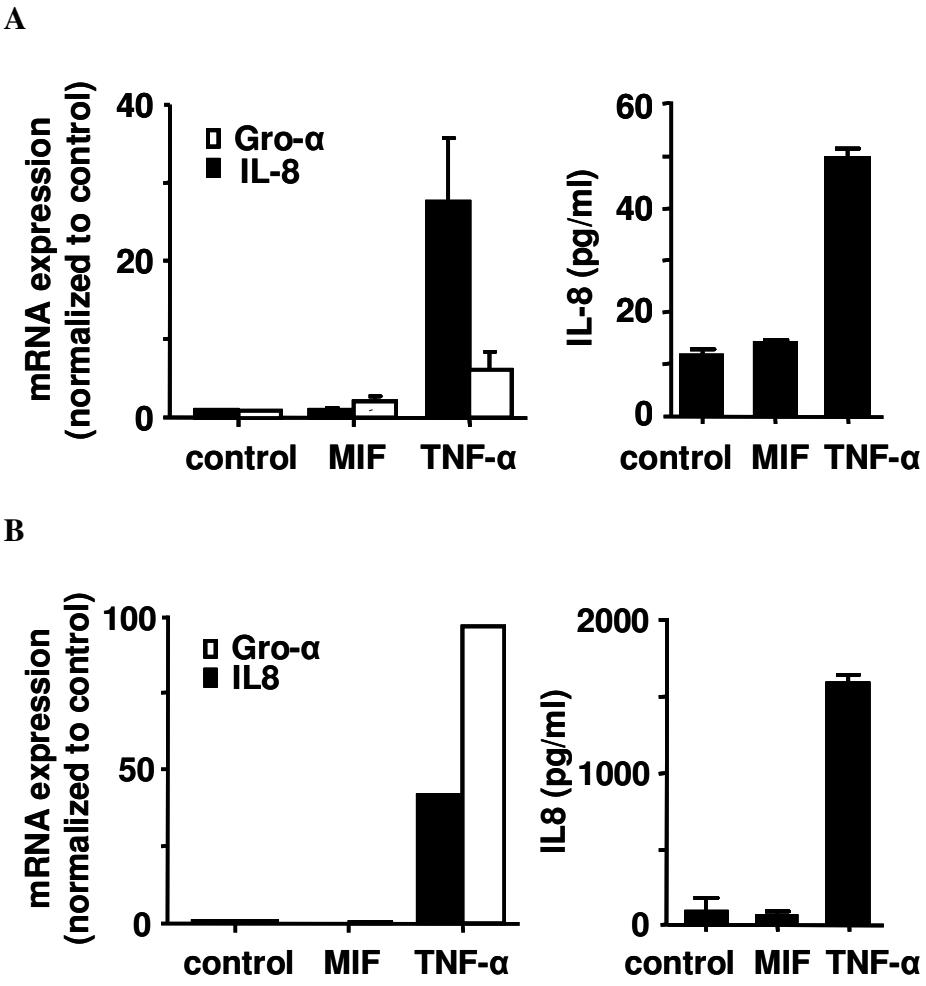

Fig. III.2.8. 2 h incubation with MIF did not lead to expression of typical CXCR2 ligands. HUVEC (A) or HAoEC (B) were stimulated with MIF or TNF-α or left untreated for 2 h, the expression of transcripts for the arrest chemokines IL-8 or Gro-α was analyzed by real-time PCR and normalized to control cells (left panel), and IL-8 protein was determined in the supernatants by ELISA (right panel). Three independent experiments were performed in duplicate. (B) Left panel shows one representative experiment of three independent experiments.

A direct short-term exposure to chemokines in solution or coated in juxtaposition to integrin ligands, e.g. vascular cell adhesion molecule (VCAM)-1 has been shown to stimulate rapid and transient up-regulation of integrin activity to mediate leukocyte arrest (Grabovsky *et al.* 2000; Chan *et al.* 2001). Integrin activation by immobilized or endothelial-bound chemokines is accomplished by induction of clustering (e.g. for α4β1) or of an extended conformation (e.g. for αLβ2) immediately preceding ligand binding. Accordingly, stimulation of monocytic cells with MIF in solution for 1-5 min triggered αLβ2-dependent arrest on CHO/ICAM-1 cells similar to IL-8 (Fig. III.2.9).

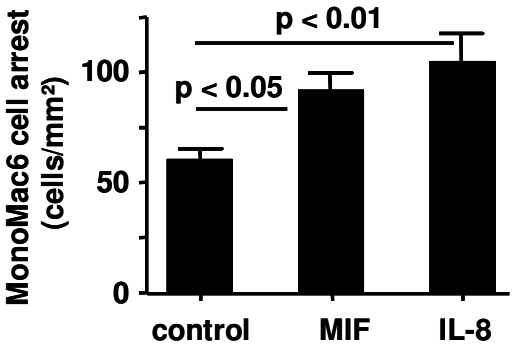

Fig. III.2.9: Direct stimulation of MonoMac6 cells with MIF triggered αLβ2-dependent arrest. MonoMac6 cells were stimulated with MIF (250 ng/mL) directly in solution and immediately perfused over CHO/ICAM-1 monolayers. Adhering cells were counted after 2 min. IL-8 (100 ng/mL) served as positive control.

Evidence for a direct stimulation of monocyte integrins was obtained by assays using the reporter mAb 327C, which recognizes an activation epitope corresponding to the extended high affinity conformation of αLβ2. MonoMac6 cells and primary monocytes were stimulated with MIF and fixed with PFA at certain time points. The activation of the αLβ2 integrin was analyzed via flow cytometry. This revealed that MIF-induced αLβ2 activation occurred as early as 1 min after exposure and persisted for 30 min in MonoMac6 cells (Fig. III.2.10, A). In isolated human blood monocytes, the activation of αLβ2 by MIF peaked at 2 min and also persisted for 30 min (Fig. III.2.10, B). To evaluate whether stimulation by MIF was restricted to αLβ2, monocytic cell arrest in flow on a VCAM-1 substrate was examined. VCAM-1 supports firm adhesion in conjunction with active α4β1. Exposure to MIF for 1-5 min triggered substantial arrest, which was mediated by CXCR2/CD74 and α4β1, as shown by mAb inhibition (Fig. III.2.11, A). In contrast, blocking CXCR2 did not affect arrest of resting cells. As for SDF-1α, stimulation of Jurkat

T cells with MIF for 1-5 min triggered CXCR4-dependent adhesion on VCAM-1 (Fig. III.2.11, B).

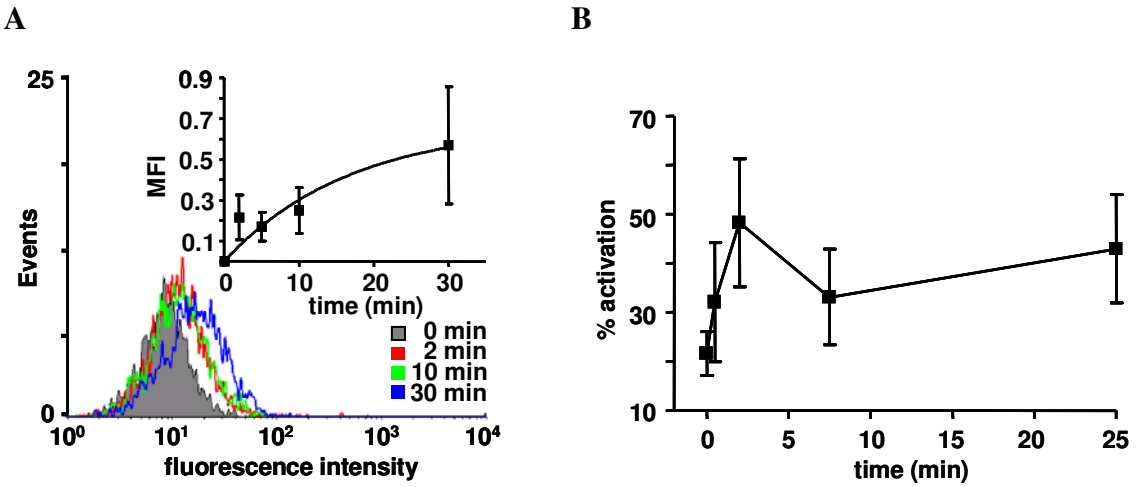

Fig. III.2.10: MIF triggered rapid activation of αLβ2 on primary monocytes and MonoMac6 cells. (A) Cells of the MonoMac6 cell line were stimulated with MIF for the indicated times. αLβ2 activation was detected by the 327C antibody and monitored by FACSAria. The activation is expressed as the increase in mean fluorescence intensity (MFI). (B) The same experiment was performed with primary monocytes isolated from PBMC. Here, data are expressed relative to maximal activation with Mg^{2+} and EGTA.

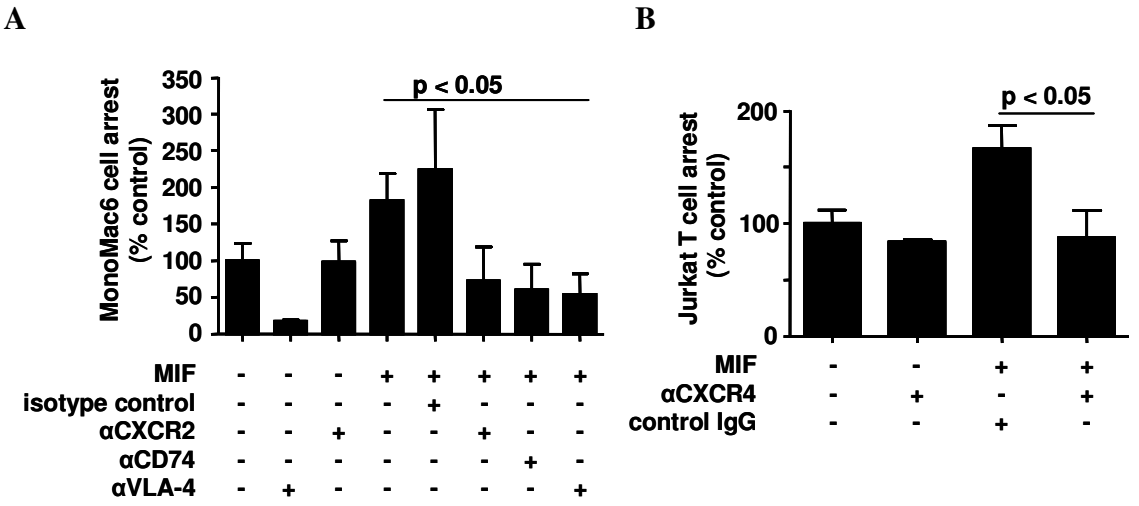

Fig. III.2.11: MIF-triggered cell arrest on VCAM-1 substrate was dependent on CD74, CXCR2, and CXCR4. (A) MonoMac6 cells were pretreated with mAbs to α4β1 (αVLA-4) , CXCR2, CD74, and stimulated with MIF for 1 min and perfused on immobilized VCAM-1.Fc at 1.5 dyne/cm2 for 5 min. (B) MIF-triggered Jurkat T cell arrest on VCAM-1 substrate was tested with or without a mAb to CXCR4 or isotype control.

Since CXCR2 is known to mediate increases in cytosolic calcium in response to IL-8 in leukocytes or transfectants (Jones *et al.* 1997), the next aim was to study the ability of MIF to induce calcium influx. To do so, neutrophils were stained with the fluorescent dye

Fluo-4 AM, which exhibits an increase in MFI when it binds Ca^{2+}. After addition of MIF (50 ng/mL), the cells were immediately analyzed in the FACSAria. MIF induced rapid calcium influx in primary human neutrophils and desensitized calcium transients in response to IL-8 and MIF, while IL-8 fully desensitized calcium signals both in response to IL-8 and MIF (Fig. III.2.12), indicating that MIF rapidly activates a GPCR/$G_{\alpha i}$ signaling pathway. The partial desensitization of IL-8 signals observed with MIF in neutrophils parallels findings with other CXCR2 ligands and likely reflects the presence of CXCR1, as MIF fully desensitized calcium influx in neutrophils that was induced by the sole CXCR2 ligand Nap-2 (Fig. III.2.12).

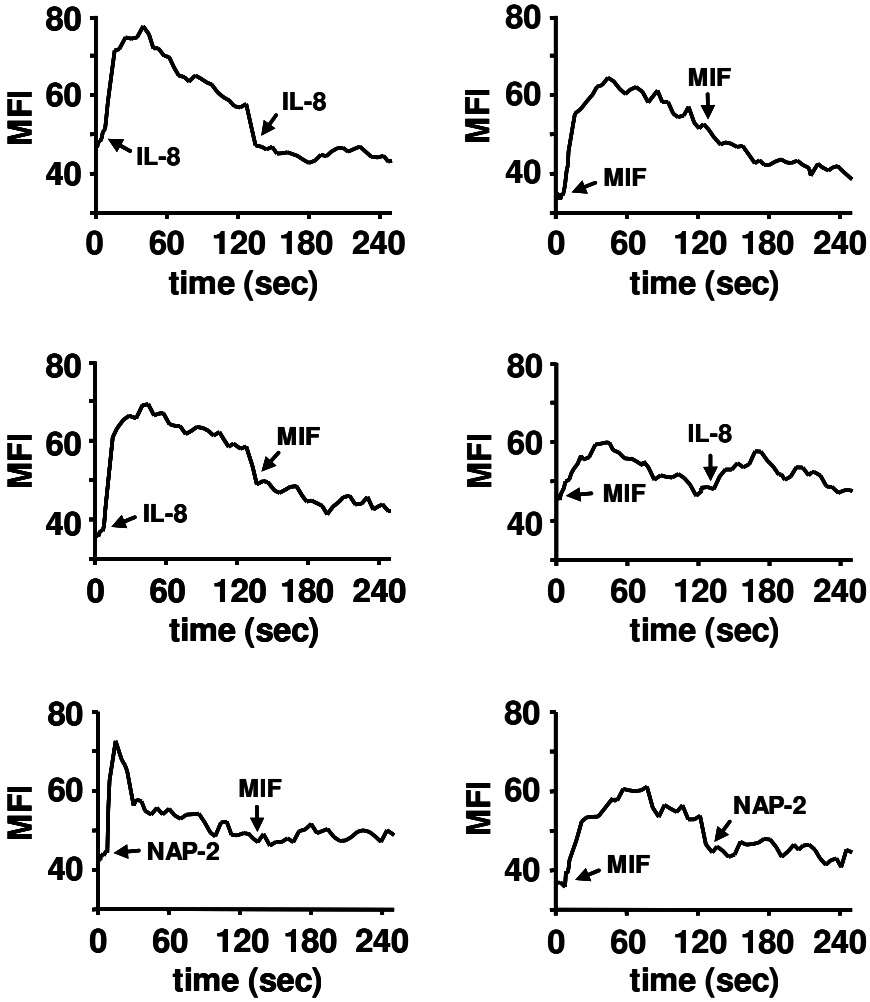

Fig. III.2.12: MIF induced rapid calcium mobilization in neutrophils. Neutrophils were stimulated with MIF, IL-8 or NAP-2 as indicated and calcium-derived mean fluorescence intensity was recorded by flow cytometry (FACSAria) for 0-240 sec. For homologous and heterologous desensitization, IL-8, NAP-2 or MIF was added 120 sec before successive stimulation with IL-8 or MIF and vice versa. The traces shown are representatives of 4 independent experiments.

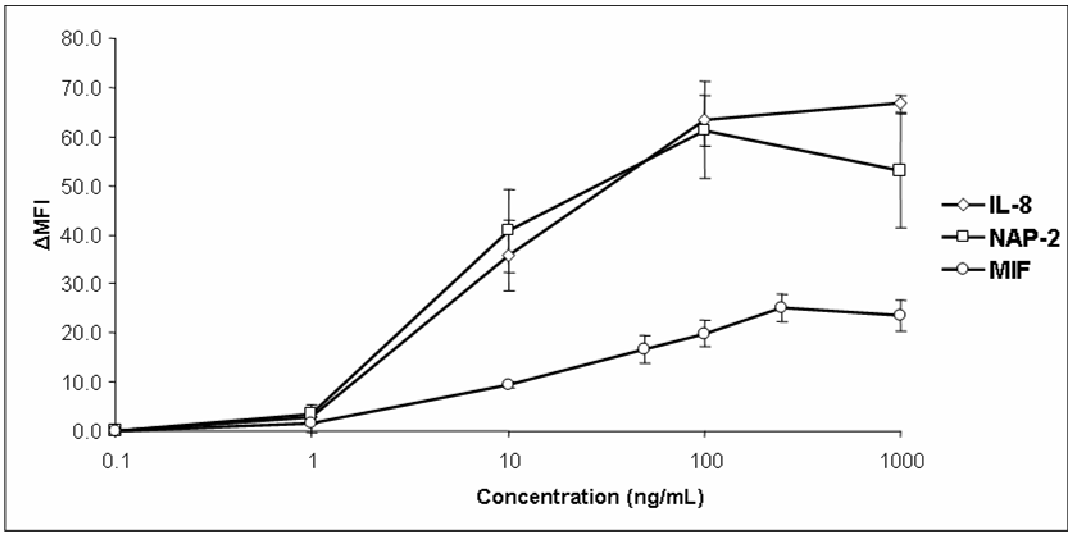

Fig. III.2.13: Dose-response curves of calcium influx triggered by IL-8, NAP-2 and MIF in L1.2/CXCR2 transfectants. L1.2 cells stably expressing CXCR2 were treated with the denoted concentrations and the change in MFI due to calcium influx was measured and recorded with the FACSAria. Data are expressed as the difference between baseline and peak MFI.

To compare MIF potency in calcium mobilization with other CXCR2 ligands, L1.2/CXCR2 transfectants were employed (Fig. III.2.13). In those transfectants, MIF dose-dependently induced calcium influx with the greatest cell response at a concentration of 250 ng/mL. MIF was less potent and effective than IL-8 and NAP-2, which both caused the highest calcium influx at 100 ng/mL.

III.2.4 MIF directly binds to the chemokine receptor CXCR2

To corroborate its interaction with CXCR2, the binding of fluorescein-labeled MIF (250 ng/mL) to HEK/CXCR2 cells compared to vector-transfected HEK cells was analyzed via flow cytometry (Fig. III.2.14, A). HEK/CXCR2 transfectants, but not vector controls, supported direct binding of labeled MIF. To support the results of the FACS analysis, coimmunoprecipitations with vector controls and CXCR2-transfectants were performed. The cells were incubated with biotinylated MIF (250 ng/mL), lyzed and biotin-MIF/protein complexes were captured with streptavidin-coated beads. Western blot analysis proved the binding of MIF to CXCR2 (Fig. III.2.14, B).

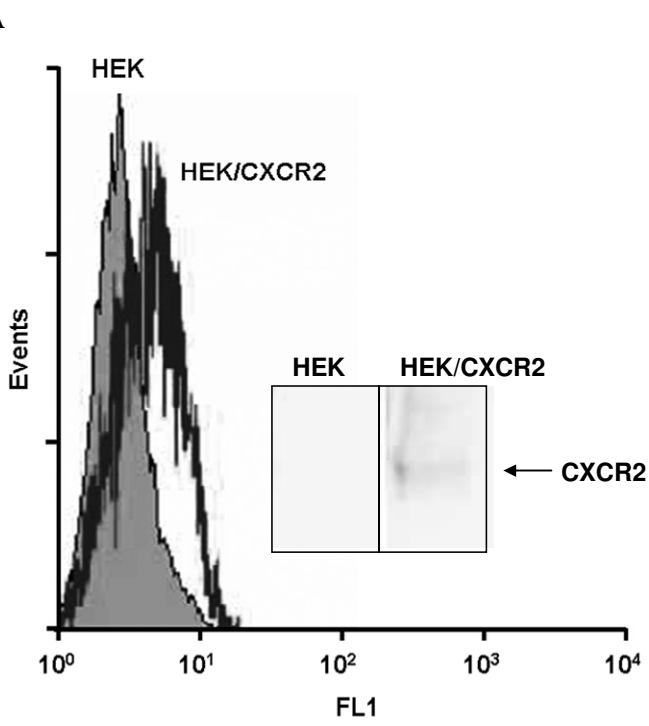

Fig. III.2.14: MIF bound to the chemokine receptor CXCR2. HEK and HEK/CXCR2 cells were incubated with biotin- or fluorescein-labeled MIF for 30 min on ice. (A) Binding of fluorescein-MIF to HEK/CXCR2 transfectants or vector controls (HEK) was analyzed by FACS. (B) Coimmunoprecipitation was performed with HEK and HEK/CXCR2 cells incubated with biotinylated MIF. Binding of biotin-MIF to CXCR2 was assessed by Western blot using the αCXCR2 RII115 after streptavidin pull-down from HEK/CXCR2 transfectants versus vector controls.

III.2.5 CXCR2 forms a complex with CD74

CD74 is a receptor for MIF as discovered earlier (Leng et al. 2003). The results above demonstrate that MIF triggers leukocyte arrest through CD74 and CXCR2 (and to a lesser extend through CXCR4), leading to the assumption that there is a receptor complex involved in MIF action. To clarify if CXCR2 and CD74 form complexes on the cell surface, coimmunoprecipitations with cells of the murine B-lymphoma cell line L1.2 stably expressing CXCR2 and transiently transfected with pcDNA/his-CD74 were performed. After pull-down of CXCR2, complexes with CD74 were detected via Western blot (Fig. III.2.15). In contrast, no complexes were observed in protein precipitates with L1.2 controls or the isotype control.

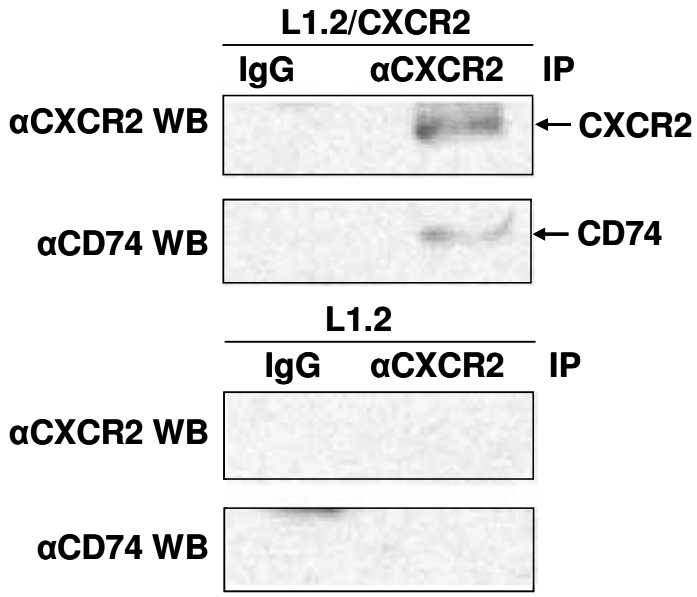

Fig. III.2.15: Coimmunoprecipitation of a CXCR2/CD74 complex. Coimmunoprecipitation was performed with precleared lysates of L1.2 cells stably expressing CXCR2 (right) and untransfected cells (left). Pull-down was done with a CXCR2-specific mAb or respective isotype control (IgG). CXCR2 (upper right) and CD74 (lower right) were detected in the protein precipitates of L1.2/CXCR2 cells as assessed by western blotting. No CXCR2 or CD74 was detected in L1.2 protein precipitates.

III.2.6 CXCR2 mediates MIF-induced monocyte arrest on atherosclerotic endothelium

The importance of MIF in the development of atherosclerosis and neointimal hyperplasia has been established by mAb blockade and genetic deletion. Furthermore, the murine CXCR2 ligand KC (IL-8 homologue) is crucial in eliciting α4β1-dependent monocyte accumulation in *ex vivo*-perfused carotid arteries of *Apoe*$^{-/-}$ mice with early atherosclerotic endothelium (Huo *et al.* 2001). To elucidate wether MIF/CXCR2 interactions are involved in monocyte accumulation in inflamed arteries, the induction of atherogenic recruitment by MIF and CXCR2 was tested in this *ex vivo* perfusion system. Carotid arteries of *Apoe*$^{-/-}$, *Mif*$^{+/+}$ and *Mif*$^{-/-}$ mice fed an atherogenic diet for 6 weeks were perfused *ex vivo* with fluorescence-labeled human MonoMac6 cells. Adhesive interactions with the atherosclerotic vessel wall were recorded using fluorescence illumination.

Monocyte arrest in carotid arteries of *Apoe*$^{-/-}$ mice fed a high-fat diet for 6 weeks was inhibited by a blocking mAb to Cxcr2, and by mAbs to CD74 and MIF (Fig. III.2.16), indicating that besides KC, MIF contributed to atherogenic recruitment via Cxcr2, and via CD74. A similar pattern for the blockade of MIF, Cxcr2 or CD74 was observed for

monocyte arrest in carotid arteries of wild-type mice treated with TNF-α for 4 h as a model of acute vascular inflammation (Fig. III.2.16, B). Inhibitory effects of CD74 mAb were attenuated and blocking MIF was ineffective in arteries of TNF-α-treated *Mif*$^{-/-}$ mice, while a remaining inhibition of Cxcr2 suggested an involvement of other TNF-α-inducible ligands (Fig. III.2.16, C).

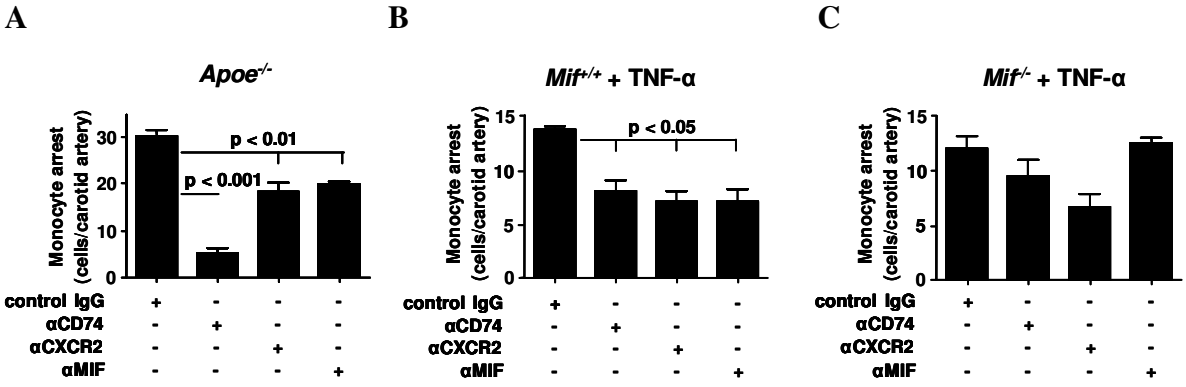

Fig. III.2.16: MIF-driven monocyte arrest in inflamed or atherosclerotic arteries involved CXCR2 and CD74. (A) Carotid arteries of *Apoe*$^{-/-}$ mice fed a western diet for 6 weeks were pre-perfused with a αMIF antibody solution or isotype control. Then the arteries were perfused with MonoMac6 cell treated with mAbs to CD74, CXCR2, isotype control (B, C) The same experiment with carotid arteries from wild-type (*Mif*$^{+/+}$) and *Mif*$^{-/-}$ mice 4 h after intraperitoneal injection of TNF-α; At 10 min MonoMac6 cells not moving for 30 sec were defined as firmly adherent. Cells were counted in 5–6 fields per carotid artery.

Compared to the effect of Mif deficiency observed with TNF-α stimulation, monocyte accumulation was more clearly impaired by Mif deficiency in arteries of *Mif*$^{-/-}$*/Ldlr*$^{-/-}$ mice versus atherogenic *Ldlr*$^{-/-}$ mice (Fig. III.2.17). A contribution of Cxcr2 was not apparent in the absence of Mif, and blocking Mif had no effect (Fig. III.2.17). In turn, both effects were restored by loading with exogenous MIF (Fig. III.2.17, C). Employment of the αCD74 mAb in *Mif*$^{-/-}$*/Ldlr*$^{-/-}$ carotid arteries led to a stronger inhibition of MonoMac6 arrest than αCXCR2 or αMIF mAbs, but all mAbs had a similar potency in reducing adhesion in MIF-treated carotid arteries (Compare Fig. III.2.17, B and C).

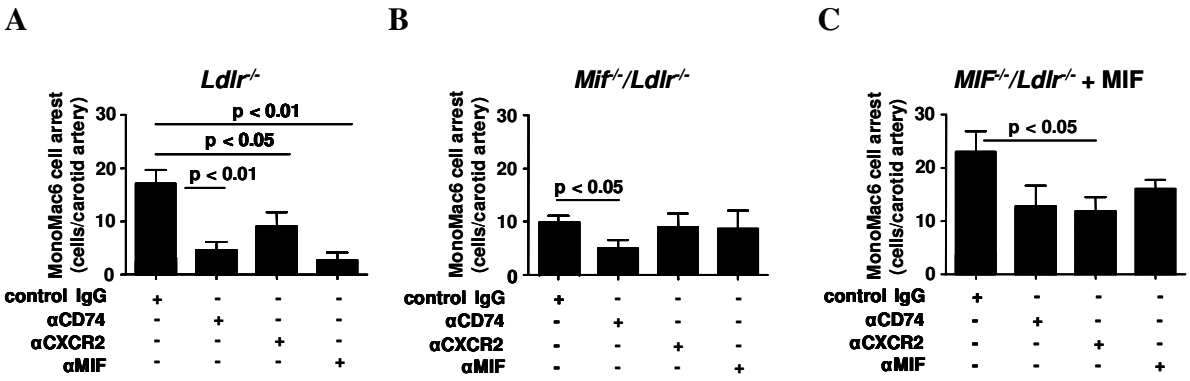

Fig. III.2.17: MIF-driven monocyte arrest in inflamed or atherosclerotic arteries involved CXCR2 and CD74. MonoMac6 cell arrest in carotid arteries from *Mif*$^{+/+}$*/Ldlr*$^{-/-}$ (designated *Ldlr*$^{-/-}$) and *Mif*$^{-/-}$*/Ldlr*$^{-/-}$ mice fed a western diet for 6 weeks; (C) Carotid arteries of *Mif*$^{-/-}$*/Ldlr*$^{-/-}$ mice were loaded with MIF for 2 h before perfusion with MonoMac6 cells. After 10 min, adherent cells in 5–6 fields per carotid artery were counted.

To further examine the relevance of CXCR2 for MIF-mediated monocyte recruitment *in vivo*, intravital microscopy on carotid arteries of chimeric wild-type and *Mif*$^{-/-}$ mice reconstituted with wild-type or *Cxcr2*$^{-/-}$ bone marrow was performed (Fig. III.2.18). 4 h following the i.p. injection of 1µg TNF-α, the accumulation of rhodamine-labeled leukocytes was evaluated. *Mif*$^{-/-}$ mice with wild-type bone marrow displayed an attenuated cell arrest, as compared to wild-type mice. The deficiency in bone marrow *Cxcr2* was associated with a more marked reduction in leukocyte accumulation in chimeric wild-type mice than in *Mif*$^{-/-}$ mice.

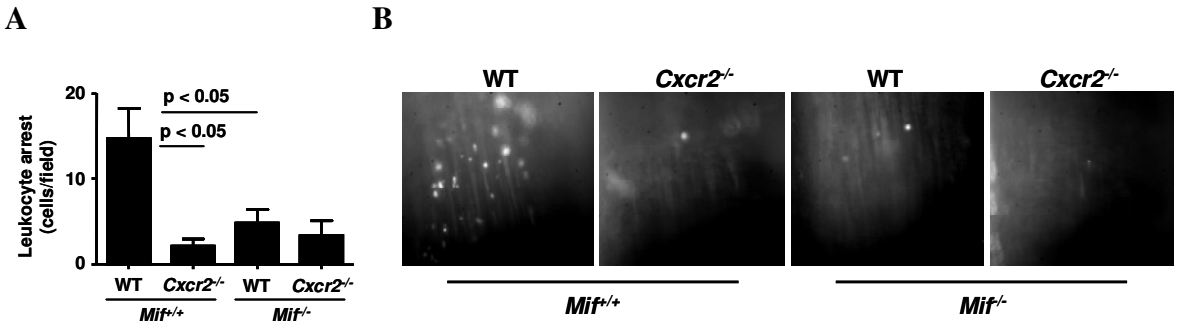

Fig. III.2.18: MIF-mediated leukocyte adhesion *in vivo* was dependent on CXCR2. For intravital microscopy, *Mif*$^{+/+}$ and *Mif*$^{-/-}$ mice reconstituted with wild-type (WT) or *Cxcr2*$^{-/-}$ bone marrow were stimulated by intraperitoneal injection of TNF-α for 4 h, and the accumulation of leukocytes labeled by intravenous injection of rhodamine G was studied after 30 min in carotid arteries *in vivo* via epifluorescence microscopy. (A) Quantification of leukocyte arrest; representative images in B.

III.2.7 MIF-induced inflammation *in vivo* relies on CXCR2

To further probe the effects of MIF *in vivo*, a model of MIF-induced peritonitis in chimeric mice reconstituted with wild-type or $CXCR2^{-/-}$ bone marrow was employed. 4 h after i.p. injection of 200 ng MIF, the peritoneal exudate was harvested by an i.p. lavage with sterile PBS. The number of immigrated neutrophils was analyzed by quantifying the number of $Gr\text{-}1^{+}CD115^{-}F4/80^{-}$ cells by flow cytometry.

MIF elicited recruitment of neutrophils after 4 h in mice with wild-type bone marrow, demonstrating neutrophil responsiveness for MIF *in vivo* (Fig. III.2.19). Conversary, the deficiency in bone marrow CXCR2 abrogated MIF-stimulated peritoneal recruitment of neutrophils (Fig. III.2.19).

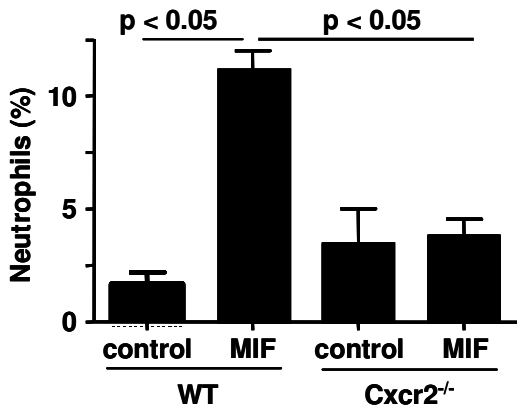

Fig. III.2.19: MIF and CXCR2 mediated inflammatory neutrophil recruitment *in vivo*. 4 h after intraperitoneal MIF injection in mice repopulated with wild-type (WT) or *Cxcr2*$^{-/-}$ bone marrow, the content of neutrophils in the abdominal cavity was evaluated by flow cytometry. MIF elicited neutrophil recruitment in mice repopulated with WT, but not *Cxcr2*$^{-/-}$ bone marrow.

III.2.8 MIF inhibition results in plaque regression

Since MIF can act through both CXCR2 and CXCR4 and given the documented role of MIF and CXCR2 in the development of atherosclerotic lesions, the next approach was to test whether targeting MIF could modify advanced lesions and their content of both CXCR2-expressing monocytes and CXCR4-expressing T cells. *Apoe*$^{-/-}$ mice, which had received a high-fat diet for 12 weeks and had developed substantial and advanced atherosclerotic lesions, were treated with neutralizing mAbs to MIF, to KC or to SDF-1α for 4 weeks. In the aortic root, blocking MIF but not KC or SDF-1α resulted in a marked reduction of plaque area compared to untreated mice at 16 weeks and a significant regression of plaque size compared to baseline at 12 weeks (Fig. III.2.20). Blocking MIF but not KC or SDF-1α was associated with a decreased content of both macrophages and

$CD3^+$ T cells at 16 weeks, indicating a more stable plaque phenotype (Fig. III.2.21).

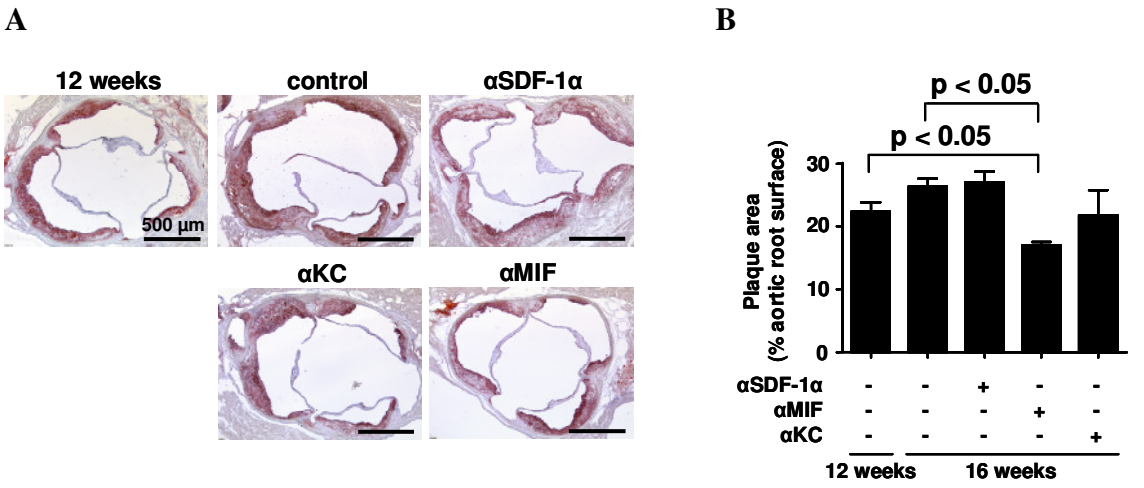

Fig. III.2.20: Blocking MIF led to a declined plaque area. *Apoe*$^{-/-}$ mice received a high-fat diet for 12 weeks and were subsequently treated with antibodies to Mif, KC or SDF-1α, or with vehicle (control) for an additional 4 weeks. Plaques in the aortic root were stained using Oil-Red-O. Blocking Mif but not KC or SDF-1α resulted in regression and stabilization of advanced atherosclerotic plaques. Representative images show the plaque area at baseline (12 weeks) and after 16 weeks. (B) Plaque area was quantified and given as % of the total aortic root surface.

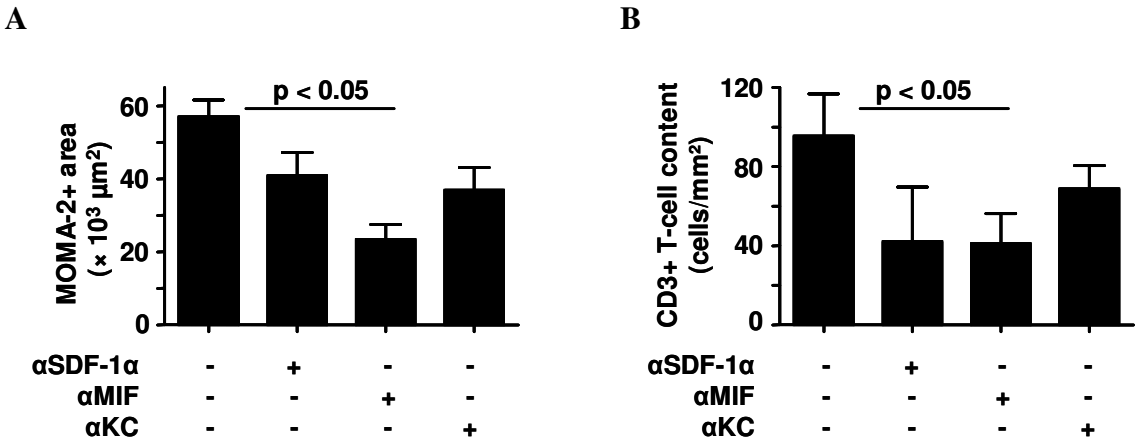

Fig. III.2.21: Targeting MIF led to a more stable plaque composition. Aortic root sections *Apoe*$^{-/-}$ mice (Fig. III.2.19) were stained with mAbs specific for the macrophage marker (MOMA2) and for the T-cell marker CD3. As revealed by quantifying the fluorescent cells, treatment with αMIF mAb lead to a significant decrease in macrophage and T-cell content.

IV Discussion

IV.1 Expression regulation of a chemokine involved in atherosclerosis

IV.1.1 YB-1 regulates RANTES expression

It has been previously reported that YB-1 affects the expression of various proliferative and inflammatory proteins, such as GM-CSF and MMP-2 at both the transcriptional and translational level (Mertens et al. 1997; Capowski et al. 2001). Depending on the cell-type, MMP-2 expression is up- or down-regulated by YB-1. Whereas YB-1 trans-activates the MMP-2 promoter in glomerular mesangial cells, the authors observed a YB-1-mediated repression of MMP-2 in the epithelial cells. Likewise, a cell-type-dependent repression of the RANTES gene by the proto-oncogene c-MYC has been described (Cappellen *et al.* 2007).

This work provides evidence that YB-1 upregulates RANTES expression in vascular SMC by the use of luciferase reporter assays, real time-PCR and ELISA. The knock-down of YB-1 by a shRNA resulted in diminished RANTES promoter activity, as well as in an inhibited secretion of RANTES by vascular SMC. The luciferase reporter experiments with the truncated promoter construct revealed that the region upstream of the -168 position was necessary for YB-1-mediated transcription activation. This finding is in concert with the EMSA results, which confirmed that YB-1 bound to the -204/-173 region of the RANTES promoter. Conversely, YB-1 seems to act as a trans-repressor for RANTES expression in macrophages, as YB-1 over-expression in RAW264.7 cells inhibited IFN-γ-induced activation of the RANTES promoter. Recently, Samuel *at al.* (2007) described an inhibitory effect of YB-1 on the MMP-13 expression by binding to AP-1 sites, suggesting that YB-1 is a new repressor in AP-1 target genes. It has also been shown that AP-1 and the NF-κB response elements participate in the LPS mediated activation of RANTES expression in macrophages (Hiura *et al.* 1999). Thus, YB-1 may repress RANTES gene activation in macrophages by binding to the AP-1 response element. Furthermore, repression might be due to preferential binding of YB-1 to single-stranded DNA, which can prevent other transcription factors from binding to enhancer regions in a cell-type specific manner, as has been described for the MHC class II genes (MacDonald *et al.* 1995).

YB-1 has been shown to synergistically interact with other transcription factors, including AP-2 and p65, a subunit of NF-κB (Raj *et al.* 1996; Mertens et al. 1998), and synergistic activators of the RANTES promoter have been described, including NF-κB, IRF-3 and IRF-7 (Genin et al. 2000). Besides the activation of RANTES in SMC by direct promoter binding, it is conceivable that YB-1 might also trans-activate other transcription factors that are involved in the regulation of RANTES, e.g. NF-κB and C/EBP (Miyamoto *et al.* 2000; Fessele et al. 2001).

IV.1.2 YB-1-regulated RANTES contributes to neointimal lesion formation

The capability of Met-RANTES to diminish diet-induced neointima formation after arterial injury in *Apoe*$^{-/-}$ mice and the protective effects of the deficiency in the RANTES receptor Ccr5 during injury-induced neointimal hyperplasia but also native and diet-induced atherosclerosis (Schober et al. 2002; Braunersreuther et al. 2007) has validated the chemokine RANTES to be of paramount importance in vascular pathophysiology and lesion formation. Thus, understanding the regulation mechanisms of the RANTES gene may provide a platform for therapeutic strategies of vascular diseases.

This study provides *in vivo* evidence that the expression of YB-1 is upregulated after injury and that it serves as a strong activator of RANTES expression in SMC. YB-1 knock-down using shRNA led to a significant decrease in neointimal and medial hyperplasia after injury, but also reduced macrophage infiltration. Interestingly, these *in vivo* effects of YB-1 knock-down during the process of remodeling resemble findings obtained on the injury-induced neointima formation in Met-RANTES-treated mice or in mice deficient in its receptor Ccr5 (Schober et al. 2002; Veillard et al. 2004; Zernecke *et al.* 2006). However, due to the fact that several chemokines, such as MCP-1 or IL-8, are non-redundantly involved in lesion formation (Weber et al. 2004), it is possible, that YB-1 effects are not exclusively mediated through the regulation of RANTES. This might be in line with the findings that the YB-1-induced monocyte arrest on SMC was not completely blocked by Met-RANTES. Moreover, besides SMC, platelets, macrophages and other cell-types not affected by YB-1 knock-down but involved in the pathogenesis of vascular remodeling may be an additional source of RANTES (Pattison et al. 1996; Schober et al. 2002).

Previously, YB-1 expression was shown to be upregulated in infarcted areas of the heart (Kamalov *et al.* 2005) and during mesangioproliferative renal disease, the latter being induced by PDGF-B via a mitogen-activated protein kinase-dependent signaling pathway in mesangial cells (van Roeyen et al. 2005). Furthermore, α-smooth muscle actin expression in lung myofibroblasts is YB-1 dependently up-regulated after exposure to thrombin or TGF (Zhang *et al.* 2005), Thrombin has also been shown to induce a cleavage-dependent activation of YB-1 protein and its nuclear translocation in endothelial cells, which can subsequently induce expression of the B chain isoform of platelet-derived growth factor (PDGF-B) (Stenina *et al.* 2000). Triggered by exposure of subendothelial matrix after endothelial-denudation injury, thrombotic events and thrombin formation might also contribute to the activation of YB-1 in this model. Since PDGF-B is also expressed after arterial injury and its inhibition is known to reduce neointima formation (Sirois *et al.* 1997; Deguchi *et al.* 1999; Raines 2004), it is not inconceivable that an auto-stimulatory loop of PDGF-B-mediated YB-1 activation may amplify the expression of PDGF-B, besides effects on RANTES expression, and may thus contribute to enhanced neointimal hyperplasia after injury. In addition, because several chemokines, such as MCP-1 and IL-8, are nonredundantly involved in lesion formation, and taking into account that the YB-1-induced monocyte arrest on SMCs was not completely blocked by Met-RANTES, one can assume that YB-1 effects were not mediated exclusively through regulation of RANTES. However, YB-1 knockdown in $Ccr5^{-/-}$ or Met-RANTES-treated mice did not lead to the expected further decline in plaque area, indicating that the contribution of YB-1 to neointima formation appears to require RANTES as a transcriptionally regulated mediator.

IV.1.3 Perspectives

This study demonstrates that YB-1 is a novel regulator of RANTES expression. An increased activity of YB-1 in inflammatory SMC and after arterial injury up-regulates the expression of RANTES and thereby controls the RANTES-mediated monocyte adhesion and contributes to neointimal lesion formation in atherosclerosis-prone *Apoe*$^{-/-}$ mice.

Since YB-1 can activate and/or repress RANTES expression, as seen in the macrophage cell line RAW264.7, the effects of YB-1 on other cell types and cell functions involved in atherogenesis clearly need to be addressed. Moreover, the exact repressive and activating mechanisms of YB-1 and a possible interaction with other transcription factors, remain to be elucidated. For instance, the possibility that YB-1 binds to the AP-1 response module in the RANTES promoter requires further examination. For a start, the employment of luciferase reporter assays using truncated or mutated promoter sequences and binding assays using EMSA epitomize suitable approaches.

The above-mentioned *in vitro* and *in vivo* experiments disclosed that YB-1 is a potent mediator of neointimal plaque growth via upregulation of RANTES expression. Thus YB-1 may be a suitable target in the treatment of vascular disease extending previous findings that suggest an interference with mechanisms regulating the expression of RANTES. Blockade of YB-1 expression might be achieved by a regional, i.e. vascular transfer of shRNA as studied in this work. But not only shRNA-mediated knock-down of YB-1, also the interference with YB-1 actions via antibodies, small molecule antagonists and inactivation by proteases may be applicable to prevent restenosis, after arterial angioplasty and stenting. This could be achieved by the use of drug-eluting stents. However, given the ubiquitous expression and pleiotropic functions of YB-1, systemic effects need to be taken into account and should be carefully scrutinized.

IV.2 Novel chemokine-like functions of MIF

IV.2.1 MIF exhibits chemokine functions through CXCR2 and CXCR4

This work identifies CXCR2 and CXCR4 as functional receptors for MIF. The *in vitro* adhesion assays revealed that MIF, immobilized on HAoEC and CHO/ICAM-1 monolayers, triggers leukocyte arrest directly through CXCR2, CXCR4 and the previously identified MIF-receptor CD74 (Leng et al. 2003). Hereby, MIF exhibited a similar efficiacy as the CXC chemokines IL-8 and SDF-1α. Involvement of other CXCR ligands was excluded by blocking mAbs and expression analysis, respectively. It was shown that MIF directly triggers integrin activation, as direct stimulation of MonoMac6 and Jurkat T cells for 1-5 min also led to αLβ2- and α4β1-dependent arrest, and rapid αLβ2 activation was demonstrated on MonoMac6 cells and primary monocytes using an antibody recognizing the active conformation of αLβ2. Furthermore, it was demonstrated that MIF diretly provokes calcium mobilization obviously not requiring CD74 as neutrophils affected by MIF do not express this cell surface protein. MIF/CXCR2-mediated Ca^{2+} mobilization led to a complete desensitization of the NAP-2 calcium signal. However, MIF was less potent in triggering calcium response compared to IL-8 and NAP-2. In addition to these data, the group of Prof. Bernhagen (UK Aachen) demonstrated that MIF also triggers leukocyte chemotaxis through the receptors CXCR2 and CXCR4, respectively (Bernhagen et al. 2007). A direct interaction of MIF and CXCR2 has been demonstrated by coimmunoprecipitation and FACS analysis in this study. Moreover, although binding of MIF to CXCR4 has not been shown yet, receptor competition experiments with I^{125}SDF-1α strongly favor a direct interaction of MIF and CXCR4 (Bernhagen et al. 2007).

Similar to IL-8, which has a wide range of actions on various types of cells (Mukaida 2003), this study proves that MIF affects monocytes and neutrophils through CXCR2. The latter was confirmed by MIF-induced peritoneal neutrophil recruitment assays with mice reconstituted *Cxcr2*$^{-/-}$ bone marrow. In addition, a recently published work demonatrated that MIF promotes mouse embryonic fibroblast migration (Dewor *et al.* 2007). The arrest activity of MIF extends to T cells, as it has the ability to interact with CXCR4.

The presented data proposes the addition of a new class of chemokines to the approved kategorization. According to the existing classification of chemokines (Murphy

et al. 2000), MIF could be referred to as a ΔC chemokine, taking into account that the MIF monomer lacks the typical N-terminal cysteines. Regarding the structural resemblance of the MIF monomer to the IL-8 dimer (Sun et al. 1996), and the pseudo-ELR motif formed by the amino acid residues R11 and D44 with appropriate spacing, MIF seems to mimic ELR^+ chemokines. It has been shown that IL-8 forms bioactive (hetero-)dimers and that homodimers form upon binding to CXCR2 but not to CXCR1 (Schnitzel *et al.* 1994; Deforge *et al.* 2000; Nesmelova *et al.* 2005), which is in line with this work, showing that MIF acts through CXCR2, but apparently does not affect leukocytes through CXCR1.

On the other hand, MIF has been proposed as a CLF-chemokine, a group comprising chemotactic polypeptides, e.g. defensins that differ from chemokines in size and shape. Like the human β-defensins HBD1 and HBD2, which bind and activate CCR6 to induce chemotaxis of immature dendritic and memory T cells (Yang et al. 1999), MIF is upregulated in various tissues after exposure to microbial products (Calandra and Roger 2003). Furthermore, MIF plays a role in sepsis similar to the proposed CLF-chemokine HMGB1 (high mobility group box) (Degryse and de Virgilio 2003). The three-dimensional resemblance of MIF and the IL-8 dimer are in accord with the postulation that some of these CLF-chemokines share tertiary structural features with the corresponding *bona fide* ligands that enable them to utilize chemokine receptors.

Beyond the functional and structural resemblance with the CLF class members and the IL-8 dimer, MIF exhibits enzymatic activities, such as D-dopachrom-tautomerase and oxidoreductase activity, which is dependent on a Cys57-Ala-Leu-Cys60 (CALC) motif. The oxidoreductase activity of MIF has also been linked to its immunogenic properties, and enzymes with chemoattractive properties have been described before: An N-terminal fragment of tyrosyl-tRNA-synthetase binds to CXCR1 stimulating chemotaxis of neutrophils, and thioredoxin, a redox enzyme released by various cell types upon activation, is a chemo-attractant for leukocytes (Bertini *et al.* 1999; Wakasugi and Schimmel 1999). As the oldest known inflammatory cytokine, MIF may represent a prototypic member of the chemokine species combining CLF, chemokine and enzymatic features.

IV.2.2 Co-function of CD74 in a CXC receptor complex

It was further demonstrated that MIF-induced activation of atherogenic or inflammatory arrest of monocytes is not only dependent on CXCR2. As a cell surface binding protein for MIF, CD74 also is involved and co-localizes with CXCR2, as shown by co-immunoprecipitation. Thus, it is conceivable that MIF signals through a functional CXCR/CD74 complex, although the Ca^{2+} mobilization experiments with neutrophils proved that the involvement of CD74 is not crucial for cell activation. However, the association with CD74 may facilitate the activation of CXCR2, as it has been shown that binding of MIF to CD74 induced a signaling cascade involving the proteoglycan CD44 and Src-family kinases (Shi *et al.* 2006). In conjunction, CD74, CD44 and Src could represent a functional receptor tyrosine kinase (RTK)-like complex, and it has been reported that RTK complexes can trans-activate GPCRs and *vice versa* (Akekawatchai *et al.* 2005; Waters *et al.* 2005). Additional binding of MIF to CD74 may facilitate GPCR activation and formation of a signaling complex with Src kinases. A similar mechanism has been described for the chemokine RANTES. The authors observed a formation of a Src kinase/CD44 signaling complex upon RANTES binding to the glycosaminoglycans of CD44 (Roscic-Mrkic *et al.* 2003). In another study, it has been shown that sphingosine-1-phosphate trans-activates CXCR4 via Src-family kinases in human progenitor cells (Walter *et al.* 2007). Fig. IV.1 shows the extended sketch of MIF-induced cell response according to the findings of this work combining CXCRs with the proposed RTK-like complex. As inferred by the profound effects of blocking CD74, this study further implies that CD74 may also participate in Gro-α/IL-8-induced signaling via CXCR2 independently of MIF to accomplish atherogenic cell recruitment. This role of CD74 is further underscored by its preferential expression on mononuclear cell types relevant to atherosclerosis (Leng *et al.* 2003).

Recapulatory, these data extend other studies pointing toward a large GPCR/RTK(-like) complex, which is able to react in a stimuli-rich environment.

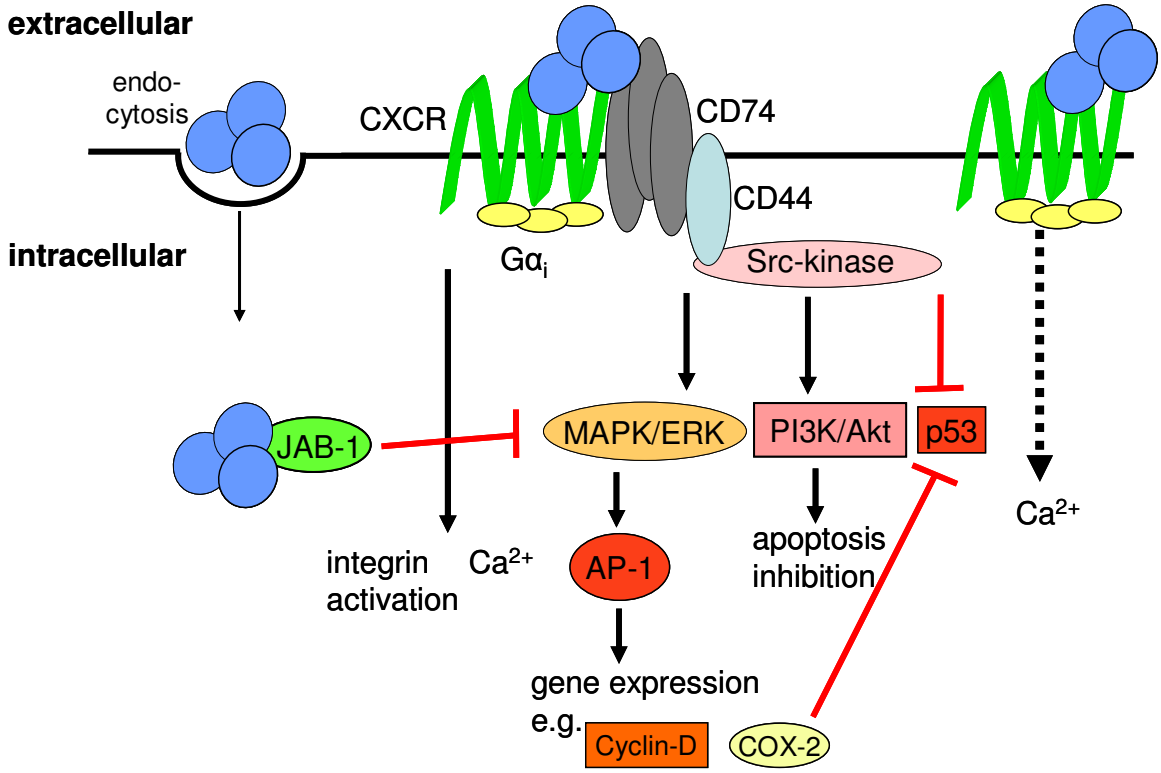

Fig.IV.I: MIF's mechanisms of action. MIF (blue trimer) binds to CXCR2 and possibly to CXCR4. MIF signaling occurs through a receptor complex formed by CD74, CD44 and at least one CXCR and elicits rapid cell responses as calcium mobilization and integrin activation. MIF signaling mechanisms through CXCR2 and CXCR4 alone remain to be elucidated (modified from Morand *et al.* 2006 and Zernecke *et al.* 2008 (in press)).

IV.2.3 Targeting MIF *in vivo* causes atherosclerosis regression

This study provides *ex vivo* and *in vivo* evidence for MIF's inflammatory actions employing perfusion of explanted carotid arteries, as well as intravital microscopy in carotid arteries with early atherosclerosis. Especially, a peritonitis model and linking CXCR2 and MIF deficiency in bone marrow chimeras demonstrated the direct functional involvement of CXCR2 in MIF-triggered monocyte recruitment *in vivo*. Previous studies investigated the contribution of MIF to atherogenesis (Pan *et al.* 2004; Schober *et al.* 2004), but its potential to activate T cells have not been taken into account, just as only the MIF function in atherosclerosis initiation has been evaluated, but its role in plaque progression has not been determined. The role of CXCR2 regarding atherosclerosis progression has been well established (Boisvert *et al.* 2006). The authors found that the genetic deletion of KC/Gro-α in *Ldlr*$^{-/-}$ mice less markedly reduced atherosclerosis than

deletion of leukocyte CXCR2, but that both predominantly affected macrophage accumulation in progressed atherosclerosis. This led to the assumption that another ligand is, at least, partially involved in CXCR2-triggered lesion formation. Accordingly, the work at hand discloses the additional role of MIF as a T cell agonist, and its potential to induce plaque progression. This study shows for the first time that antibody blockade of MIF but not of the cognate CXCR2 and CXCR4 ligands KC/Gro-α or SDF-1α alone leads to a marked regression of advanced pre-existing atherosclerotic plaques in *Apoe*$^{-/-}$ mice on a high-fat diet, and that inflammatory cell content (both macrophages and T cells) was reduced, entailing a more stable plaque phenotype. The present data recognizes MIF as being the additional CXCR2 ligand actively involved in advanced atherosclerosis. As an additional feature, blocking MIF impairs CXCR4-supported T cell recruitment, which is also a critical force driving lesion formation.

IV.2.4 Perspectives

This work unveils that MIF is a non-cognate CXCR ligand. Furthermore, the intrinsic effects of MIF/CXCR2 interaction on inflammation and atherosclerosis progression have been investigated to a great extent. The next goal is to clarify the interaction of MIF with CXCR4, and if CXCR4 also forms a receptor complex with CD74 (and CD44/Src kinase signaling complex) and CXCR2. This could be done by coimmunoprecipitation experiments or, alternatively, by making use of the Fluorescence Resonance Energy Transfer (FRET) which occurs, if a CFP- and YFP-coupled protein, respectively, are in immediate vicinity. Besides, future studies should clearify, if GPCRs trans-activate CD74/CD44/Src complex or if the RTK-like complex acts upstream of the GPCRs. Since the activation of the CXCR2 receptor requires the presence of an ELR motif (Jones et al. 1997), and because of the pseudo-ELR motif (Fig. I.4) which is formed by the amino acid residues on two adjacent β-helices, it is important to examine, if this pseudo-ELR motif is crucial for MIF/CXCR2/4 and CD74 interaction. This could be accomplished by binding assays and functional experiments with MIF mutants (with substituted amino acids at position 11 and/or 44). Furthermore, it would be interesting to discover the CXCR/MIF interface by exchanging the three extracellular loops and the N-terminus of the CXCR2 receptor with the respective parts of a non-MIF-interacting GPCR, for example with the extracellular domains of CXCR3.

The number of chemokine receptor antagonists developed to target atherosclerosis and other inflammatory diseases, e.g. the above-mentioned CCR5 antagonist Met-RANTES, is rapidly expanding and a substantial amount of evidence has been gathered in favor of this therapeutic strategy despite the apparent redundancy in the chemokine system (Proudfoot 2002). This study identifies MIF as a non-cognate CXCR agonist, thereby extending the approaches for therapeutic strategies that target MIF effects on atherosclerosis and other inflammatory diseases. Small peptide antagonists based on the MIF structure may be able to inhibit CXCR2 and/or CXCR4-mediated inflammatory events.

Beyond current strategies promoting reverse cholesterol transport by apolipoprotein mimetics and raising HDL-cholesterol levels by interfering with the cholesterol metabolism or altering the cholesterol composition (Navab *et al.* 2004), targeting MIF may emerge as a suitable strategy to achieve therapeutic regression and stabilization of manifest and advanced atherosclerosis.

V Summary

This study surveys the expression control and the down-stream effects of two mediators that have a severe impact on atherosclerosis progression.

The first approach identified YB-1 as a new transcriptional regulator of the CC chemokine RANTES. RANTES is upregulated in mononuclear cells or deposited by activated platelets during inflammation and has been implicated in atherosclerosis and neointimal hyperplasia. Here, the influence of YB-1 on RANTES expression and its contribution to neointima formation after guide-wire injury has been investigated. The binding of YB-1 to position -214/-173 was confirmed by DNA binding studies. Increased expression of both YB-1 and RANTES mRNA in neointimal versus medial SMC suggested a regulatory function of YB-1 for RANTES expression and, indeed, overexpression of YB-1 in smooth muscle cells (but not macrophages) enhanced RANTES transcriptional activity in reporter assays, mRNA and protein expression, and RANTES-dependent monocyte arrest in shear flow. Furthermore, intraluminal transfection of carotid arteries of hyperlipidemic *Apoe*$^{-/-}$ mice with a lentivirus encoding YB-1 shRNA directly after wire injury led to a significant reduction in plaque area and macrophage content. YB-1 was expressed in neointimal SMC but not macrophages and colocalized with neointimal RANTES, which was downregulated by YB-1 shRNA. A further reduction of lesion formation by YB-1 knockdown was not observed in *Apoe*$^{-/-}$ mice deficient in the RANTES receptor Ccr5 or after treatment with the RANTES receptor antagonist Met-RANTES, which indicates that YB-1 effects were dependent on RANTES. Thus, local blockade of YB-1 might become a suitable strategy in preventing restenosis after balloon angioplasty.

The second part of this work intended to elucidate the mechanisms of the pleiotropic functions of the CLF chemokine MIF. MIF plays a critical role in inflammatory diseases and atherogenesis and attracts immune cells to sites of inflammation. The only known cell surface receptor for MIF is CD74, which can mediate sustained activation of ERK/MAPK. Yet, no receptor had been discovered that would be able to confer MIF's chemokine-like functions in cells devoid of CD74, as neutrophils and fibroblast, which are also affected by MIF. This thesis introduces the two chemokine receptors CXCR2 and CXCR4 as functional receptors for MIF. MIF triggered $G_{\alpha i}$ and integrin-dependent arrest of monocytes and T cells specifically through CXCR2 and, to a lesser extent, CXCR4,

inducing rapid integrin activation and calcium influx. MIF directly bound to CXCR2 as revealed by FACS analysis and coimmunoprecipitation. Monocyte arrest mediated by MIF in inflamed or atherosclerotic arteries involved CXCR2 and CD74, which occur in a receptor complex. *In vivo*, MIF deficiency impaired monocyte adhesion to the aortic/arterial wall in atherosclerosis-prone mice, and MIF-induced leukocyte adhesion as well as peritoneal recruitment required CXCR2, as evidenced by intravital microscopy and MIF/CXCR2 chimeric mice. Blocking MIF but not *bona fide* ligands of CXCR2 or CXCR4 in mice with advanced atherosclerosis reduced plaque area, monocyte and T-cell content. These data open the possibility of achieving therapeutic regression and stabilization of advanced atherosclerotic lesions by targeting MIF.

VI Zusammenfassung

Die vorliegende Arbeit beschäftigt sich mit der Expressionskontrolle und Effekten von zwei Proteinen, die eine große Auswirkung auf den Krankheitsverlauf der Atherosklerose haben.

Im ersten Forschungsansatz wurde YB-1 als der Transkriptionsregulator des CC Chemokins RANTES identifiziert. Während einer Entzündungsreaktion wird die Expression von RANTES in mononukleären Zellen hochreguliert, oder RANTES wird von aktivierten Plättchen auf dem Endothel deponiert, wo es an der Entstehung von Atherosklerose und neointimaler Hyperplasie beteiligt ist. In der vorliegenden Studie wurde der Einfluss von YB-1 auf die RANTES-Expression, sowie seine Mitwirkung an der Neointimabildung nach Drahtverletzung der *Carotis* ermittelt. Die Bindung von YB-1 an Position -214/-173 des RANTES-Promotors wurde durch DNA-Bindungsstudien bestätigt. Die gesteigerte Expression von YB-1 und RANTES-mRNA in neointimalen *versus* medialen glatten Muskelzellen deutete auf eine regulatorische Funktion von YB-1 für die RANTES-Expression hin, und tatsächlich führte die Überexpression von YB-1 in glatten Muskelzellen (aber nicht in Makrophagen) zu einer verstärkten RANTES-Promotoraktivität, sowie zu einer gesteigerten Produktion von RANTES-mRNA und -Protein. Außerdem bewirkte die YB-1 Überexpression in glatten Muskelzellen einen verstärkten Monozytenarrest in Scherfluss, der durch den RANTES-Rezeptorantagonisten Met-RANTES signifikant inhibiert wurde. Darüber hinaus führte der lentivirale Transfer von YB-1 shRNA in die Karotidenlumina von hyperlipidämischen *Apoe*$^{-/-}$-Mäusen nach Drahtverletzung zu einer signifikant reduzierten Plaquefläche, sowie reduziertem Makrophagengehalt. YB-1 wurde in neointimalen SMC aber nicht in Makrophagen exprimiert und kolokalisierte mit neointimalem RANTES, dessen Expression durch YB-1-Silencing herunterreguliert wurde. Eine weitere Reduktion der Neointimafläche durch YB-1-Silencing wurde weder in Met-RANTES-behandelten noch in RANTES-Rezeptor-defizienten (*Ccr5*$^{-/-}$) *Apoe*$^{-/-}$-Mäusen beobachtet. Dieser Umstand ließ darauf schließen, dass der YB-1-Effekt auf die Neointimabildung RANTES-abhängig war. Folglich könnte die lokale Blockade von YB-1 eine neue Strategie zur Restenose-Prävention nach Angioplastie darstellen.

Im zweiten Teil dieser Arbeit sollte den Funktionsmechanismen des CLF Chemokins MIF auf den Grund gegangen werden. MIF spielt eine wichtige Rolle bei Entzündungserkrankungen wie der Atherogenese und lockt Immunzellen zu Entzündungsherden. Der einzige bekannte Zelloberflächenrezeptor für MIF ist CD74, welcher eine anhaltende Aktivierung von ERK/MAPK vermitteln kann. Es wurde bisher jedoch kein Rezeptor gefunden, der die Chemokinfunktionen von MIF in Zellen ohne CD74, wie Fibroblasten und Neutrophile, erkären würde. Diese Studie identifiziert die zwei Chemokinrezeptoren CXCR2 und CXCR4 als funktionelle Rezeptoren für MIF.

MIF vermittelte $G_{\alpha i}$- und Integrin-abhängige Adhäsion von Monozyten und T-Zellen spezifisch durch CXCR2 und, zu einem kleineren Teil, durch CXCR4. Dabei induzierte MIF eine schnelle Integrinaktivierung und Calciummobilisierung. FACS Analyse und Co-Immunpräzipitation bestätigten die direkte Bindung von MIF an CXCR2. MIF-vermittelter Monozytenarrest in entzündlichen oder atherosklerotischen Arterien war abhängig von CXCR2 und CD74, welche einen Rezeptorkomplex bilden. MIF-Defizienz verhinderte Monozytenarrest an der Aorta-/Arterienwand in Atherosklerose-anfälligen Mäusen *in vivo*, und, wie intravitale Mikroskopie und MIF/CXCR2-Chimäre bestätigten, war CXCR2 verantwortlich für MIF-induzierte Leukozytenadhäsion, sowie für die Neutrophileninfiltration im Peritonitismodell. Die Blockade von MIF, aber nicht von den bekannten CXCR2/CXCR4-Liganden in Mäusen mit fortgeschrittener Atherosklerose reduzierte die Plaquefläche und deren Monozyten-und T-Zellgehalt.

Die Aufklärung der Wirkungsmechanismen von MIF in dieser Studie eröffnet neue Möglichkeiten für Therapien zur Regression und Stabilisierung von atherosklerotischen Läsionen.

VII References

Akekawatchai, C., Holland, J. D., Kochetkova, M., Wallace, J. C. and McColl, S. R. (2005). "Transactivation of CXCR4 by the insulin-like growth factor-1 receptor (IGF-1R) in human MDA-MB-231 breast cancer epithelial cells." *J Biol Chem* **280**(48): 39701-8.

Ammit, A. J., Lazaar, A. L., Irani, C., O'Neill, G. M., Gordon, N. D., Amrani, Y., Penn, R. B. and Panettieri, R. A., Jr. (2002). "Tumor necrosis factor-alpha-induced secretion of RANTES and interleukin-6 from human airway smooth muscle cells: modulation by glucocorticoids and beta-agonists." *Am J Respir Cell Mol Biol* **26**(4): 465-74.

Baugh, J. A., Chitnis, S., Donnelly, S. C., Monteiro, J., Lin, X., Plant, B. J., Wolfe, F., Gregersen, P. K. and Bucala, R. (2002). "A functional promoter polymorphism in the macrophage migration inhibitory factor (MIF) gene associated with disease severity in rheumatoid arthritis." *Genes Immun* **3**(3): 170-6.

Bendrat, K., Al-Abed, Y., Callaway, D. J., Peng, T., Calandra, T., Metz, C. N. and Bucala, R. (1997). "Biochemical and mutational investigations of the enzymatic activity of macrophage migration inhibitory factor." *Biochemistry* **36**(49): 15356-62.

Berndt, K., Kim, M., Meinhardt, A. and Klug, J. (2007). "Macrophage migration inhibitory factor does not modulate co-activation of androgen receptor by Jab1/CSN5." *Mol Cell Biochem*.

Bernhagen, J., Calandra, T., Mitchell, R. A., Martin, S. B., Tracey, K. J., Voelter, W., Manogue, K. R., Cerami, A. and Bucala, R. (1993). "MIF is a pituitary-derived cytokine that potentiates lethal endotoxaemia." *Nature* **365**(6448): 756-9.

Bernhagen, J., Krohn, R., Lue, H., Gregory, J. L., Zernecke, A., Koenen, R. R., Dewor, M., Georgiev, I., Schober, A., Leng, L., Kooistra, T., Fingerle-Rowson, G., Ghezzi, P., Kleemann, R., McColl, S. R., Bucala, R., Hickey, M. J. and Weber, C. (2007). "MIF is a noncognate ligand of CXC chemokine receptors in inflammatory and atherogenic cell recruitment." *Nat Med* **13**(5): 587-96.

Bertini, R., Howard, O. M., Dong, H. F., Oppenheim, J. J., Bizzarri, C., Sergi, R., Caselli, G., Pagliei, S., Romines, B., Wilshire, J. A., Mengozzi, M., Nakamura, H., Yodoi, J., Pekkari, K., Gurunath, R., Holmgren, A., Herzenberg, L. A., Herzenberg, L. A. and Ghezzi, P. (1999). "Thioredoxin, a redox enzyme released in infection and inflammation, is a unique chemoattractant for neutrophils, monocytes, and T cells." *J Exp Med* **189**(11): 1783-9.

Blocki, F. A., Ellis, L. B. and Wackett, L. P. (1993). "MIF protein are theta-class glutathione S-transferase homologs." *Protein Sci* **2**(12): 2095-102.

Bloom, B. R. and Bennett, B. (1966). "Mechanism of a reaction in vitro associated with delayed-type hypersensitivity." *Science* **153**(731): 80-2.

Boehlk, S., Fessele, S., Mojaat, A., Miyamoto, N. G., Werner, T., Nelson, E. L.,

Schlondorff, D. and Nelson, P. J. (2000). "ATF and Jun transcription factors, acting through an Ets/CRE promoter module, mediate lipopolysaccharide inducibility of the chemokine RANTES in monocytic Mono Mac 6 cells." *Eur J Immunol* **30**(4): 1102-12.

Boisvert, W. A., Rose, D. M., Johnson, K. A., Fuentes, M. E., Lira, S. A., Curtiss, L. K. and Terkeltaub, R. A. (2006). "Up-regulated expression of the CXCR2 ligand KC/GRO-alpha in atherosclerotic lesions plays a central role in macrophage accumulation and lesion progression." *Am J Pathol* **168**(4): 1385-95.

Braunersreuther, V., Zernecke, A., Arnaud, C., Liehn, E. A., Steffens, S., Shagdarsuren, E., Bidzhekov, K., Burger, F., Pelli, G., Luckow, B., Mach, F. and Weber, C. (2007). "Ccr5 but not Ccr1 deficiency reduces development of diet-induced atherosclerosis in mice." *Arterioscler Thromb Vasc Biol* **27**(2): 373-9.

Burger-Kentischer, A., Gobel, H., Kleemann, R., Zernecke, A., Bucala, R., Leng, L., Finkelmeier, D., Geiger, G., Schaefer, H. E., Schober, A., Weber, C., Brunner, H., Rutten, H., Ihling, C. and Bernhagen, J. (2006). "Reduction of the aortic inflammatory response in spontaneous atherosclerosis by blockade of macrophage migration inhibitory factor (MIF)." *Atherosclerosis* **184**(1): 28-38.

Calandra, T., Bernhagen, J., Mitchell, R. A. and Bucala, R. (1994). "The macrophage is an important and previously unrecognized source of macrophage migration inhibitory factor." *J Exp Med* **179**(6): 1895-902.

Calandra, T. and Bucala, R. (1995). "Macrophage migration inhibitory factor: a counter-regulator of glucocorticoid action and critical mediator of septic shock." *J Inflamm* **47**(1-2): 39-51.

Calandra, T. and Roger, T. (2003). "Macrophage migration inhibitory factor: a regulator of innate immunity." *Nat Rev Immunol* **3**(10): 791-800.

Capowski, E. E., Esnault, S., Bhattacharya, S. and Malter, J. S. (2001). "Y box-binding factor promotes eosinophil survival by stabilizing granulocyte-macrophage colony-stimulating factor mRNA." *J Immunol* **167**(10): 5970-6.

Cappellen, D., Schlange, T., Bauer, M., Maurer, F. and Hynes, N. E. (2007). "Novel c-MYC target genes mediate differential effects on cell proliferation and migration." *EMBO Rep* **8**(1): 70-6.

Chan, J. R., Hyduk, S. J. and Cybulsky, M. I. (2001). "Chemoattractants induce a rapid and transient upregulation of monocyte alpha4 integrin affinity for vascular cell adhesion molecule 1 which mediates arrest: an early step in the process of emigration." *J Exp Med* **193**(10): 1149-58.

Charo, I. F. and Taubman, M. B. (2004). "Chemokines in the pathogenesis of vascular disease." *Circ Res* **95**(9): 858-66.

Chook, Y. M., Gray, J. V., Ke, H. and Lipscomb, W. N. (1994). "The monofunctional chorismate mutase from Bacillus subtilis. Structure determination of chorismate mutase and its complexes with a transition state analog and prephenate, and implications for the mechanism of the enzymatic reaction." *J Mol Biol* **240**(5): 476-500.

Chung, C. T., Niemela, S. L. and Miller, R. H. (1989). "One-step preparation of competent Escherichia coli: transformation and storage of bacterial cells in the same solution." *Proc Natl Acad Sci U S A* **86**(7): 2172-5.

Cockwell, P., Calderwood, J. W., Brooks, C. J., Chakravorty, S. J. and Savage, C. O. S. (2002). Chemoattraction of T cells expressing CCR5, CXCR3 and CX3CR1 by proximal tubular epithelial cell chemokines. **17:** 734-744.

David, J. R. (1966). "Delayed hypersensitivity in vitro: its mediation by cell-free substances formed by lymphoid cell-antigen interaction." *Proc Natl Acad Sci U S A* **56**(1): 72-7.

Deforge, L. E., Lowman, H. B., Leong, S. R., Chuntharapai, A., Jin Kim, K. and Hebert, C. A. (2000). "A neutralizing monoclonal antibody specific for the dimer interface region of IL-8." *Cytokine* **12**(11): 1620-9.

Degryse, B. and de Virgilio, M. (2003). "The nuclear protein HMGB1, a new kind of chemokine?" *FEBS Lett* **553**(1-2): 11-7.

Deguchi, J., Abe, J., Makuuchi, M. and Takuwa, Y. (1999). "Inhibitory effects of trapidil on PDGF signaling in balloon-injured rat carotid artery." *Life Sci* **65**(26): 2791-9.

Dewor, M., Steffens, G., Krohn, R., Weber, C., Baron, J. and Bernhagen, J. (2007). "Macrophage migration inhibitory factor (MIF) promotes fibroblast migration in scratch-wounded monolayers in vitro." *FEBS Lett* **581**(24): 4734-42.

Elsner, J., Petering, H., Hochstetter, R., Kimmig, D., Wells, T. N., Kapp, A. and Proudfoot, A. E. (1997). "The CC chemokine antagonist Met-RANTES inhibits eosinophil effector functions through the chemokine receptors CCR1 and CCR3." *Eur J Immunol* **27**(11): 2892-8.

Evdokimova, V., Ruzanov, P., Anglesio, M. S., Sorokin, A. V., Ovchinnikov, L. P., Buckley, J., Triche, T. J., Sonenberg, N. and Sorensen, P. H. (2006). "Akt-mediated YB-1 phosphorylation activates translation of silent mRNA species." *Mol Cell Biol* **26**(1): 277-92.

Feigelson, S. W., Grabovsky, V., Winter, E., Chen, L. L., Pepinsky, R. B., Yednock, T., Yablonski, D., Lobb, R. and Alon, R. (2001). "The Src kinase p56(lck) up-regulates VLA-4 integrin affinity. Implications for rapid spontaneous and chemokine-triggered T cell adhesion to VCAM-1 and fibronectin." *J Biol Chem* **276**(17): 13891-901.

Fessele, S., Boehlk, S., Mojaat, A., Miyamoto, N. G., Werner, T., Nelson, E. L., Schlondorff, D. and Nelson, P. J. (2001). "Molecular and in silico characterization of a promoter module and C/EBP element that mediate LPS-induced RANTES/CCL5 expression in monocytic cells." *Faseb J* **15**(3): 577-9.

Fessele, S., Maier, H., Zischek, C., Nelson, P. J. and Werner, T. (2002). "Regulatory context is a crucial part of gene function." *Trends in Genetics* **18**(2): 60-63.

Fingerle-Rowson, G., Petrenko, O., Metz, C. N., Forsthuber, T. G., Mitchell, R., Huss, R., Moll, U., Muller, W. and Bucala, R. (2003). "The p53-dependent effects of

macrophage migration inhibitory factor revealed by gene targeting." *Proc Natl Acad Sci U S A* **100**(16): 9354-9.

Gaudreault, I., Guay, D. and Lebel, M. (2004). "YB-1 promotes strand separation in vitro of duplex DNA containing either mispaired bases or cisplatin modifications, exhibits endonucleolytic activities and binds several DNA repair proteins." *Nucleic Acids Res* **32**(1): 316-27.

Genin, P., Algarte, M., Roof, P., Lin, R. and Hiscott, J. (2000). "Regulation of RANTES chemokine gene expression requires cooperativity between NF-kappa B and IFN-regulatory factor transcription factors." *J Immunol* **164**(10): 5352-61.

Gerszten, R. E., Garcia-Zepeda, E. A., Lim, Y. C., Yoshida, M., Ding, H. A., Gimbrone, M. A., Jr., Luster, A. D., Lucsinskas, F. W. and Rosenzweig, A. (1999). "MCP-1 and IL-8 trigger firm adhesion of monocytes to vascular endothelium under flow conditions." *Nature* **398**: 718-723.

Grabovsky, V., Feigelson, S., Chen, C., Bleijs, D. A., Peled, A., Cinamon, G., Baleux, F., Arenzana-Seisdedos, F., Lapidot, T., van Kooyk, Y., Lobb, R. R. and Alon, R. (2000). "Subsecond induction of alpha4 integrin clustering by immobilized chemokines stimulates leukocyte tethering and rolling on endothelial vascular cell adhesion molecule 1 under flow conditions." *J Exp Med* **192**(4): 495-506.

Hansson, G. K. (2005). "Inflammation, atherosclerosis, and coronary artery disease." *N Engl J Med* **352**(16): 1685-95.

Hiura, T. S., Kempiak, S. J. and Nel, A. E. (1999). "Activation of the human RANTES gene promoter in a macrophage cell line by lipopolysaccharide is dependent on stress-activated protein kinases and the IkappaB kinase cascade: implications for exacerbation of allergic inflammation by environmental pollutants." *Clin Immunol* **90**(3): 287-301.

Hoi, A. Y., Hickey, M. J., Hall, P., Yamana, J., O'Sullivan, K. M., Santos, L. L., James, W. G., Kitching, A. R. and Morand, E. F. (2006). "Macrophage migration inhibitory factor deficiency attenuates macrophage recruitment, glomerulonephritis, and lethality in MRL/lpr mice." *J Immunol* **177**(8): 5687-96.

Horuk, R. (2001). "Chemokine receptors." *Cytokine Growth Factor Rev* **12**(4): 313-35.

Hudson, J. D., Shoaibi, M. A., Maestro, R., Carnero, A., Hannon, G. J. and Beach, D. H. (1999). "A proinflammatory cytokine inhibits p53 tumor suppressor activity." *J Exp Med* **190**(10): 1375-82.

Huo, Y., Weber, C., Forlow, S. B., Sperandio, M., Thatte, J., Mack, M., Jung, S., Littman, D. R. and Ley, K. (2001). "The chemokine KC, but not monocyte chemoattractant protein-1, triggers monocyte arrest on early atherosclerotic endothelium." *J Clin Invest* **108**(9): 1307-14.

Jonasson, L., Holm, J., Skalli, O., Bondjers, G. and Hansson, G. K. (1986). "Regional accumulations of T cells, macrophages, and smooth muscle cells in the human atherosclerotic plaque." *Arteriosclerosis* **6**(2): 131-8.

Jones, S. A., Dewald, B., Clark-Lewis, I. and Baggiolini, M. (1997). "Chemokine

antagonists that discriminate between interleukin-8 receptors. Selective blockers of CXCR2." *J Biol Chem* **272**(26): 16166-9.

Jordan, N. J., Watson, M. L., Williams, R. J., Roach, A. G., Yoshimura, T. and Westwick, J. (1997). "Chemokine production by human vascular smooth muscle cells: modulation by IL-13." *Br J Pharmacol* **122**(4): 749-57.

Jung, H., Kim, T., Chae, H. Z., Kim, K. T. and Ha, H. (2001). "Regulation of macrophage migration inhibitory factor and thiol-specific antioxidant protein PAG by direct interaction." *J Biol Chem* **276**(18): 15504-10.

Kamalov, G., Varma, B. R., Lu, L., Sun, Y., Weber, K. T. and Guntaka, R. V. (2005). "Expression of the multifunctional Y-box protein, YB-1, in myofibroblasts of the infarcted rat heart." *Biochem Biophys Res Commun* **334**(1): 239-44.

Kleemann, R., Hausser, A., Geiger, G., Mischke, R., Burger-Kentischer, A., Flieger, O., Johannes, F. J., Roger, T., Calandra, T., Kapurniotu, A., Grell, M., Finkelmeier, D., Brunner, H. and Bernhagen, J. (2000). "Intracellular action of the cytokine MIF to modulate AP-1 activity and the cell cycle through Jab1." *Nature* **408**(6809): 211-6.

Kleemann, R., Kapurniotu, A., Frank, R. W., Gessner, A., Mischke, R., Flieger, O., Juttner, S., Brunner, H. and Bernhagen, J. (1998). "Disulfide analysis reveals a role for macrophage migration inhibitory factor (MIF) as thiol-protein oxidoreductase." *J Mol Biol* **280**(1): 85-102.

Kleemann, R., Rorsman, H., Rosengren, E., Mischke, R., Mai, N. T. and Bernhagen, J. (2000). "Dissection of the enzymatic and immunologic functions of macrophage migration inhibitory factor. Full immunologic activity of N-terminally truncated mutants." *Eur J Biochem* **267**(24): 7183-93.

Lan, H. Y., Bacher, M., Yang, N., Mu, W., Nikolic-Paterson, D. J., Metz, C., Meinhardt, A., Bucala, R. and Atkins, R. C. (1997). "The pathogenic role of macrophage migration inhibitory factor in immunologically induced kidney disease in the rat." *J Exp Med* **185**(8): 1455-65.

Laudanna, C. and Alon, R. (2006). "Right on the spot. Chemokine triggering of integrin-mediated arrest of rolling leukocytes." *Thromb Haemost* **95**(1): 5-11.

Lee, A. H., Hong, J. H. and Seo, Y. S. (2000). "Tumour necrosis factor-alpha and interferon-gamma synergistically activate the RANTES promoter through nuclear factor kappaB and interferon regulatory factor 1 (IRF-1) transcription factors." *Biochem J* **350 Pt 1**: 131-8.

Leech, M., Metz, C., Hall, P., Hutchinson, P., Gianis, K., Smith, M., Weedon, H., Holdsworth, S. R., Bucala, R. and Morand, E. F. (1999). "Macrophage migration inhibitory factor in rheumatoid arthritis: evidence of proinflammatory function and regulation by glucocorticoids." *Arthritis Rheum* **42**(8): 1601-8.

Leitinger, N. (2003). "Oxidized phospholipids as modulators of inflammation in atherosclerosis." *Curr Opin Lipidol* **14**(5): 421-30.

Leng, L., Metz, C. N., Fang, Y., Xu, J., Donnelly, S., Baugh, J., Delohery, T., Chen, Y.,

Mitchell, R. A. and Bucala, R. (2003). "MIF signal transduction initiated by binding to CD74." *J Exp Med* **197**(11): 1467-76.

Ley, K. (2003). "Arrest chemokines." *Microcirculation* **10**(3-4): 289-95.

Libby, P. (2002). "Inflammation in atherosclerosis." *Nature* **420**(6917): 868-74.

Lindner, V., Fingerle, J. and Reidy, M. A. (1993). "Mouse model of arterial injury." *Circ Res* **73**(5): 792-796.

Lue, H., Kapurniotu, A., Fingerle-Rowson, G., Roger, T., Leng, L., Thiele, M., Calandra, T., Bucala, R. and Bernhagen, J. (2006). "Rapid and transient activation of the ERK MAPK signalling pathway by macrophage migration inhibitory factor (MIF) and dependence on JAB1/CSN5 and Src kinase activity." *Cell Signal* **18**(5): 688-703.

Lue, H., Thiele, M., Franz, J., Dahl, E., Speckgens, S., Leng, L., Fingerle-Rowson, G., Bucala, R., Luscher, B. and Bernhagen, J. (2007). "Macrophage migration inhibitory factor (MIF) promotes cell survival by activation of the Akt pathway and role for CSN5/JAB1 in the control of autocrine MIF activity." *Oncogene* **26**(35): 5046-59.

MacDonald, G. H., Itoh-Lindstrom, Y. and Ting, J. P. (1995). "The transcriptional regulatory protein, YB-1, promotes single-stranded regions in the DRA promoter." *J Biol Chem* **270**(8): 3527-33.

Maione, T. E., Gray, G. S., Petro, J., Hunt, A. J., Donner, A. L., Bauer, S. I., Carson, H. F. and Sharpe, R. J. (1990). Inhibition of angiogenesis by recombinant human platelet factor-4 and related peptides. **247:** 77-79.

Mertens, P. R., Alfonso-Jaume, M. A., Steinmann, K. and Lovett, D. H. (1998). "A synergistic interaction of transcription factors AP2 and YB-1 regulates gelatinase A enhancer-dependent transcription." *J Biol Chem* **273**(49): 32957-65.

Mertens, P. R., Harendza, S., Pollock, A. S. and Lovett, D. H. (1997). "Glomerular mesangial cell-specific transactivation of matrix metalloproteinase 2 transcription is mediated by YB-1." *J Biol Chem* **272**(36): 22905-12.

Mischke, R., Kleemann, R., Brunner, H. and Bernhagen, J. (1998). "Cross-linking and mutational analysis of the oligomerization state of the cytokine macrophage migration inhibitory factor (MIF)." *FEBS Lett* **427**(1): 85-90.

Mitchell, R. A., Liao, H., Chesney, J., Fingerle-Rowson, G., Baugh, J., David, J. and Bucala, R. (2002). "Macrophage migration inhibitory factor (MIF) sustains macrophage proinflammatory function by inhibiting p53: regulatory role in the innate immune response." *Proc Natl Acad Sci U S A* **99**(1): 345-50.

Miyamoto, N. G., Medberry, P. S., Hesselgesser, J., Boehlk, S., Nelson, P. J., Krensky, A. M. and Perez, H. D. (2000). "Interleukin-1beta induction of the chemokine RANTES promoter in the human astrocytoma line CH235 requires both constitutive and inducible transcription factors." *J Neuroimmunol* **105**(1): 78-90.

Morand, E. F., Leech, M. and Bernhagen, J. (2006). "MIF: a new cytokine link between rheumatoid arthritis and atherosclerosis." *Nat Rev Drug Discov* **5**(5): 399-410.

Moser, B. and Willimann, K. (2004). "Chemokines: role in inflammation and immune surveillance." *Ann Rheum Dis* **63 Suppl 2**: ii84-ii89.

Mukaida, N. (2003). "Pathophysiological roles of interleukin-8/CXCL8 in pulmonary diseases." *Am J Physiol Lung Cell Mol Physiol* **284**(4): L566-77.

Muller, R., Bullesfeld, L., Gerckens, U. and Grube, E. (2002). "[State of treatment of coronary artery disease by drug releasing stents]." *Herz* **27**(6): 508-13.

Murphy, P. M., Baggiolini, M., Charo, I. F., Hebert, C. A., Horuk, R., Matsushima, K., Miller, L. H., Oppenheim, J. J. and Power, C. A. (2000). "International union of pharmacology. XXII. Nomenclature for chemokine receptors." *Pharmacol Rev* **52**(1): 145-76.

Navab, M., Anantharamaiah, G. M., Reddy, S. T., Van Lenten, B. J., Datta, G., Garber, D. and Fogelman, A. M. (2004). "Human apolipoprotein A-I and A-I mimetic peptides: potential for atherosclerosis reversal." *Curr Opin Lipidol* **15**(6): 645-9.

Nelson, P. J., Kim, H. T., Manning, W. C., Goralski, T. J. and Krensky, A. M. (1993). "Genomic organization and transcriptional regulation of the RANTES chemokine gene." *J Immunol* **151**(5): 2601-12.

Nesmelova, I. V., Sham, Y., Dudek, A. Z., van Eijk, L. I., Wu, G., Slungaard, A., Mortari, F., Griffioen, A. W. and Mayo, K. H. (2005). "Platelet factor 4 and interleukin-8 CXC chemokine heterodimer formation modulates function at the quaternary structural level." *J Biol Chem* **280**(6): 4948-58.

Oh, W., Lee, E. W., Sung, Y. H., Yang, M. R., Ghim, J., Lee, H. W. and Song, J. (2006). "Jab1 induces the cytoplasmic localization and degradation of p53 in coordination with Hdm2." *J Biol Chem* **281**(25): 17457-65.

Pan, J. H., Sukhova, G. K., Yang, J. T., Wang, B., Xie, T., Fu, H., Zhang, Y., Satoskar, A. R., David, J. R., Metz, C. N., Bucala, R., Fang, K., Simon, D. I., Chapman, H. A., Libby, P. and Shi, G. P. (2004). "Macrophage migration inhibitory factor deficiency impairs atherosclerosis in low-density lipoprotein receptor-deficient mice." *Circulation* **109**(25): 3149-53.

Pattison, J. M., Nelson, P. J., Huie, P., Sibley, R. K. and Krensky, A. M. (1996). "RANTES chemokine expression in transplant-associated accelerated atherosclerosis." *J Heart Lung Transplant* **15**(12): 1194-9.

Proudfoot, A. E. (2002). "Chemokine receptors: multifaceted therapeutic targets." *Nat Rev Immunol* **2**(2): 106-15.

Raffetseder, U., Frye, B., Rauen, T., Jurchott, K., Royer, H. D., Jansen, P. L. and Mertens, P. R. (2003). "Splicing factor SRp30c interaction with Y-box protein-1 confers nuclear YB-1 shuttling and alternative splice site selection." *J Biol Chem* **278**(20): 18241-8.

Raines, E. W. (2004). "PDGF and cardiovascular disease." *Cytokine Growth Factor Rev* **15**(4): 237-54.

Raj, G. V., Safak, M., MacDonald, G. H. and Khalili, K. (1996). "Transcriptional regulation of human polyomavirus JC: evidence for a functional interaction between RelA (p65) and the Y-box-binding protein, YB-1." *J Virol* **70**(9): 5944-53.

Reape, T. J. and Groot, P. H. (1999). "Chemokines and atherosclerosis." *Atherosclerosis* **147**(2): 213-25.

Roger, T., David, J., Glauser, M. P. and Calandra, T. (2001). "MIF regulates innate immune responses through modulation of Toll-like receptor 4." *Nature* **414**(6866): 920-4.

Roscic-Mrkic, B., Fischer, M., Leemann, C., Manrique, A., Gordon, C. J., Moore, J. P., Proudfoot, A. E. and Trkola, A. (2003). "RANTES (CCL5) uses the proteoglycan CD44 as an auxiliary receptor to mediate cellular activation signals and HIV-1 enhancement." *Blood* **102**(4): 1169-77.

Rosengren, E., Bucala, R., Aman, P., Jacobsson, L., Odh, G., Metz, C. N. and Rorsman, H. (1996). "The immunoregulatory mediator macrophage migration inhibitory factor (MIF) catalyzes a tautomerization reaction." *Mol Med* **2**(1): 143-9.

Ross, R. (1993). "The pathogenesis of atherosclerosis: a perspective for the 1990s." *Nature* **362**(6423): 801-9.

Sackstein, R. (2005). "The lymphocyte homing receptors: gatekeepers of the multistep paradigm." *Curr Opin Hematol* **12**(6): 444-50.

Sambrook, J. and Russell, D. W. (2001). "Molecular cloning : a laboratory manual." *Cold Spring Harbor: Cold Spring Harbor Laboratory Press.*

Samuel, S., Beifuss, K. K. and Bernstein, L. R. (2007). "YB-1 binds to the MMP-13 promoter sequence and represses MMP-13 transactivation via the AP-1 site." *Biochim Biophys Acta* **1769**(9-10): 525-31.

Sanchez, E., Gomez, L. M., Lopez-Nevot, M. A., Gonzalez-Gay, M. A., Sabio, J. M., Ortego-Centeno, N., de Ramon, E., Anaya, J. M., Gonzalez-Escribano, M. F., Koeleman, B. P. and Martin, J. (2006). "Evidence of association of macrophage migration inhibitory factor gene polymorphisms with systemic lupus erythematosus." *Genes Immun* **7**(5): 433-6.

Schall, T. J., Bacon, K., Toy, K. J. and Goeddel, D. V. (1990). "Selective attraction of monocytes and T lymphocytes of the memory phenotype by cytokine RANTES." *Nature* **347**(6294): 669-71.

Schall, T. J., Jongstra, J., Dyer, B. J., Jorgensen, J., Clayberger, C., Davis, M. M. and Krensky, A. M. (1988). "A human T cell-specific molecule is a member of a new gene family." *J Immunol* **141**(3): 1018-25.

Schnitzel, W., Monschein, U. and Besemer, J. (1994). "Monomer-dimer equilibria of interleukin-8 and neutrophil-activating peptide 2. Evidence for IL-8 binding as a dimer and oligomer to IL-8 receptor B." *J Leukoc Biol* **55**(6): 763-70.

Schober, A., Bernhagen, J., Thiele, M., Zeiffer, U., Knarren, S., Roller, M., Bucala, R.

and Weber, C. (2004). "Stabilization of atherosclerotic plaques by blockade of macrophage migration inhibitory factor after vascular injury in apolipoprotein E-deficient mice." *Circulation* **109**(3): 380-5.

Schober, A., Knarren, S., Lietz, M., Lin, E. A. and Weber, C. (2003). "Crucial role of stromal cell-derived factor-1alpha in neointima formation after vascular injury in apolipoprotein E-deficient mice." *Circulation* **108**(20): 2491-7.

Schober, A., Manka, D., von Hundelshausen, P., Huo, Y., Hanrath, P., Sarembock, I. J., Ley, K. and Weber, C. (2002). "Deposition of platelet RANTES triggering monocyte recruitment requires P-selectin and is involved in neointima formation after arterial injury." *Circulation* **106**(12): 1523-9.

Shamri, R., Grabovsky, V., Gauguet, J. M., Feigelson, S., Manevich, E., Kolanus, W., Robinson, M. K., Staunton, D. E., von Andrian, U. H. and Alon, R. (2005). "Lymphocyte arrest requires instantaneous induction of an extended LFA-1 conformation mediated by endothelium-bound chemokines." *Nat Immunol* **6**(5): 497-506.

Shen, L., Hu, J., Lu, H., Wu, M., Qin, W., Wan, D., Li, Y. Y. and Gu, J. (2003). "The apoptosis-associated protein BNIPL interacts with two cell proliferation-related proteins, MIF and GFER." *FEBS Lett* **540**(1-3): 86-90.

Shi, X., Leng, L., Wang, T., Wang, W., Du, X., Li, J., McDonald, C., Chen, Z., Murphy, J. W., Lolis, E., Noble, P., Knudson, W. and Bucala, R. (2006). "CD44 is the signaling component of the macrophage migration inhibitory factor-CD74 receptor complex." *Immunity* **25**(4): 595-606.

Sirois, M. G., Simons, M. and Edelman, E. R. (1997). "Antisense oligonucleotide inhibition of PDGFR-beta receptor subunit expression directs suppression of intimal thickening." *Circulation* **95**(3): 669-76.

Skalen, K., Gustafsson, M., Rydberg, E. K., Hulten, L. M., Wiklund, O., Innerarity, T. L. and Boren, J. (2002). "Subendothelial retention of atherogenic lipoproteins in early atherosclerosis." *Nature* **417**(6890): 750-4.

Sorokin, A. V., Selyutina, A. A., Skabkin, M. A., Guryanov, S. G., Nazimov, I. V., Richard, C., Th'ng, J., Yau, J., Sorensen, P. H., Ovchinnikov, L. P. and Evdokimova, V. (2005). "Proteasome-mediated cleavage of the Y-box-binding protein 1 is linked to DNA-damage stress response." *Embo J* **24**(20): 3602-12.

Stemme, S., Holm, J. and Hansson, G. K. (1992). "T lymphocytes in human atherosclerotic plaques are memory cells expressing CD45RO and the integrin VLA-1." *Arterioscler Thromb* **12**(2): 206-11.

Stenina, O. I., Poptic, E. J. and DiCorleto, P. E. (2000). "Thrombin activates a Y box-binding protein (DNA-binding protein B) in endothelial cells." *J Clin Invest* **106**(4): 579-87.

Strieter, R. M., Polverini, P. J., Kunkel, S. L., Arenberg, D. A., Burdick, M. D., Kasper, J., Dzuiba, J., Van Damme, J., Walz, A., Marriott, D., Chan, S.-Y., Roczniak, S. and Shanafelt, A. B. (1995). The Functional Role of the ELR Motif in CXC Chemokine-

mediated Angiogenesis. **270:** 27348-27357.

Subramanya, H. S., Roper, D. I., Dauter, Z., Dodson, E. J., Davies, G. J., Wilson, K. S. and Wigley, D. B. (1996). "Enzymatic ketonization of 2-hydroxymuconate: specificity and mechanism investigated by the crystal structures of two isomerases." *Biochemistry* **35**(3): 792-802.

Sun, H. W., Bernhagen, J., Bucala, R. and Lolis, E. (1996). "Crystal structure at 2.6-A resolution of human macrophage migration inhibitory factor." *Proc Natl Acad Sci U S A* **93**(11): 5191-6.

Takata, H., Tomiyama, H., Fujiwara, M., Kobayashi, N. and Takiguchi, M. (2004). Cutting Edge: Expression of Chemokine Receptor CXCR1 on Human Effector CD8+ T Cells. **173:** 2231-2235.

Ting, J. P., Painter, A., Zeleznik-Le, N. J., MacDonald, G., Moore, T. M., Brown, A. and Schwartz, B. D. (1994). "YB-1 DNA-binding protein represses interferon gamma activation of class II major histocompatibility complex genes." *J Exp Med* **179**(5): 1605-11.

van Roeyen, C. R., Eitner, F., Martinkus, S., Thieltges, S. R., Ostendorf, T., Bokemeyer, D., Luscher, B., Luscher-Firzlaff, J. M., Floege, J. and Mertens, P. R. (2005). "Y-box protein 1 mediates PDGF-B effects in mesangioproliferative glomerular disease." *J Am Soc Nephrol* **16**(10): 2985-96.

Veillard, N. R., Kwak, B., Pelli, G., Mulhaupt, F., James, R. W., Proudfoot, A. E. and Mach, F. (2004). "Antagonism of RANTES receptors reduces atherosclerotic plaque formation in mice." *Circ Res* **94**(2): 253-61.

von Hundelshausen, P., Weber, K. S., Huo, Y., Proudfoot, A. E., Nelson, P. J., Ley, K. and Weber, C. (2001). "RANTES deposition by platelets triggers monocyte arrest on inflamed and atherosclerotic endothelium." *Circulation* **103**(13): 1772-7.

Wakasugi, K. and Schimmel, P. (1999). "Two distinct cytokines released from a human aminoacyl-tRNA synthetase." *Science* **284**(5411): 147-51.

Walter, D. H., Rochwalsky, U., Reinhold, J., Seeger, F., Aicher, A., Urbich, C., Spyridopoulos, I., Chun, J., Brinkmann, V., Keul, P., Levkau, B., Zeiher, A. M., Dimmeler, S. and Haendeler, J. (2007). "Sphingosine-1-phosphate stimulates the functional capacity of progenitor cells by activation of the CXCR4-dependent signaling pathway via the S1P3 receptor." *Arterioscler Thromb Vasc Biol* **27**(2): 275-82.

Waters, C. M., Connell, M. C., Pyne, S. and Pyne, N. J. (2005). "c-Src is involved in regulating signal transmission from PDGFbeta receptor-GPCR(s) complexes in mammalian cells." *Cell Signal* **17**(2): 263-77.

Weber, C., Schober, A. and Zernecke, A. (2004). "Chemokines: key regulators of mononuclear cell recruitment in atherosclerotic vascular disease." *Arterioscler Thromb Vasc Biol* **24**(11): 1997-2008.

Weber, C., Weber, K. S., Klier, C., Gu, S., Wank, R., Horuk, R. and Nelson, P. J. (2001). "Specialized roles of the chemokine receptors CCR1 and CCR5 in the

recruitment of monocytes and T(H)1-like/CD45RO(+) T cells." *Blood* **97**(4): 1144-6.

Weber, K. S., Draude, G., Erl, W., de Martin, R. and Weber, C. (1999). "Monocyte Arrest and Transmigration on Inflamed Endothelium in Shear Flow Is Inhibited by Adenovirus-Mediated Gene Transfer of Ikappa B-alpha " *Blood* **93**(11): 3685-3693.

Weber, K. S., von Hundelshausen, P., Clark-Lewis, I., Weber, P. C. and Weber, C. (1999). "Differential immobilization and hierarchical involvement of chemokines in monocyte arrest and transmigration on inflamed endothelium in shear flow." *Eur. J. Immunol.* **29**: 700-712.

Weber, K. S., Weber, C., Ostermann, G., Dierks, H., Nagel, W. and Kolanus, W. (2001). "Cytohesin-1 is a dynamic regulator of distinct LFA-1 functions in leukocyte arrest and transmigration triggered by chemokines." *Curr. Biol.* **11**: 1969-1974.

Yang, D., Chertov, O., Bykovskaia, S. N., Chen, Q., Buffo, M. J., Shogan, J., Anderson, M., Schroder, J. M., Wang, J. M., Howard, O. M. and Oppenheim, J. J. (1999). "Beta-defensins: linking innate and adaptive immunity through dendritic and T cell CCR6." *Science* **286**(5439): 525-8.

Yusuf, S. (2002). "MRC/BHF Heart Protection Study of antioxidant vitamin supplementation in 20,536 high-risk individuals: a randomised placebo-controlled trial." *Lancet* **360**(9326): 23-33.

Zernecke, A., Liehn, E. A., Gao, J. L., Kuziel, W. A., Murphy, P. M. and Weber, C. (2006). "Deficiency in CCR5 but not CCR1 protects against neointima formation in atherosclerosis-prone mice: involvement of IL-10." *Blood* **107**(11): 4240-3.

Zhang, A., Liu, X., Cogan, J. G., Fuerst, M. D., Polikandriotis, J. A., Kelm, R. J., Jr. and Strauch, A. R. (2005). "YB-1 coordinates vascular smooth muscle alpha-actin gene activation by transforming growth factor beta1 and thrombin during differentiation of human pulmonary myofibroblasts." *Mol Biol Cell* **16**(10): 4931-40.

VIII Acknowledgements

I am very grateful to Prof. Dr. Christian Weber for the possibility to work on a very interesting topic in his research group and for supervision and scientific support. I would also like to thank Prof. Dr. Jürgen Bernhagen for his scientific support.

I am also very grateful to PD Dr. Christoph Peterhänsel for reviewing my thesis and for his support.

Special thanks go to Dr. Rory Koenen for excellent supervision in the lab and helpful discussions.

Thanks to Prof. Dr. Peter Mertens and his research group, especially Dr. Ute Raffetseder, for helping with the luciferase reporter assays and performing the EMSA.

A special thanks to Dr. Alma Zernecke for perfoming the regression studies in mice *in vivo*. In this regard I would also like to thank Dr. Elisa Liehn and Dr. Erdenechimeg Guenther for their help with the animal experiments.

Thanks to Dr. Hongqi Lue for performing CoIP in HEK cells and FACS measurement of CXCR2/MIF.

Last but not least, I would like to thank all my colleagues from the Institute of Molecular Cardiovascular Research (IMCAR) and from the Institute of Biochemistry at the University Hospital RWTH Aachen for good collaboration and a great working atmosphere.

IX Curriculum Vitae

Persönliche Daten:

Name:	Regina Krohn
Geburtsdatum/ort:	25.07.1977 in Xanten, Deutschland
Nationalität:	Deutsch
Familienstand:	ledig, keine Kinder

Bildungsweg:

August 1988 - Juni 1997	Besuch des Stiftsgymnasiums Xanten
Juni 1997	Schulabschluss mit der Allgemeinen Hochschulreife am Stiftsgymnasium Xanten
Oktober 1997 - Dezember 2003	Diplomstudium Biologie an der Rheinisch-Westfälischen Technischen Hochschule (RWTH) Aachen
Februar 2003 - Dezember 2003	Diplomandin am Institut für Molekulare Biotechnologie an der RWTH Aachen unter der Leitung von Prof. Dr. Rainer Fischer. Die Arbeit fand in Kooperation mit dem Fraunhofer Institut für Molekularbiologie und Angewandte Ökologie (IME) Aachen statt.
2004 - 2007	Doktorandin am Institut für Kardiovaskuläre Molekularbiologie unter der Leitung von Univ.-Prof. Dr. med. Christian Weber in Kooperation mit dem Institut für Biochemie unter der Leitung von Univ.-Prof. Dr. rer. nat. Jürgen Bernhagen

Auslandsaufenthalte:

September 1994 - Juli 1995	Besuch der Highschool in Brunswick, Georgia, USA
Mai 2000 – Juli 2000	Sprachkurs an der Universität von Salamanca, Spanien

Publikationen:

Tur, M.K., Huhn, M., Thepen, T., Stocker, M., **Krohn, R.**, Vogel, S., Jost, E., Osieka, R., van de Winkel, J. G., Fischer, R., Finnern, R. and Barth, S. (2003). Recombinant CD64-specific single chain immunotoxin exhibits specific cytotoxicity against acute myeloid leukemia cells. *Cancer Res* **63**(23): 8414-9.

Bernhagen, J., **Krohn, R.**, Lue, H., Gregory, J. L., Zernecke, A., Koenen, R. R., Dewor, M., Georgiev, I., Schober, A., Leng, L., Kooistra, T., Fingerle-Rowson, G., Ghezzi, P., Kleemann, R., McColl, S. R., Bucala, R., Hickey, M. J., Weber**,** C. (2007). MIF is a noncognate ligand of CXC receptors in inflammatory and atherogenic cell recruitment. *Nat Med* **13**(5), 587-96.

Krohn, R., Raffetseder, U., Bot, I., Zernecke, A., Shagdarsuren, E., Liehn, E. A., van Sandbrink, J. P., Nelson, P. J., Biessen, E. A., Mertens, P. R., Weber, C. (2007). Y-box binding protein-1 controls CC chemokine ligand-5 (CCL5) expression in smooth muscle cells and contributes to neointima formation in atherosclerosis-prone mice. *Circulation* **116**(16), 1812-20.

Dewor, M., Steffens, G., **Krohn, R.**, Weber, C., Baron, J., Bernhagen, J. (2007). Macrophage migration inhibitory factor (MIF) promotes fibroblast migration in scratch-wounded monolayers in vitro. *FEBS Lett* **581**(24), 4734-42.

Zernecke, A., Bot, I., Talab, Y. D., Shagdarsuren, E., Bidzhekov, K., Meiler, S., **Krohn, R.**, Schober, A., Sperandio, M., Soehnlein, O., Bornemann, J., Tacke, F., Biessen, E. A. and Weber, C. (2008). Protective role of CXC receptor 4/CXC ligand 12 unveils the importance of neutrophils in atherosclerosis. *Circ Res* **102**(2), 209-17.